ENVIRONMENTAL AND ECONOMIC ASSESSMENT OF CARBON DIOXIDE RECOVERY AND MITIGATION IN THE INDUSTRIAL AND ENERGY SECTORS

by

Sarang D. Supekar

A dissertation submitted in partial fulfillment
of the requirements for the degree of
Doctor of Philosophy
(Mechanical Engineering)
in the University of Michigan
2015

Doctoral Committee:

Professor Steven J. Skerlos, Chair
Assistant Professor Neil P. Dasgupta
Professor Mark S. Daskin
David A. Stephenson, Ford Motor Company
Assistant Professor Ming Xu

For Aai and Baba

ACKNOWLEDGEMENTS

As I look back at my educational journey up to this moment, it is the unconditional love, unyielding support, and untiring hard work of my parents and grandparents for which I am most thankful. It is from them that I learnt that compassion, patience, resilience, and tenacity are more powerful than anything else in helping one achieve personal goals – an invaluable lesson that has been particularly useful during these last five years. From my brother, I have learnt the importance of quiet observation in assessing, analyzing, and solving problems.

In addition to my family, I want to acknowledge the crucial support and encouragement that some of my close friends have provided during my graduate life. A big thanks to Deepti for being a true friend, and for always inspiring kindness and excellence in whatever I did, since our undergraduate days in Pune. I am immensely grateful to Devki for the countless hours of happiness and fun-filled conversations about art, music, and science that we have shared in the last two years – I have learnt so much about creativity and expression from her. Life as a new international student can be tough, but thanks to Sachin, the transition from one culture and lifestyle to another was relatively smooth, and I always felt that I could count on him in any situation. Neha, Mark, the Deshmukh family, Taylor, Hurf, Vikram, Vikrant, Vineet, Laura, Sam, and friends from the Combustion Lab, Ceramics Club, the BLUElab Living Building Challenge team, and Tau Beta Pi – I am so lucky to have had your company and friendship. You have all made my years in Ann Arbor really memorable.

I am incredibly thankful to my dissertation committee members for their generous support and valuable critique of my work. Mark Daskin's patient guidance on notations and thorough review of the mathematical framework has been instrumental in the successful implementation of the optimization model in this thesis. Neil Dasgupta's critical questions about the data, model assumptions, and policy implications have really helped refine the work in this thesis on carbon mitigation in the energy and transportation sectors. The discussions on allocation in life cycle assessment with Ming Xu contributed significantly to the validation of the environmental assessment framework discussed in the sections on CO_2 recovery. I am also grateful to Dave Stephenson and Andres Clarens for sharing their experimental work that contributed to the papers on supercritical CO_2-assisted machining. Thank you to Burak Ozdoganlar and his research group at Carnegie Mellon for sharing their experimental setup and data processing techniques, which contributed to the work on supercritical CO_2-assisted micromachining. I am very grateful to my EASTlab colleagues Katie Whitefoot, Vineet Raichur, Katie Caruso and Sherri Cook for sharing their knowledge and experience in their fields of expertise. I particularly want to thank Katie Caruso for her work on, and help with transitioning from the first iteration of the optimization model, and thank Karsten Kieckhäfer from TU Braunschweig for providing the data on vehicle value depreciation and battery technology cost projections.

And finally, to Steve Skerlos, for the pivotal role he has played in shaping the work presented in this entire thesis, and in my overall professional development over the last five years, all I can say is that I cannot thank you enough! I have learned so much about sustainability, design, and the guiding principles for conducting and evaluating sound research from you. But I believe this knowledge is just

incidental to having worked with you as my academic advisor. The lessons in servant leadership in the context of scholarship and education, and in being a good mentor, are what I value the most among all the skills and philosophies that I learnt during my apprenticeship with you. For all your support, and all your kindness, I humbly express my gratitude.

TABLE OF CONTENTS

LIST OF FIGURES

LIST OF TABLES

LIST OF APPENDICES

LIST OF ABBREVIATIONS

ACIDP	Acidification Potential (Life Cycle Impact Assessment)
B	Biomass (Electricity Generation Capacity)
BAU	Business as Usual
BEV	Battery Electric Vehicle
C	Coal (Electricity Generation Capacity)
CAFE	Corporate Average Fuel Economy (Standard)
CCS	Carbon Capture and Sequestration
CFC	Chlorofluorocarbon
cLCA	Consequential Life Cycle Assessment
CV	Conventional Vehicle
ECOTX	Ecotoxicity (Life Cycle Impact Assessment)
ENER	Energy Use (Life Cycle Impact Assessment)
EOR	Enhanced Oil Recovery
G	Geothermal (Electricity Generation Capacity)
GHG	Greenhouse Gas
GWP	Global Warming Potential (Life Cycle Impact Assessment)
H	Hydroelectric (Electricity Generation Capacity)
HCFC	Hydrochlorofluorocarbon
HEV	Hybrid Electric Vehicle
HRE	Heat Removal Efficacy
HRP	Heat Removal Potential
LCA	Life Cycle Assessment
LCI	Life Cycle Inventory
LE	Lubrication Efficacy
LN2	Liquid Nitrogen
MDEA	Methyldiethanolamine
MEA	Monoethanolamine
MMT	Million Metric Tons
MQL	Minimum Quantity Lubrication
MW	Megawatt
MWF	Metalworking Fluid
MWh	Megawatt-Hour
N	Nuclear (Electricity Generation Capacity)

NG	Natural Gas (Electricity Generation Capacity)
OZDP	Ozone Depletion Potential (Life Cycle Impact Assessment)
P	Petroleum (Electricity Generation Capacity)
PCO3	Propylene Carbonate
PFC	Perfluorocarbon
PHEV	Plug-in Hybrid Electric Vehicle
RESP	Respiratory Effects (Life Cycle Impact Assessment)
RO	Reverse Osmosis
S	Solar (Electricity Generation Capacity)
$scCO_2$	Supercritical Carbon Dioxide
SMOG	Smog Potential (Life Cycle Impact Assessment)
tCO_2	Metric tons of CO_2
UPW	Ultrapure Water
VOC	Volatile Organic Compound
W	Off-shore Wind (Electricity Generation Capacity)
WATER	Water Use (Life Cycle Impact Assessment)
WRI	World Resources Institute

ABSTRACT

Environmental and Economic Assessment of Carbon Dioxide Recovery and Mitigation in the Industrial and Energy Sectors

by

Sarang D. Supekar

Chair: Steven J. Skerlos

Anthropogenic carbon dioxide (CO_2) is a global pollutant that needs urgent control to prevent large-scale vitiation of ecosystems. Generally speaking, anthropogenic CO_2 emissions can be reduced through (1) CO_2 capture for long-term sequestration or use in other applications, (2) renewable and low-carbon energy sources and technologies, and (3) demand reduction of carbon-intensive services and products through reduced consumption and efficiency improvements. The first two approaches constitute the "supply-side" of carbon abatement measures, and are the focus of this dissertation in which I examine the environmental and economic attributes of CO_2 recovery and mitigation technologies in the U.S. industrial and energy sectors.

Starting by developing a comprehensive picture of the recovered CO_2 supply chain, this dissertation provides process-based emissions inventories for recovering and purifying CO_2 from

combustion flue gases and higher purity point sources for sequestration and use in industrial applications. The strong influence of CO_2 quality on the emissions, energy consumption, and costs of carbon capture found through this analysis warrants deeper scientific and economic analyses of carbon capture and sequestration as a carbon abatement option. To estimate the marginal emissions from use of recovered CO_2 in industrial applications, a market-based allocation methodology is developed in a consequential life cycle assessment framework, along with new greenhouse gas accounting procedures that incorporate reuse and sequestration as fates for CO_2. This methodology is presented with results from experimental studies on recovered CO_2-based metalworking fluids, and motivates further exploration of applications employing the thermal and chemical properties of CO_2 for pollution prevention and carbon abatement.

The dissertation concludes with an examination of carbon mitigation strategies from the standpoint of CO_2 prevention in the U.S. electric and automotive sectors. By creating a stock-and-flow model of the U.S. automotive and power generation fleets, and considering the evolution of all major technologies in both sectors in an optimization framework, cost-minimizing technology trajectories are identified, which collectively cut about 55 gigatons of CO_2 emissions by 2050. The analysis reveals that despite anticipated advancements and cost reductions in carbon abatement technologies with time, the technological costs of carbon abatement are likely to increase markedly with delay in climate-action.

CHAPTER 1

INTRODUCTION AND BACKGROUND

The United States (U.S.) is the world's second largest emitter of greenhouse gases (GHGs) behind China, and the largest emitter when considering population density. In 2011, the total U.S. GHG emission was equivalent to 6700 million metric tons of carbon dioxide (MMT CO_2 eq.). Serious climate change mitigation efforts within the U.S. over the next two to three decades will thus be critical in achieving meaningful short as well as long term reductions in greenhouse gas emissions. Figure 1.1 illustrates a decomposition of U.S. GHG emissions by economic sector, their sub-sectors, and fossil fuel type. The vast majority of U.S. GHG emissions (over 80%) come from the industrial sector, which includes fossil fuel supply chain industries, and the energy sector, which includes transportation. Furthermore, nearly 85% of the total U.S. GHG inventory is comprised of CO_2 emissions, although the impact of the more potent GHGs such as methane (CH_4), nitrous oxide (N_2O), and haloalkanes (CFCs, HCFCs, and PFCs) is not negligible. Thus, from a climate change mitigation standpoint, CO_2 is not only the most significant GHG of concern, but concurrently also the GHG with the largest potential for achieving meaningful reductions in emissions.

Several technology options exist on the supply side to achieve significant cuts in CO_2 emissions over the next few decades, in addition to conservation measures on the demand side of the services provided by these sectors. Since a majority of GHG emissions are from combustion of fossil fuels

(nearly 80% in the U.S.), carbon capture and sequestration (CCS) has been identified as potentially playing a significant role in stabilizing carbon emissions by many of the studies on GHG trajectory projections (IPCC, 2005; Pacala & Socolow, 2004; Stern, 2008; Williams et al., 2012). Captured CO_2 can be "stored" through geological, ocean, or mineral sequestration . It can also be used as a feedstock or solvent in niche industrial applications such as food and beverage manufacturing (Raventos, Duarte, & Alarcon, 2002), pharmaceutical manufacturing (Subramaniam, Rajewski, & Snavely, 1997), pH control, welding and solvent extraction (Aresta & Dibenedetto, 2007; DeSimone, 2002).

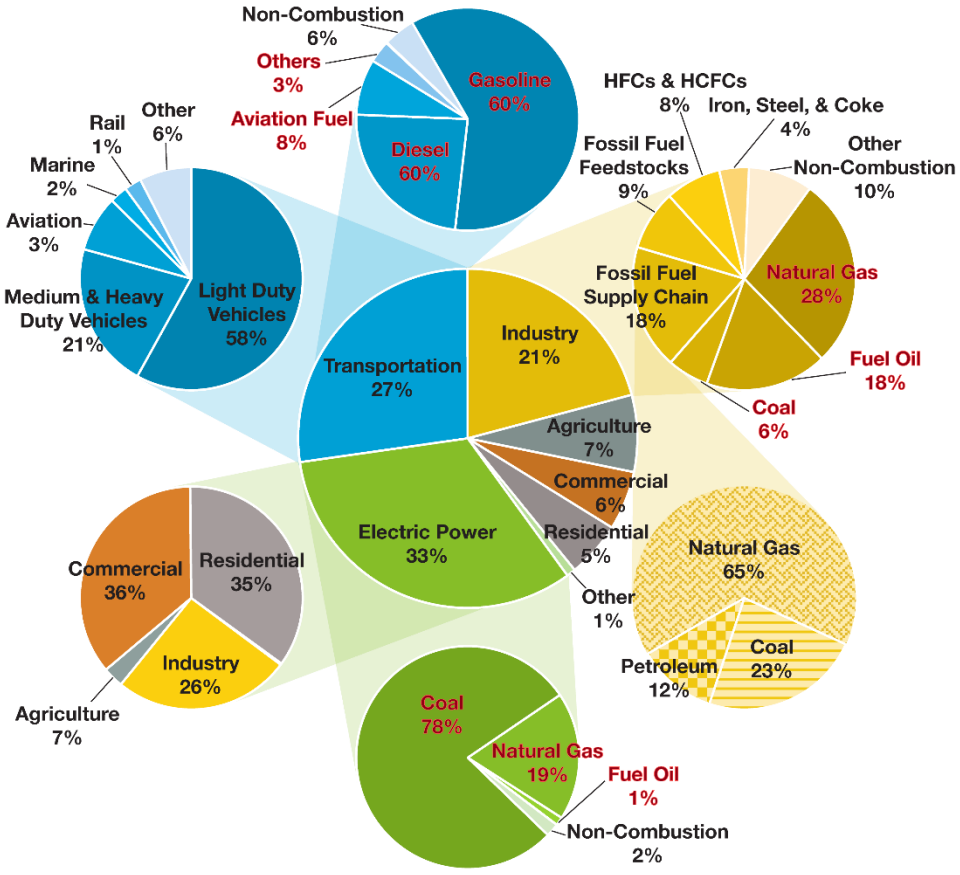

Figure 1.1. Breakdown of U.S. greenhouse gas emissions by sector and fuel type. Red typeface indicates greenhouse gases produced from fossil fuel combustion.

The capture of CO_2 is an energy intensive process that has its own carbon footprint among other environmental impacts. As in the case of biofuels (Clarens, Resurreccion, White, & Colosi, 2010), it is thus important to account for the energy and material inflows and outflows for CCS systems to evaluate the net reduction in CO_2. Several studies in the literature (Khoo & Tan, 2006; Koornneef, van Keulen, Faaij, & Turkenburg, 2008; Singh, Strømman, & Hertwich, 2011) have examined the life cycle environmental impacts of CCS from coal and natural gas power plants. These studies estimate that every metric ton of CO_2 captured leads to 200-350 kg of emissions on-site or from upstream processes depending on the fuel source, and separation method. The energy penalties assumed in these studies however only take into the basic steps of separation, compression, and refrigeration involved in CO_2 capture. They do not account for the steps that may be required to purify the CO_2 to a level that is safe (from an environmental and occupational standpoint) for transportation, as well as sequestration or use as an industrial feedstock. Thus, they do not account for the influence of the quality of CO_2 on the net energy balance and carbon footprint (Zapp et al., 2012), which may lead to underestimation of CCS impacts.

Furthermore, current greenhouse gas accounting guidelines lack a clear formulation of accounting strategies for either sequestered CO_2 (IPCC, 2005) or for CO_2 that is used as a feedstock or solvent in industrial applications. For instance, guidelines from the World Resources Institute (WRI) classify the direct and indirect emissions from an organization into three operational boundaries. Under this classification, Scope 1 emissions are the direct on-site emissions, Scope 2 emissions are those caused by electricity use, and finally Scope 3 accounts for emissions that occur upstream or downstream of the organization due to its activities. The key problem leading to concerns about proper accounting

in case of sequestration or reuse of recovered CO_2 is that Scope 1 does not distinguish between *generation* of greenhouse gases and their *emission* into the atmosphere. In the case of sequestration, this can lead to overestimation or underestimation of GHG inventories for instance, in cases where the CO_2 is removed from a fuel prior to combustion using gasification in one place, but is combusted for energy in another. In the case of reuse, the lack of distinction between generation and emission can lead to the CO_2 generated from a power plant to be counted towards the Scope 1 emissions of the recovered CO_2 end-user. In the event of some sort of a carbon penalty being levied in the future, the current accounting system will thus impose a penalty for reusing CO_2 before emitting it to the atmosphere, even if this reuse offsets large amounts of other Scope 3 emissions that are usually unmeasured and unreported.

For instance, the well known environmental and human health hazards associated with the use of conventional organic solvents and refrigerants have motivated the development of alternate CO_2-based technologies sans these hazards. CO_2 acts as a non-flammable and non-corrosive substitute due to its favorable chemical and physical properties. CO_2 has found application as a feedstock, chilling agent, or solvent in several industrial applications such as food and beverage manufacturing (Raventos et al., 2002), pharmaceutical manufacturing (Subramaniam et al., 1997), pH control, welding and solvent extraction (Aresta & Dibenedetto, 2007; Beckman, 2004). Most of the CO_2 used in the merchant market is recovered as a byproduct in ammonia, hydrogen, ethylene oxide, titanium dioxide and ethanol plants, and in rare instances from flue gases resulting from fossil fuel combustion.

One of the main barriers to adoption of recovered CO_2 in pollution prevention and sustainable manufacturing applications is the legitimate concern of industries to reduce their 'carbon footprints' which runs counter to the benefits of using CO_2. This concern emanates from two main factors: 1) the focus of current greenhouse gas accounting practice being on the point-of-release of GHG emissions rather than point-of-generation, and 2) the inability of the traditional (attributional) life cycle assessment methods to allocate causal emissions to a co-product or byproduct in a multiple output process. A market-based allocation and GHG accounting approach is thus needed to develop a more thorough understanding of the environmental impacts of recovered CO_2 for sequestration or reuse. This serves as the first motivation for the dissertation. As such, the first part of this dissertation aims to bridge this gap by using a process-based consequential life cycle assessment approach to (1) evaluate the impacts of CO_2 recovery and processing for sequestration and reuse, (2) develop a complementary GHG accounting methodology, and (3) evaluate the marginal environmental impacts of using recovered CO_2 in manufacturing applications to substitute current emission intensive products/processes.

For CO_2 sources where CCS could either be technologically or economically infeasible several other technology options have been identified in the literature. For instance, studies on the transportation sector (Bandivadekar et al., 2008; Grimes-Casey, Keoleian, & Willcox, 2009; McCollum & Yang, 2009; Rentziou, Gkritza, & Souleyrette, 2012) analyze the relative potentials of various powertrain technologies, fuels, and demand reduction strategies in reducing greenhouse gas emissions. Other studies focus on analyzing specific technologies such as plugin hybrids (Shiau et al., 2010), hydrogen fuel cell vehicles (Greene, Leiby, & Bowman, 2007), and biofuels (Kromer,

Bandivadekar, & Evans, 2010), demand reduction measures (Cervero & Duncan, 2006), or policy measures such as CAFE (Whitefoot & Skerlos, 2012) or carbon taxes (Morrow et al. 2010). Although each study focuses on selected strategies, and uses different scenarios for future demand and technology costs/emissions within those strategies, their common message is that the most effective approach to achieving deep cuts in GHG emissions is a combination of different strategies. Similarly, studies on GHG mitigation in the electric utility sector (Pacala & Socolow, 2004; Turton & Barreto, 2006; van Vuuren et al., 2009; Williams et al., 2012) have examined the role of various technologies and strategies such as renewables, biomass-derived fuels, nuclear, and natural gas using both top-down models (macroeconomic- or econometrics-based) and bottom up (technology- or engineering-based) models. These studies emphasize the importance of using a combination of strategies to achieve deep cuts in GHG emissions, and establish the value of both macroeconomic and technology-based models in designing effective climate change policies.

Studies in the literature that are based on macroeconomic models use some form of profit maximizing objective function to generate economic, technological and emission outcomes. Most of the bottom-up model-based studies on the other hand are simulation-based. While simulation-based models are valuable in understanding the range of possible technology and emission trajectories, they predict emission trajectories based on a spectrum of "what if" scenarios with projections for factors such as economic growth, demand growth, technology progression, fuel prices, fuel economy standards, and taxes or penalties. Although such analyses provide valuable insights for policy makers as to what *could* happen under the "what if" scenarios assessed, they may not provide adequate information on what *should* happen from the point of view of minimizing total societal cost. In this

regard, an optimization-based approach in bottom-up models is equally important for a concerted analysis with profit-maximizing macroeconomic models for developing effective policies. Such a model, together with a comprehensive sensitivity analysis of parameters such as fuel prices, which are known to cause variability in the outcomes of simulation-based models, can also predict a narrower and more confident range of technology and emission trajectories. This is an important requirement for informing public policy, and the lack of optimization-based bottom-up models in energy and transportation climate change policy analysis studies constitutes a critical gap in the published literature. This gap serves the second motivation for this dissertation.

The second part of the dissertation thus aims to start filling this gap in the literature by developing a bottom-up cost minimization framework. The model that implements the framework allows us to determine the techno-economic emission reduction potential of various currently available technologies, and predict emission trajectories in the auto and electricity sectors. The model considers lifetime use-phase costs borne by producers, consumers, and government over the analysis time horizon. To estimate GHG abatement costs and compare technology trajectories under emission regulated scenarios in both sectors, the model uses a reference business-as-usual case without emission regulations. The business-as-usual case is also assumed to operate under a cost-minimization framework.

CHAPTER 2

CARBON DIOXIDE RECOVERY

2.1 CO_2 SUPPLY CHAIN AND RECOVERY PROCESS

Figure 1.1 shows that fossil fuel combustion from various sectors and sub-sectors accounts for 94% of the total CO_2 emissions in the U.S, of which roughly 32% is from fossil fuel-based thermal power plants. To mitigate this large volume of combustion-related CO_2 emissions, technologies for various carbon capture and sequestration (CCS) options such as pre-combustion, oxy-fuel, and post-combustion capture have been explored, and their technological potential has been well established (IPCC, 2005). Four pilot CCS projects (< 30 MW) have been in operation in the U.S. since 2005, and five full-scale projects are either in the construction or planning phase (MIT CC&ST Program, 2014). Since post-combustion capture remains the "most common and commercially mature" technology option according to a recent study on the prospects of CCS technologies (Eide, 2013), it is studied in detail in this dissertation. In addition to CO_2 capture from fossil fuel combustion, there are opportunities for CO_2 recovery from industrial processes that generate CO_2 as a byproduct of chemical or biological processes. Examples of such processes are iron and steel production, cement production, ammonia production, and ethanol production, and together these non-combustion CO_2 sources in the industrial sector account for roughly 3.5% of the total U.S. CO_2 emissions.

The recovered CO_2 supply chain begins with a source of CO_2, which could either be an anthropogenic point source or a natural reservoir of CO_2. Nearly three quarters of the U.S. merchant market CO_2 capacity of 14.3 million metric tons (MMT) per year (Advanced Cryogenics, 2013) comprises of ammonia, ethanol, and hydrogen plants in which the CO_2 is produced as a co-product of chemical processes (hereafter referred to as co-product sources). A fifth of the total capacity comes from natural CO_2 wells, and the remaining is comprised of natural gas processing plants, post-combustion capture plants, and ethylene oxide and titanium dioxide manufacturing plants.

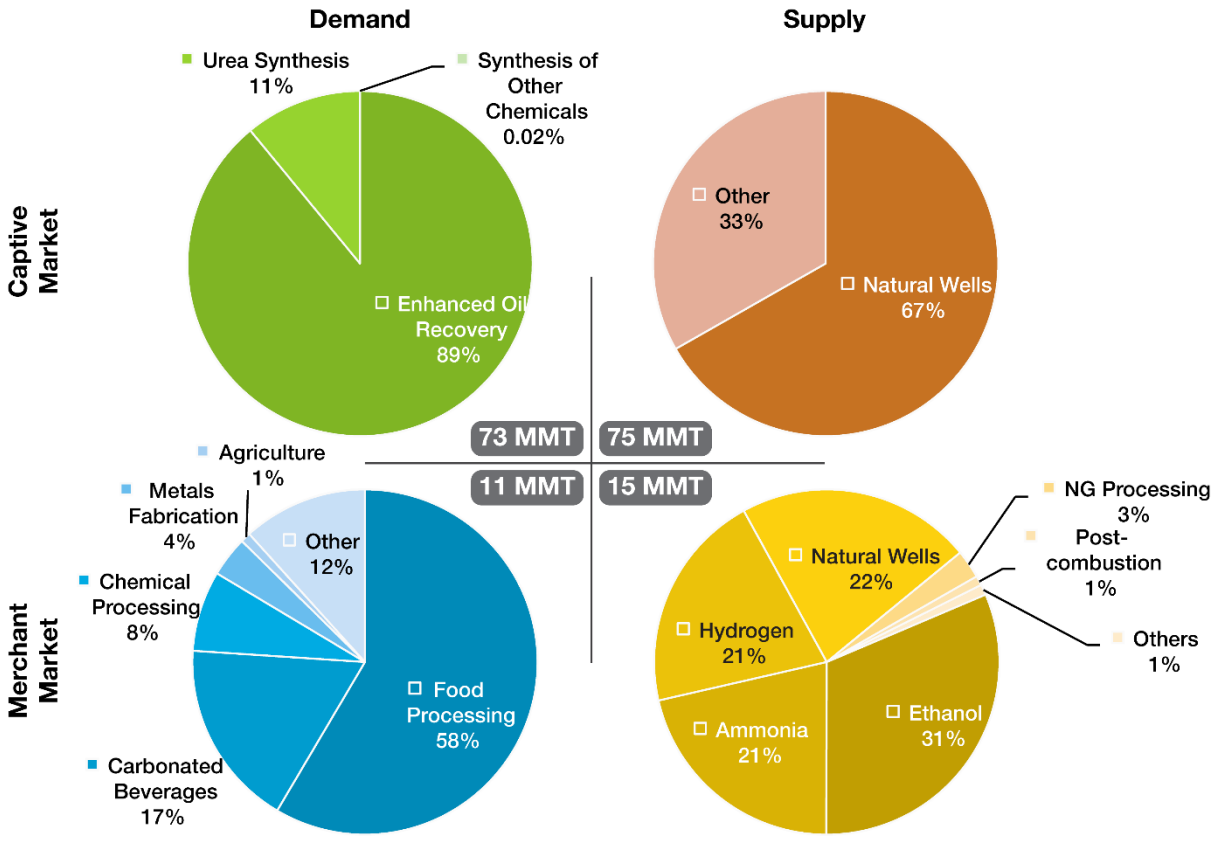

Figure 2.1. Recovered CO_2 merchant and captive markets in the U.S. broken down by source and end-use application.

It should be noted that this *merchant* market CO_2 capacity is in addition to the nearly 44 MMT CO_2 capacity (Meyer, 2007) used for *captive* market applications such as enhanced oil recovery (EOR), for which there exists a dedicated supply network largely of natural wells in parts of the Rocky Mountain, Appalachian, and Southwest regions of the U.S. Merchant markets are distinguished from captive markets, where the suppliers and buyers of a commodity are usually owned by the same entity and/or serve a niche industry in which the commodity is used in bulk. The recovered CO_2 supply and demand in the U.S. including merchant and captive sources is summarized in Figure 2.1.

The purity of the raw CO_2 feed stream from ammonia, ethanol, and hydrogen plants, is over 97% (v/v), while the purity of raw CO_2 from natural wells is between 80 - 98% (v/v) (Feinberg & Karpuk, 1990). Irrespective of the source, raw CO_2 streams contain various amounts of alcohols, water, alkanes, aldehydes, ketones, air gases, carbon monoxide, sulfides, mercaptans, and volatile organic compounds (VOCs) such as toluene, xylene, and benzene (European Industrial Gases Association, 2008) Impurities such as mercury, amines, and nitrogen oxides may also be present depending on the CO_2 source. Most merchant market CO_2 is purified to meet food grade quality of 99.9% (v/v) or higher, with a few plants producing 99.5% (v/v) pure industrial grade CO_2.

Recovery of CO_2 from combustion sources begins with separating the CO_2 from a mixture of other gases such as nitrogen and its oxides, sulfur compounds, oxygen, and water vapor present in the combustion flue gas. The separation process, which is akin to enrichment of CO_2 from the waste stream for further processing, nearly eliminates all dissolved gases leaving behind trace impurities. Separation is mainly carried out using a chemical absorption/stripping processes, although other

techniques such as membrane or cryogenic separation that can be used depending on the CO_2 partial pressure are also being explored. An aqueous solution of monoethanolamine (MEA) is most ubiquitously used solvent for absorption of CO_2, but other solvents such as methyl-diethanolamine (MDEA), potassium carbonate, and chilled ammonia are also used in certain plants (Kothandaraman, 2010). The key processes following separation are high-pressure compression to about 100 bar, cooling, scrubbing (if SO_2 content is more than 10 ppmv), drying, activated carbon treatment, and distillation if removal of non-condensable air gases such as oxygen is necessary for downstream conditions. These processes prepare the CO_2 for pipeline transportation to a geological storage facility without causing two-phase flow conditions in the pipelines, or environmental problems during or after storage. The purity of CO_2 obtained from these processes meets the industrial grade standard (≥ 99.5% v/v) set by EIGA (European Industrial Gases Association, 2008).

During the production of ammonia, hydrogen and CO_2 are produced as a result of natural gas steam reforming and water gas shift reactions. To facilitate the reaction between this hydrogen and nitrogen, an amine absorption-stripping process is used to remove the CO_2 from the gas stream. This CO_2 then serves as the raw feed gas for further processing. Similarly, in the refinery hydrogen production process, CO_2 is separated from hydrogen usually using pressure swing adsorption. The CO_2 stream, which still contains significant quantities of hydrogen, methane, and carbon monoxide, is reacted with oxygen in a furnace. After the heat from this exothermic reaction recovered, the CO_2 stream acts as the raw feed gas for further processing. In an ethanol production facility, the CO_2 off-gas released during the biomass fermentation process serves as the feed gas for further processing.

The purification train (and associated process conditions) used for recovery of CO_2 from both ethanol and ammonia production is identical due to the similar composition, temperature, and pressure conditions of the raw byproduct CO_2 feed gas, and follows the steps listed above for recovery and purification of CO_2 from post-combustion sources. The two significant differences here are that if the CO_2 is to be sold in the merchant market, it is only necessary to compress it to a pressure of about 21 bar, and since CO_2 is not in the supercritical state these conditions, a refrigeration step at the end of the purification process is required to facilitate easier and cheaper storage and transport of the CO_2. Recovery of CO_2 from hydrogen plants requires an additional catalytic oxidation step before purification with activated carbon since the upstream process of steam reforming of natural gas introduces a higher concentration of hydrocarbon and sulfur compounds than in CO_2 from fermentation. In the case of ammonia production, which also involves steam reforming of natural gas, the hydrocarbon and sulfur impurities are removed to a greater extent in the amine absorption process used to separate ammonia from CO_2 than the pressure swing adsorption process used to separate hydrogen from CO_2 (Yu, Huang, & Tan, 2012). A catalytic oxidation step is thus generally not required to recover industrial or high purity grade CO_2 from ammonia. It should be noted that CO_2 recovery plants are usually owned and operated by an independent firm that buys the raw CO_2 feed gas from the CO_2 producer. The firm designs the CO_2 purification and handling system for the purity grade that they wish to sell, which also governs the operating conditions and controls to which the various processes are calibrated. Operating the plant to obtain a different purity grade than what it is designed for can thus result in destabilization of the process and production losses.

The processes and operating conditions used to characterize the inputs and environmental emissions from the production of industrial and high purity grade CO_2 recovered were developed based on existing studies in the literature (Finley, 2006; Häring, 2008; Kohl & Nielson, 1997; Overcash, Li, Griffing, & Rice, 2007) and inputs from gas industry professionals and companies (Rushing, 2013; The Wittemann Company, 2012). Figure 2.1 through Figure 2.5 present the block flow diagrams for recovery and purification of CO_2 from all the major sources of CO_2. Appendix A provides a detailed summary of these steps and process conditions, and data sources used to characterize the process.

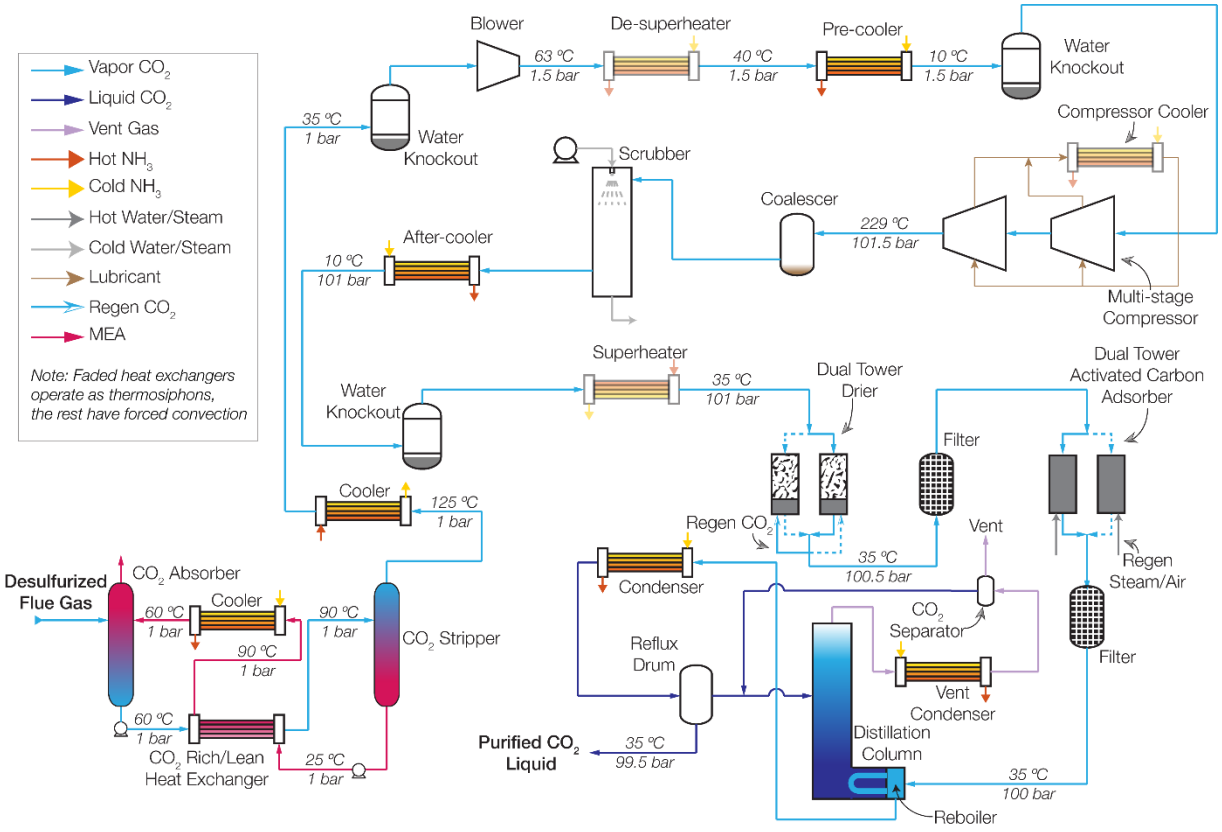

Figure 2.2. Block flow diagram of a typical recovery process for CO_2 from post-combustion flue gases as well as high-purity sources.

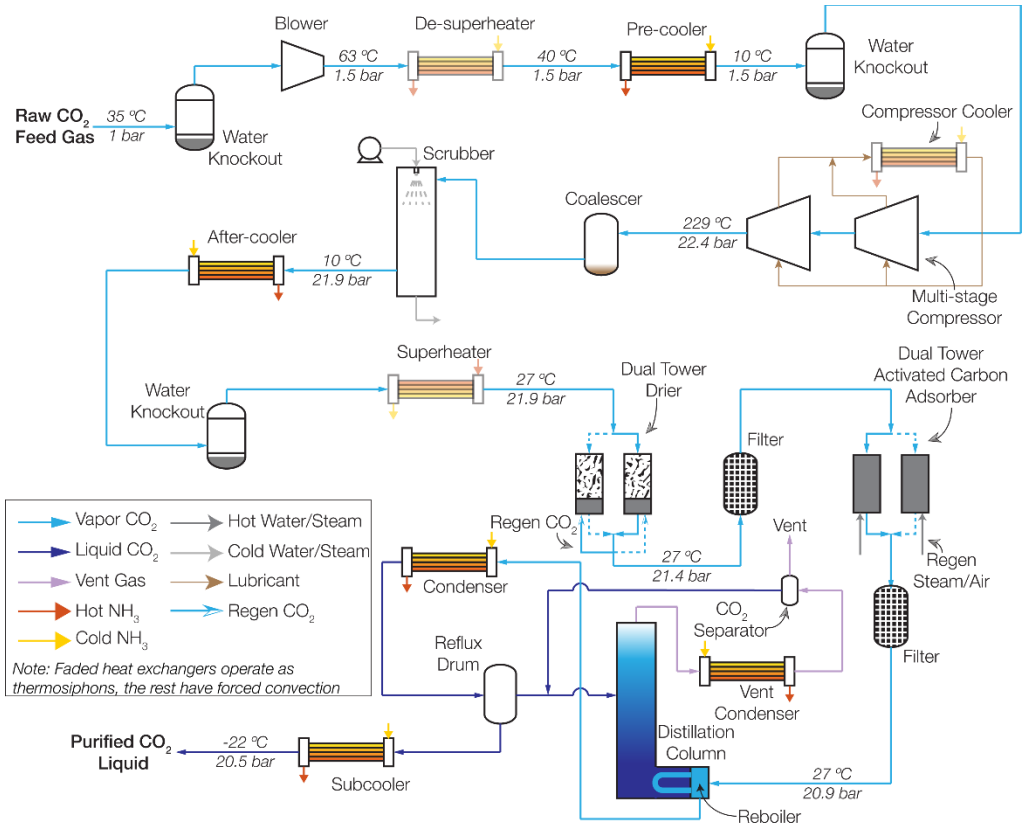

Figure 2.3. Block flow diagram for recovery of high purity grade CO_2 from ethanol or ammonia production.

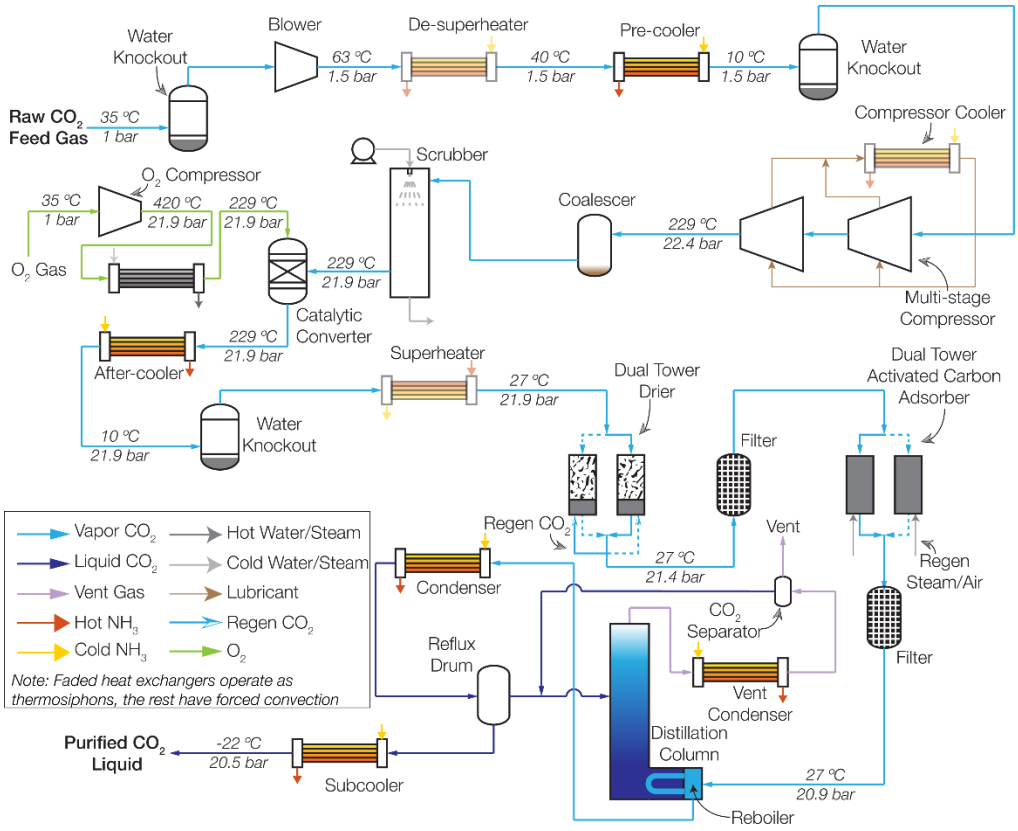

Figure 2.4. Block flow diagram for recovery of high purity grade CO_2 from hydrogen production.

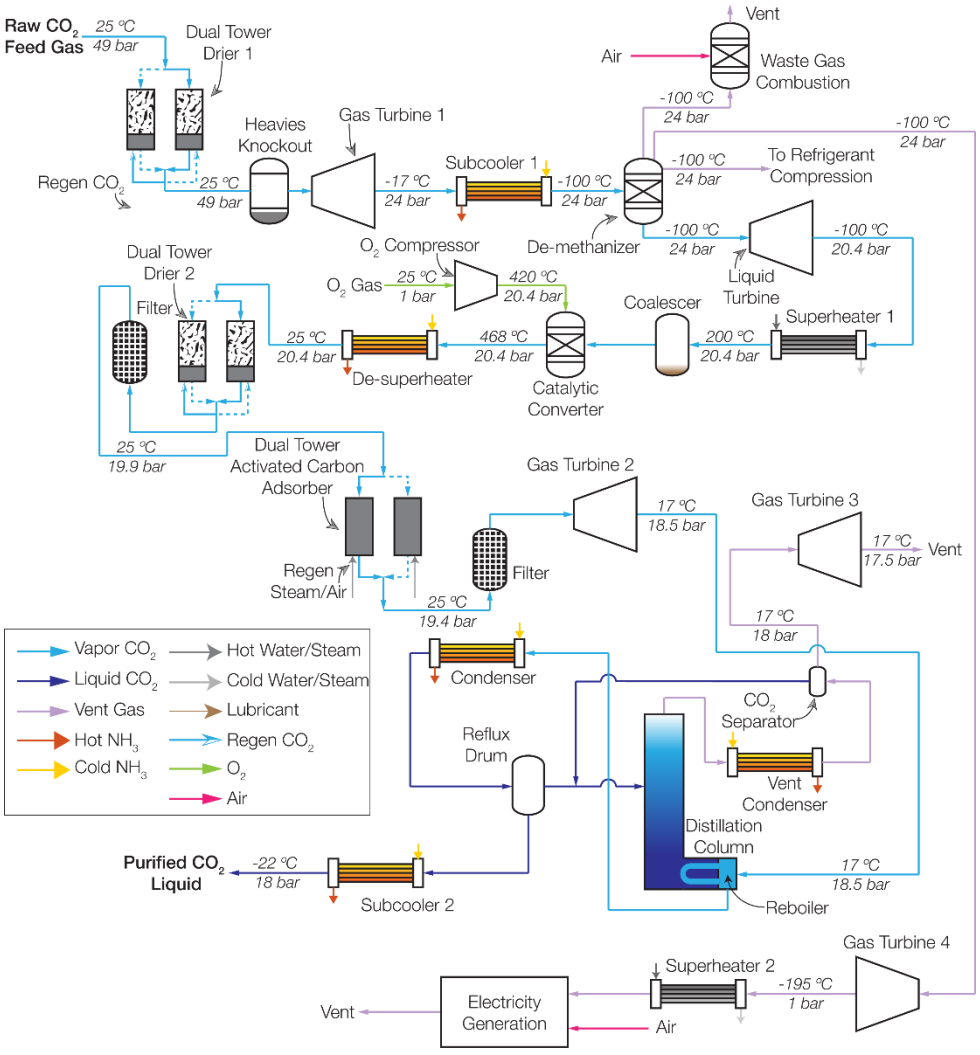

Figure 2.5. Block flow diagram for recovery of high purity grade CO_2 from natural wells.

Upstream emissions for bituminous coal and natural gas were obtained from the U.S. LCI database (National Renewable Energy Laboratory, 2012), and those for compressed air, oxygen gas, and desiccant were obtained from the Ecoinvent database (*Ecoinvent Database v2.2*, 2010). Emission factors for combustion of coal and natural gas were obtained from U.S. EPA's Stationary Combustion Emissions Report (U.S. Environmental Protection Agency, 1998a, 1998b). Degradation products of MEA and their respective concentrations in the vent gas of the stripper were adapted from Veltman, Singh, & Hertwich (2010) to match the heat rate adjustments in this analysis. Efficiencies of baghouse,

FGD, low-NOx, and scrubber units, and activated carbon bed for VOC and heavy metal removal were obtained from various sources in the literature (Karnib, Kabbani, Holail, & Olama, 2014; U.S. Environmental Protection Agency, 1998a; U.S. EPA, 2003a, 2003b). Production emissions of coconut shell GAC were developed using the process details outlined in Hung (2012). Infrastructure-related emissions such as those occurring from building of the recovery plant were excluded from the analysis. Useful heat recovered and fugitive emissions from processes within the CO_2 recovery plant were estimated using the guidelines provided by Jiménez-González, Kim, & Overcash (2000). Electric energy recovery in a CO_2 plant by expanding the pressurized process fluid or combustion gases in a gas turbine, wherever practical, was assumed to occur at a mechanical to electrical energy conversion efficiency of 40%. Consumption of materials such as activated carbon (Finley, 2006), desiccant (Finley, 2006), and scrubber sump water (Jiménez-González et al., 2000) which are replenished at frequencies roughly independent of CO_2 production rate, were estimated per unit of CO_2 assuming a recovery plant capacity of 300 metric tons CO_2/day.

2.2 PRODUCTION IMPACTS OF CO_2 RECOVERED FROM COMBUSTION SOURCES

Using the process details and operating conditions established for recovery of CO_2 from post-combustion sources, the production emissions inventory was developed for capture of CO_2 from a pulverized bituminous coal power plant (PC) and a natural gas combined cycle power plant (NGCC). Heat rates for both fuel sources were obtained from U.S. Energy Information Administration (2013b), and include parasitic energy consumption from pre-treatment processes such as flue gas desulfurization (FGD) and baghouse (for particulates removal). These pre-treatment steps are required, specifically for CO_2 capture from coal-fired plants since high concentration of sulfur and nitrogen oxides, together

with other acid gases such can lead to equipment corrosion and high rates of consumption of the chemical absorbent MEA. CO_2 capture from natural gas plants does not require such extensive pre-treatment due to insignificant concentrations of sulfur and particulate impurities in its flue gas. They however do require low-NOx burners, and the assumed heat rate for natural gas plants accounts for this. It should be noted that several coal and natural gas units across the U.S. already have such units installed to be in compliance with local and federal criteria pollutant control regulations, and thus the parasitic load form pre-treatment of flue gases is not ascribed to the recovered CO_2 in such cases.

Emission inventories were characterized using the U.S. EPA's TRACI 2.0 method (Bare, 2011). Impact categories chosen for analysis were global warming (GWP), ozone depletion potential (OZDP), smog formation (SMOG), acidification (ACIDP), eutrophication potential (EUTP), respiratory effects (RESP), energy use (ENER), and water use (WATER). Characterization factors for each pollutant examined were obtained from the Ecoinvent database (*Ecoinvent Database v2.2*, 2010). The emissions inventory includes upstream as well as on-site emissions.

The upstream, on-site, and total environmental emissions from the production of 1 MWh of electricity for sale from PC, PC-CCS, NGCC, and NGCC-CCS are shown in Appendix C, and Figure 2.6 shows the relative impacts from production of 1 MWh of electricity for sale from PC-CCS (top) and NGCC-CCS (bottom) plants relative to their non-CCS counterparts. PC-CCS and NGCC-CCS show a net reduction of about 48% and 61% respectively when considering upstream and on-site emissions in the nominal case examined (85% chemical absorption capture efficiency, raw gas purity post-MEA treatment 99%, solvent regeneration energy = 4850kJ/kg CO_2). These values are at least

25% lower than values reported in the literature on LCA of CCS plants. Energy penalty, defined as the additional amount of heat input required for maintaining the same level of electricity output from the power plant, is found to be about 32% for NGCC plants, which is closer to values reported in some studies (Kothandaraman, 2010), but the 124% energy penalty for coal plants is significantly higher than any values reported in the literature.

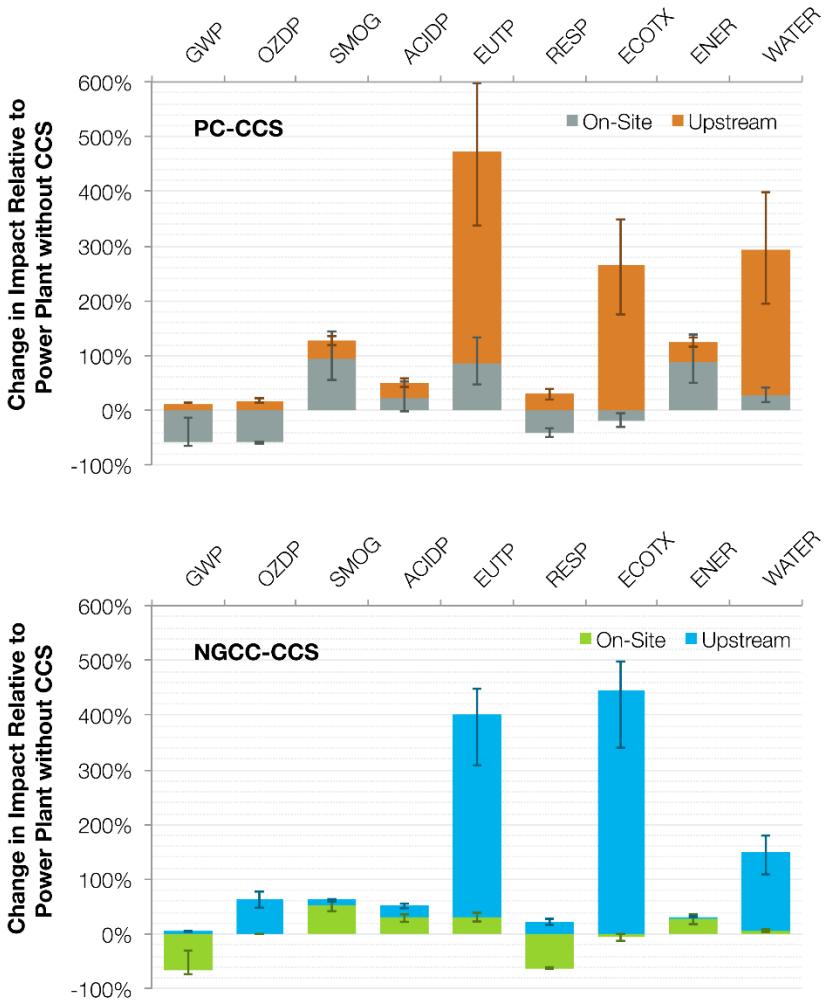

Figure 2.6. Comparison of environmental impacts from 1 MWh of electricity generation for sale in PC and NGCC plants with and without capture (CCS) units.

The life cycle analysis here assumes that the heat source for the recovery plant is coal instead of natural gas, which reduces the overall efficiency of the PC-CCS plant more than an NGCC-CCS plant

since the heating value of coal is lower, and its carbon content per unit of heat output is higher than natural gas. As such, energy penalty of a PC-CCS plant can be reduced by using a separate natural gas boiler for steam generation and heating in the capture plant, although this will change the mass-balance equation of the capture process from its form used for this analysis. Although the process conditions used for the LCA here are for producing industrial grade CO_2 (≥ 99.5 % v/v purity), the MEA absorption/striping process contributes to more than 90% of the total energy use in the capture plant per kg of CO_2 captured, and thus the results for ≥ 95.5 % v/v purity as recommended in the DYNAMIS CO_2 quality guidelines for CCS (de Visser et al., 2008) are not expected to be significantly different.

A potential benefit often associated with of post-combustion CCS plants is the added removal of particulate matter, sulfur oxides, and nitrogen oxides emitted to the atmosphere during the various recovery and purification steps in the capture plant. The resulting reduction in concentrations of these pollutants can reduce smog formation, eutrophication, and harmful respiratory effects. However, our life cycle analysis shows that apart from the noticeable reduction in particulates and respiratory effects likely in NGCC-CCS plants, the overall reduction of the remaining pollutants when considering both upstream and on-site emissions are marginal, or in fact negative, meaning the emissions of these pollutants actually increase due to the CCS process. Increase in SMOG is primarily due to the fugitive emissions of MEA and its degradation products, formaldehyde and acetaldehyde, which are all strong smog forming chemicals. Further, fuel supply chains of both coal and natural gas have high eutrophication and ecotoxicity impacts, and thus the significant increase in fuel consumption

overshadows any marginal on-site reduction in the emission of pollutants contributing to these impact categories.

Thus from a life cycle point of view, NGCC-CCS plants can potentially be a more viable carbon abatement option than PC-CCS, unless advanced combustion technologies such as gasified coal and oxy-fuel combustion, or advanced CO_2 separation techniques such as membrane separation are able to reduce the energy penalty of coal-fired CCS plants significantly. Despite differences in the magnitude of CO_2 reduction and energy penalties for PC-CCS and NGCC-CCS, this overall conclusion of the analysis agrees with the recommendations provided in other CCS LCA studies in the literature (Khoo & Tan, 2006; Singh et al., 2011) over the highly uncertain techno-economic feasibility of coal-fired CCS plants.

2.3 RECOVERED CO_2 IN INDUSTRIAL APPLICATIONS

Carbon dioxide is used as a feedstock, chilling agent, and solvent in industrial applications such as food and beverage manufacturing (Raventos et al., 2002) pharmaceutical manufacturing (Subramaniam et al., 1997) polymer and chemical synthesis (Desimone & Tumas, 2003) pH control, welding, solvent extraction (Aresta & Dibenedetto, 2007) and heat pumps (Volkswagen AG, 2013). These applications are a part of the roughly 11 million metric ton (MMT) CO_2 merchant market in the U.S. (Garvey, 2014) where suppliers (merchants) sell their CO_2 on the free market to buyers. Merchant markets are distinguished from captive markets, where the suppliers and buyers of a commodity are usually owned by the same entity and/or serve a niche industry in which the commodity is used in bulk.

Emerging technologies that are based on merchant market CO_2 have been reported to significantly reduce toxicity, energy consumption, and water consumption in numerous industrial applications, receiving over a dozen green chemistry awards in the last two decades ("Green Chemistry Award 2014 Winner," 2014, *Kenneth G. Hancock Memorial Award*, 1999; U.S. EPA, 2014). Such applications, while presently small in volume, can potentially be another way of directly reducing CO_2 emissions by "fixing" the CO_2 to other non-greenhouse gas products, or by using the CO_2 in CO_2-based technologies to substitute energy and carbon intensive processes and thereby offsetting those emissions.

In the United States and other industrialized countries, the merchant market CO_2 used in such industrial applications is recovered as a co-product from the production of ammonia, hydrogen, ethanol, ethylene oxide, and titanium dioxide, as well as from natural gas processing plants, natural CO_2 wells, and in rare instances from the flue gases of fossil fuel combustion. A notable barrier to achieving higher adoption rates of CO_2-based technologies is a concern companies have in regards to increasing their 'carbon footprint' by embracing these technologies. This concern emanates from two main factors: 1) the focus of current greenhouse gas (GHG) accounting practice on the point-of-release of GHG emissions rather than point-of-generation, and 2) the inability of attributional life cycle assessment (LCA) methods to allocate causal emissions to a co-product in multiple output processes such as those used to produce CO_2.

2.3.1 Greenhouse Gas Accounting Practices

The World Resources Institute (WRI) and World Business Council for Sustainable Development (WBCSD) provide guidance and a comprehensive standard for businesses and organizations regarding how to measure, classify, and report GHG emissions (*Corporate Value Chain (Scope 3) Accounting and*

Reporting Standard, 2012, *Product Life Cycle Accounting and Reporting Standard*, 2011, *The Greenhouse Gas Protocol - A Corporate Accounting and Reporting Standard*, 2004). Since its creation in 2001, the WRI GHG protocol has served as a polestar for corporations and countries who have adopted a systematic GHG accounting system ("Looking Back on 15 Years of Greenhouse Gas Accounting," 2014). Companies define their organizational boundary by using an 'equity' or 'control' based approach. There are operational boundaries within these organizational boundaries, which divide emissions into three 'Scopes.' Scope 1 accounts for GHG releases that occur from operations owned or controlled by the company. Scope 2 accounts for emissions arising from the generation of electricity that is purchased by the company and its entities. Scope 3 encompasses indirect emissions outside Scope1 and Scope 2 (e.g., upstream production processes associated with materials procured by a company).

The guidelines from WRI regarding operational boundaries clearly distinguish between direct (Scope 1) and indirect (Scope 3) GHG emissions from an organization. However, as identified by WRI itself (*The Greenhouse Gas Protocol - A Corporate Accounting and Reporting Standard*, 2004) there is yet to be a clear consensus on an appropriate set of accounting guidelines on reuse and sequestration. Recent studies in the literature advance this discussion by focusing on certain aspects of GHG accounting for reuse and sequestration such as defining baseline scenarios (*Federal Greenhouse Gas Accounting and Reporting Guidance*, 2010; McCormick, 2012) and ascertaining the allocation along a product or commodity value chain (Brandão et al., 2012; McCoy, Pollak, & Jaramillo, 2011). However, we believe that accounting for emissions from reuse and sequestration would be fundamentally easier to address if the accounting standard distinguished between the *generation* of

GHGs and the *emission* of GHGs into the atmosphere. Since current protocols do not make this distinction, the CO_2 generated by an ammonia manufacturer will, for instance, be reported under its Scope 3 indirect emissions, while being counted towards the Scope 1 emissions of the end-user of this CO_2 such as a CO_2-based decaffeination plant. This reduces Scope 1 emissions of the CO_2 generating plant, potentially encouraging more generation of CO_2 from it. It may alternatively reduce incentives to purchase recovered CO_2 if, for instance, a carbon penalty is levied on companies based on their Scope 1 emissions, even if this reuse offsets large amounts of other unreported Scope 3 emissions (via process substitution). Classifying the emission of recovered CO_2 as a Scope 1 emission for the end-user firms might also create an incentive for those firms to recover their own CO_2 emissions that are likely to be dilute and/or highly contaminated with impurities, leading to high costs. Such forces may create disincentives for firms to adopt CO_2-based technologies in emerging sustainability applications, as suggested by Vogtländer, Brezet, & Hendriks (2001) who note that placing penalties on recovered materials by treating firms that eventually scrap the material as creators of the scrap ultimately reduces the incentive for using recovered materials.

2.3.2 Limitations of Allocation Practices in Life Cycle Assessment

CO_2 sold in the merchant market for various applications is largely recovered as a co-product of chemical processing plants that produce chemical commodities such as fertilizer and hydrogen as their primary product. In LCA practice, the allocation of environmental impacts from such processes with multiple co-products is nebulous at best (Guinée et al., 2011) and contentious at worst (Ekvall & Finnveden, 2001). Kim & Overcash (2000) suggest allocation factors based on ratios of physical and/or economic attributes of products and co-products. They also caution against blind

interpretation of their impact-assessment results, and advise that allocation methods be in accordance with the goal and scope of the study, since molecular weight or specific volume of a co-product have little relevance to the environmental burdens created by that co-product. For instance, in the case of ammonia production, a ton of ammonia output from the plant creates about 1.18 tons of CO_2 as a co-product (Jiménez-González et al., 2000), and so a mass-based allocation would attribute over half the impacts of ammonia production to the production of CO_2 co-product. Clarens, Zimmerman, Keoleian, Hayes, & Skerlos (2008) acknowledge this problem with mass-based allocation for recovered CO_2, stating that it is unreasonable given the disparity between the economic value of CO_2 and ammonia, and use price-based allocation instead. However, as noted by Overcash, Li, Griffing, & Rice (2007), there is temporal variability in prices, and prices fluctuate in manners irrelevant to environmental emissions.

When considering how to allocate environmental impacts to recovered CO_2, we contend that the key question is whether the demand for CO_2 as a co-product influences the production of the primary product. We also note the essential requirement to fully account for the emissions and resource use that occur during the process of recovering and purifying the co-product CO_2 so as to meet quality and regulatory requirements. To address these issues, we first discuss the supply- and demand-side dynamics of the merchant CO_2 market as well as the primary products that generate CO_2 for the merchant market. We then apply consequential LCA (cLCA) to allocate generation emissions to CO_2 as a market-driven product, and add the emissions associated with purifying the CO_2 and delivering it to an end-user. Finally, we present guidelines to account for emissions that may be created or avoided from processes that are affected by the reuse of CO_2.

2.4 CONSEQUENTIAL LCA FRAMEWORK FOR RECOVERED CO_2

A market-based allocation method for recovered CO_2 examines the processes and/or technologies that are affected on the margin due to a change in the demand for recovered CO_2. These affected processes are generally referred to as 'marginal processes', and a detailed set of guidelines for identifying marginal processes in general, and determining co-product allocation for multi-output processes is provided in B. P. Weidema, Frees, & Nielsen (1999). Based on these guidelines, the marginal processes for CO_2 in general are those involved in purification and delivery of CO_2 as discussed in the following paragraphs.

2.4.1 Merchant CO_2 Supply Chain

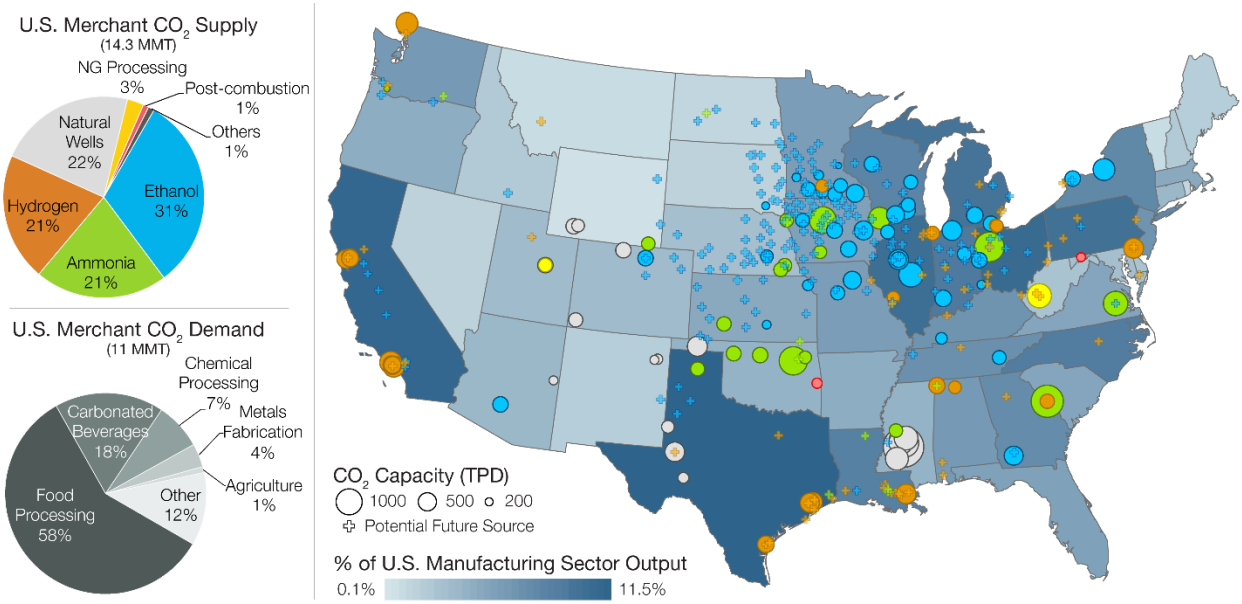

Figure 2.7. Sources and end-use markets of merchant market CO_2 in the United States. CO_2 source colors on the map correspond to CO_2 source colors on the CO2 supply pie chart (Supekar & Skerlos, 2014).

Figure 2.7 shows the U.S. merchant CO_2 sources by type and location, along with the market shares of major CO_2 using industries (Aresta, 2003; Garvey, 2014). As discussed earlier, CO_2 processing at a typical recovery plant involves compression of the raw CO_2 to about 20 bar pressure,

followed by a series of purification steps to remove impurities, and finally refrigeration to about -22 °C. Refrigerated CO_2 is stored in tanks on-site at the recovery plant, sent to a dry ice production unit within the plant, or dispatched immediately for delivery depending on the quantity and form of the final product demand. On-site storage capacity for liquid CO_2 is usually limited to about two to three days of production volume. Merchant CO_2 is usually delivered using tanker trailers. Deliveries by distributor firms to high-volume end-users, which constitute the largest merchant market-share, are made using bulk containers that can hold up to 250 tons of CO_2. Deliveries to low-volume end-users are made using trucks containing dewars or cylinders.

2.4.2 Market-based Allocation

Storing recovered CO_2 is expensive due to the high costs of the heavily insulated or refrigerated containers required for maintaining the recovered CO_2 at its delivery pressure and temperature. Merchant market CO_2 production is thus roughly equal to the demand (since inventory is small) and a recovery plant is operational only to the extent that there is a demand from the merchant market. Furthermore, CO_2 plants are generally located near areas of demand. Figure 2.7 shows the locations of existing suppliers of merchant CO_2 relative to the U.S. manufacturing sector economic activity ("Manufactures Summary by State: 2009," 2012; NAICS Association, 2014) where manufacturing sector output includes applications such as food processing and refrigeration, beverage carbonation, production of carbonates, bicarbonates, and pharmaceuticals, and shielding gas in welding. In 2013, the demand for merchant CO_2 was about 11 MMT (Garvey, 2014), which means that, on average, about 25% of the total production capacity of 14.3 MMT was unutilized. Installing CO_2 recovery plants at existing ammonia, ethanol, and hydrogen plants without CO_2 recovery (BBI International,

2014; Pacific Northwest National Lab, 2014; U.S. Geological Survey, 2012b) (marked by + in Figure 2.7) can alone add about 52 MMT of annual merchant CO_2 capacity. A marginal increase in the demand for CO_2 in the near-term will thus likely be met by the surplus regional capacity. However, order-of-magnitude increases in CO_2 demand would require the installation of additional recovery plants.

Using the detailed set of allocation rules for consequential LCA described in Weidema (2000), we propose that under a market-based allocation, only those emissions that occur from marginal technologies or processes should be ascribed to recovered CO_2. For CO_2, the marginal processes are compression, purification, refrigeration, storage, and transportation of the raw CO_2 feed gas obtained from ammonia, ethanol, and hydrogen plants, as long as CO_2 demand is less than the installed production capacity. The marginal production processes for CO_2 from natural wells are purification, refrigeration, and transportation of recovered CO_2.

To determine whether any part of the production emissions of ethanol, ammonia, and hydrogen qualify as marginal processes for recovered CO_2 production, we examine the production volumes of these commodities as recommened by Weidema (2003) Based on publicly available data (BBI International, 2014; U.S. Energy Information Administration, 2013c; U.S. Geological Survey, 2012a), it is notable that the markets for ethanol, ammonia, and hydrogen have been stable or increasing over the last decade. In contrast, the CO_2 merchant market has been relatively stable over this period (Baker & Garvey, 2013; Garvey & Turley, 2011, 2012; Garvey, 2010, 2014; U.S. Census Bureau, 2005), with existing CO_2 recovery plants operating on average at 65 - 80% of their production

capacity. Additionally, the market value of ethanol, ammonia, and hydrogen is at least four, eight, and forty times higher respectively than the highest purity grade of merchant CO_2 (USD 150/ton).

Based on this market information, it can be assumed that marginal increases in the demand for CO_2 are highly unlikely to affect the production of ethanol, ammonia or hydrogen. Therefore, in the framework of Weidema (2000) ethanol, ammonia, and hydrogen are the 'determining co-products' of their respective production process, where the determining co-product is the co-product whose market demand governs the operation, resource use, and emissions from the plant. The framework would designate CO_2 as the 'dependent co-product' since its production depends on the production of the determining co-product. Following Weidema (2000) none of the production emissions of the determining co-products should be ascribed to the dependent co-product. Furthermore, the processes used to separate CO_2 from the determining co-product are not marginal processes since they would be operational even without the demand for CO_2. In the case of CO_2 obtained from natural wells, CO_2 itself is the determining co-product, and emissions from its extraction from the wells should be included in the production emissions.

2.4.3 Product Substitution

If a CO_2-based technology provides an identical or a higher value (from an economic or regulatory standpoint) than an existing product/process in a certain market, it will likely substitute the existing product/process. This is refered to as product substitution. For instance, manufacturing firms choosing to adopt supercritical CO_2 metalworking fluids (rapidly expanding sprays of $scCO_2$ and dissolved vegetable oil) (Clarens et al., 2008) over water-based metalworking fluids may offset the life cycle resource use and emissions associated with a functionally equivalent quantity of water-based

metalworking fluids. We established in the previous section that the use of CO_2 in the merchant market is highly unlikely to affect ammonia production and its associated emissions. In this case, where the dependent co-product (CO_2) capacity is only partially utilized, Weidema, (2000) recommends that emissions from all marginal processes, as well as credit from avoided emissions should be ascribed to the dependent co-product. This is because although the volume of CO_2 (*dependent* co-product) produced is governed by the production of ammonia (*determining* co-product), the volume of CO_2 utilized is governed *solely* by the demand for CO_2. If no product substitution occurs due to the use of CO_2 in the end-use application of interest, as is the case with beverage carbonation, there will be no offset emissions, and the credit from displaced emissions will be zero. It should be noted that regardless of product substitution, the recovery of CO_2 generated during ammonia production for use in CO_2-based technologies, over 99% of which eventually emit all the recovered CO_2 to the atmosphere, does *not* reduce the CO_2 footprint of ammonia production since this CO_2 would have been emitted to the atmosphere even in the absence of a market for recovered CO_2.

The current (2014) demand for CO_2 is met without fully utilizing the installed capacity, and shortages in regional supply are generally met by neighboring regions since transportation is fast and inexpensive (at the expense of increased transportation emissions). As such, a marginal increase in demand for CO_2 is unlikely to affect the supply to existing and established markets. A significant increase in regional CO_2 demand in a new end-use application may sometimes lead to CO_2 shortages and thus *short-term* product substitution in established local CO_2 markets, but this phenomenon is likely to be reversed by additional CO_2 supply from neighboring regions or new CO_2 recovery plants. If new CO_2 capacity is added to meet the demand, the emissions from production and installation of

any capital equipment or technologies needed in the new recovery plants will be ascribed to the recovered CO_2. Any increased emissions from quantity-dependent (as opposed to fixed) operation and maintenance processes occurring due to marginal increases in demand should also be ascribed to the recovered CO_2. However, over the lifespan of the plant, these emissions are likely to be insignificant in comparison to the marginal production emissions per unit of recovered CO_2.

2.5 IMPLICATIONS FOR GREENHOUSE GAS ACCOUNTING

The proposed market-based allocation for recovered CO_2 hinges on the distinction between GHG generation and GHG emission in accounting practice so as to avoid double counting or leakage of recovered CO_2. To distinguish between GHG generation and GHG emission, we propose to divide Scope 1 for direct emissions into three sub-scopes: 1a, 1b, and 1c. Under this new scheme, Scope 1a accounts for GHGs *generated and emitted* within the organizational boundary of a firm, Scope 1b accounts for GHGs *generated but not emitted* within the organizational boundary, and Scope 1c accounts for GHGs *emitted but not generated* within the organizational boundary. A vast majority of firms either emit all the GHGs they generate, or recover any GHGs generated for use and eventual emission within their own organizational boundary. The direct emissions from such firms will fall entirely under Scope 1a. However, for firms such as ammonia plants that partially recover their CO_2 for sale on the merchant market will report emissions under both Scope 1a and 1b. Additionally, if a firm imports GHGs as a material input (and not embodied emissions) into their organizational boundary, and if these GHGs are eventually released into the atmosphere, the firm will report such GHG emissions under Scope 1c.

Further, if operations such as mineral carbonation (von der Assen, Jung, & Bardow, 2013) or production of biofuel feedstocks (Cherubini & Strømman, 2011; Clarens et al., 2010) within a firm fix GHGs during any step, the fixing or 'anti-generation' will be reported as a negative value in Scope 1b. Under the revised set of accounting rules, the direct GHG emissions for which a firm is responsible are the sum of emissions under Scopes 1a and 1b. Reported Scope 1c emissions, if any, will be added to Scopes 1a and 1b emissions if and only if the Scope 1c GHGs were generated specifically for use within the firm, as is the case with CO_2 obtained from natural wells.

Scopes 2 and 3 that account for indirect emissions from electricity use and product value chain respectively remain unchanged from their current definition (*Corporate Value Chain (Scope 3) Accounting and Reporting Standard*, 2012). As with current GHG accounting guidelines, the revised Scopes are additive, i.e. they can be added to obtain the total GHG inventory of a firm. Thus, assuming that they maintain a clear inventory of primary product sales, fuel consumption, sales of recovered GHGs, if any, and sources of purchased GHGs, if any, firms can calculate their carbon footprint with the data they have. Figure 2.8 illustrates the proposed accounting and market-based allocation framework.

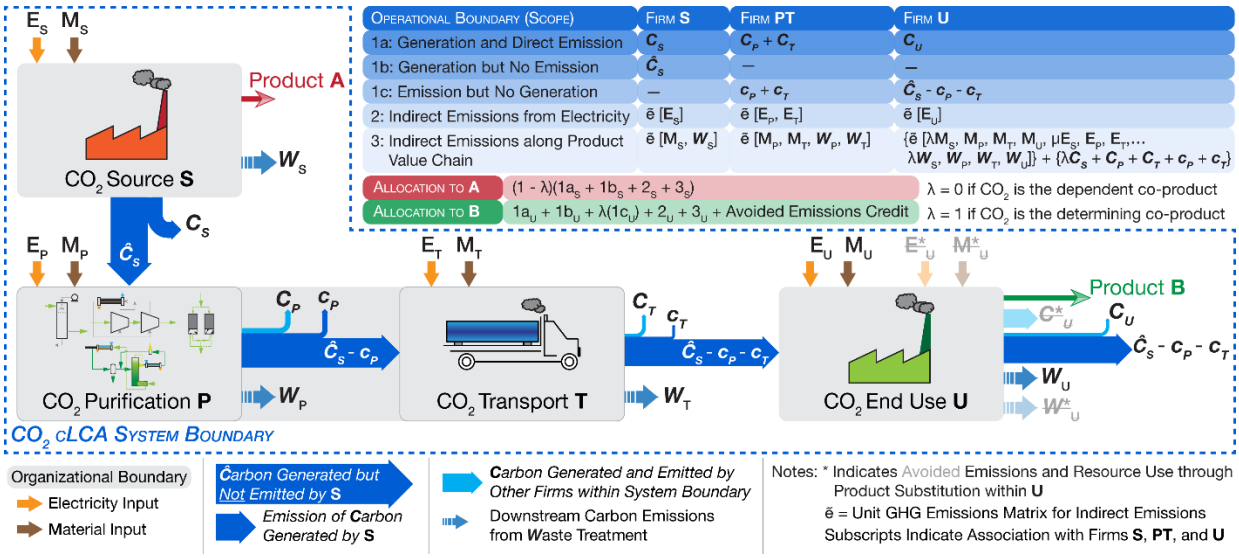

Figure 2.8. Market-based allocation and GHG accounting framework for CO_2 as a commodity (Supekar & Skerlos, 2014).

Having a separate classification for generated GHGs not emitted (Scope 1b), and for direct emission of GHGs generated elsewhere (Scope 1c) eliminates the ambiguity about whether such emissions should be reported under the current definition of Scope 1 or Scope 3. Scopes 1b and 1c thus allow greater transparency in the tracking and reporting of emissions by preventing firms within a product's value chain from either double-counting or discounting their direct emissions. For instance, CO_2 generators such as firm **S** in Figure 2.8, whose primary product market is unaffected by the market for its recovered CO_2 co-product, cannot claim a reduction in the carbon footprint of their primary product **A**. At the same time, it will also ensure that users of CO_2 recovered from natural reservoirs are accountable for the extraction and eventual emission, if any, of the recovered CO_2 to the atmosphere.

2.6 PRODUCTION IMPACTS OF MERCHANT CO_2

The allocation method and system boundaries described in Figure 2.8 were used to estimate the market-driven production emissions associated with recovering CO_2. Inventories for the CO_2 production from ethanol, ammonia, hydrogen, and natural well sources were developed using published literature and inputs from practitioners in the gas industry. Inventories were developed for two ranges of purity grades that are defined as industrial (≥ 99.5% v/v) and high purity (99.9 - 99.999% v/v). This distinction is made based on whether or not the purity grade requires removal of trace air gases such as oxygen, nitrogen, and argon, with the grades requiring distillation categorized as high purity. Appendix A provides a summary of the grades, processes, and the main process operating conditions used to calculate production emissions of recovered CO_2.

Under the market-based allocation proposed here, the emission of compounds such as hydrocarbons or heavy metals that are already present along with CO_2 in the waste stream of co-product sources, is not allocated to recovered CO_2. However, the emissions of hydrocarbons, heavy metals, and other compounds that occur from fossil fuel combustion within the recovery plant are allocated to the recovered CO_2. Appendix A also provides a detailed explanation of various assumptions and data sources in the analysis.

Figure 2.9 reports the impacts of producing 1 metric ton of high purity CO_2, which are divided into four categories: upstream impacts of inputs, impacts from electricity use, on-site impacts from combustion of fossil fuels within the recovery plant, and on-site impacts not related to combustion such as those from fugitive emissions of ammonia refrigerant and natural gas. Appendix B lists the operating conditions and parameters, and the sources and assumptions that are used to estimate the

impacts shown in Figure 2.9, and also provides the range of high and low values for these conditions and parameters.

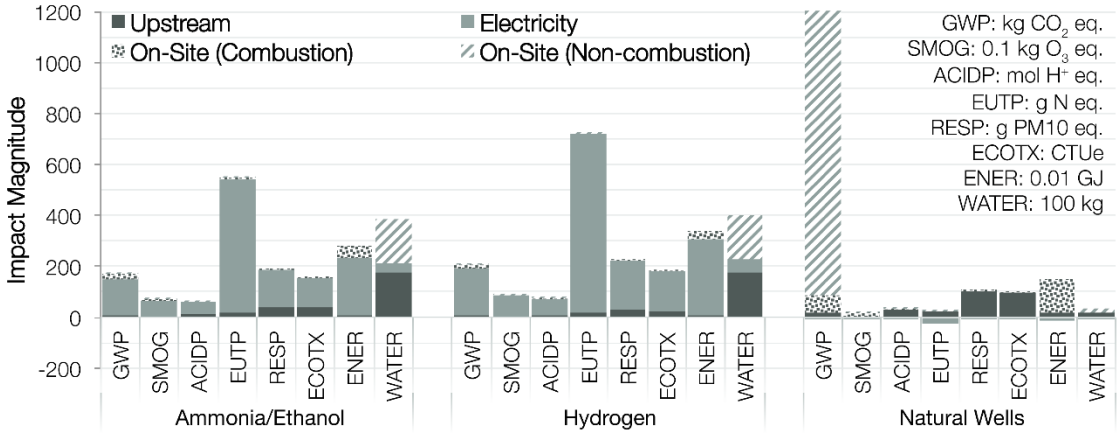

Figure 2.9. Production impacts of 1 metric ton of high purity merchant CO_2 recovered from various sources. Units for impact magnitude for each impact category are indicated in the top right corner of the figure. CO_2 from co-product sources has a lower carbon footprint than CO_2 from natural wells (Supekar & Skerlos, 2014).

Figure 2.9 also shows that recovered CO_2 has a global warming footprint six times less than CO_2 from a natural reservoir. This result may seem somewhat counterintuitive since the CO_2 from co-product sources is often be viewed as an industrial pollutant, whereas the CO_2 from wells may be perceived as a natural resource. However, the CO_2 from natural wells is extracted solely for sale to end-users who eventually release the CO_2 to the atmosphere. Natural wells contain CO_2 that is nearly at 50 bar pressure, which is much higher than the typical merchant market delivery pressure of 18 bar. The pressure energy stored in the CO_2 is harnessed by using the high pressure CO_2 to run a series of gas or liquid turbines that in turn generate electricity. Additional energy is recovered by combusting methane and other hydrocarbons mixed in small quantities with the CO_2 in the wells. As a result, the electricity consumption of recovered CO_2 from natural wells is often negative, which means that the recovery plant can feed electricity into the grid and the total energy consumption is less than half that

of CO_2 recovered from co-product sources. This offset is modeled in this work using emissions from U.S. average electricity production as a proxy for marginal electricity production emissions. However, when performing an application-specific cLCA of CO_2 from natural wells, we recommend using marginal electricity production data, particularly for wells in the U.S. given the large variance in the electricity grid mix of the states where these wells are located (WY, UT, CO, NM, and AZ). Lower energy consumption of CO_2 from natural wells does not translate to lower global warming potential, as its CO_2 footprint is 6 times larger than CO_2 from co-product sources (see Figure 2.9).

Although cheaper to operate due to lower energy costs, the capacity of natural CO_2 wells to supply the merchant market is quite restricted due their commitment to the large captive market of enhanced oil and natural gas recovery. CO_2 used in EOR applications has lower purity requirements, and more importantly, over 90% of the recovered CO_2 is sequestered in the oil and gas wells once they are depleted beyond the point of commercial viability (Melzer, 2012). Therefore from a GHG mitigation perspective, it is best for natural wells to be only used for EOR applications, if at all. Further, any expansion in capacity of merchant CO_2 should only come from co-product sources that currently do not capture their CO_2, which are generally located near to current and potential industrial areas within the U.S. to minimize transportation and storage emissions.

In the production of CO_2 from co-product sources, electricity use accounts for the largest share of impacts. Increased electricity use for production of high purity grades also increases impacts in other categories besides energy use, particularly global warming, smog, acidification, ecotoxicity, and water

use. Combustion of natural gas for steam or heat generation in the recovery plant is the other major contributor to greenhouse gas emissions and energy use.

2.6.1 Effects of Purity on Merchant CO_2 Production Emissions

Electricity, natural gas, and water use scale up non-linearly as initial purity decreases and final purity increases. For instance, energy use, which includes electricity, heat, and steam, can be almost three times higher for supercritical fluid extraction grade CO_2, which is ≥ 99.998% (v/v) pure compared to industrial grade CO_2, which is ≥ 99.5 % (v/v) pure. This increase in energy use is in part due to the higher regeneration time, gas flow rate, and temperature required for carbon and desiccant beds. Additionally, a distillation step is required to remove trace air gases, which uses the final purified dry CO_2 as reflux to selectively cool and condense the pure CO_2 out of the mixture of CO_2 and trace air gases. The higher the reflux ratio is for a given distillation tower design, the higher will be the distillation efficiency or purity of the final CO_2 product.

Supercritical fluid extraction grade CO_2, which should have an oxygen concentration of less than 2 ppmv, may require a reflux ratio up to 0.3 (Häring, 2008). This reflux ratio corresponds to a loss of about 25% in the yield of the final purified CO_2 product. Similar yield losses occur in the drying step, where about 8% of the dried CO_2 product is used for desiccant bed regeneration (Kohl & Nielson, 1997). Vent losses of up to 1% in other parts of the purification train also contribute to yield loss indirectly, and together with CO_2 product use for bed regeneration and reflux, increase the impacts of recovering highly pure CO_2. For instance, the energy required to compress a kg of CO_2 in the feed gas from atmospheric pressure to about 18 bars is about 294 kJ assuming adiabatic and mechanical efficiencies to be about 80%. However, due to yield losses in subsequent steps, only about 70% of

this CO_2 will be recovered as final product. Therefore compression energy increases to 412 kJ/kg CO_2 output. Appendix B provides the range of operating conditions and process parameters used to estimate the environmental emissions and resource consumption from the different commercially relevant grades of CO_2 recovered from the major merchant market sources. Appendix D lists the range of environmental impacts and process inputs for different commercially relevant grades of CO_2 recovered from the major merchant market sources. These values are estimated using the range of key parameters such as initial purity, carbon bed regeneration steam flow rate, and distillation reflux ratio shown in Appendix B. Figure 2.10 uses values from Appendix D to provide a comparison between the impacts associated with recovering various grades of CO_2 from different sources, and the range within which these impact values lie.

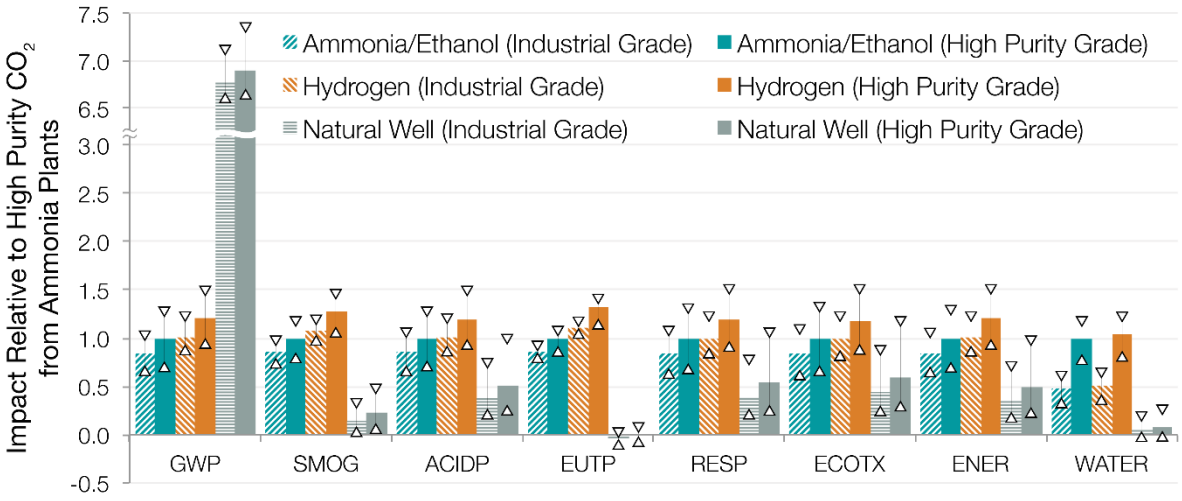

Figure 2.10. Range of environmental impact values for industrial and high purity grades of CO_2 from major merchant market sources. △ and ▽ respectively indicate lower and upper bounds for each impact value relative to the corresponding impact value for high purity grade CO_2 from ammonia plants (Supekar & Skerlos, 2014).

2.6.2 Market-Based vs. Attribute-Based Allocation

To illustrate the difference between market- and attribute-based allocation methods for recovered CO_2, we analyzed the ammonia production process, which generates 1,180 kg of CO_2 per ton of ammonia produced (Jiménez-González et al., 2000; Overcash et al., 2007). Ammonia is manufactured through a series of energy and resource intensive steps that include desulfurization and subsequent steam reforming of natural gas, shift conversion of carbon monoxide, removal of CO_2 using amines, compression, and refrigeration. The CO_2 removed using an amine wash is then sent to the recovery plant for further processing. Using production impact data for liquid ammonia (Argonne National Laboratory, 2012; Jiménez-González et al., 2000), the impacts of the CO_2 recovery and purification process calculated in this study, and prices and sales of ammonia and merchant CO_2 (Baker & Garvey, 2013; Farm Futures, 2014; Rushing, 2011; U.S. Geological Survey, 2012a), we estimated the production impacts of recovered CO_2 using mass-, revenue-, and market-based allocation methods associated with LCA.

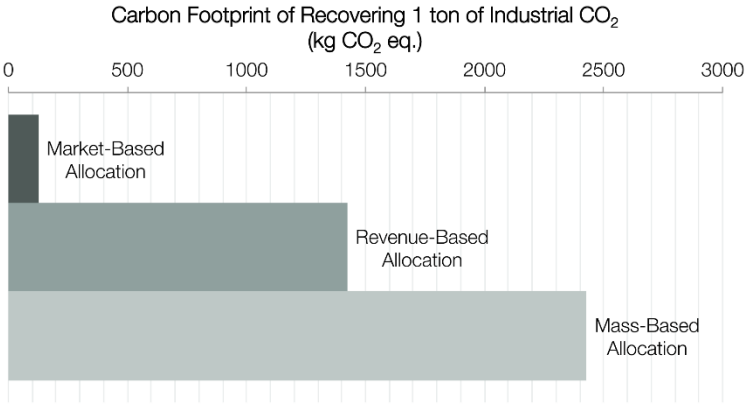

Figure 2.11. Comparison of GWP of 1 ton of recovered CO_2 from ammonia/ethanol source using market-based allocation and attribute-based allocation methods.

Revenue- and mass-based allocation methods estimate that global warming potential of the production of recovered CO_2 is 11 and 19 times higher than estimates made using market-based allocation as shown in Figure 2.11. This is because in addition to sharing the environmental burdens of the determining co-product ammonia, attributional allocation also ascribes the global warming impact from its ultimate atmospheric emission to the recovered CO_2. Correspondingly, estimates of energy use with revenue- and mass-based allocation methods are 1.75 and 9 times higher than market-based allocation. It should be noted that although a price of $100/ton and $650/ton have been assumed for CO_2 and ammonia in this analysis, the prices of ammonia may have a regional and monthly variation of as much as 25%.

2.6.3 Merchant CO_2 Transportation

Over 99% of merchant market CO_2 is delivered to consumers using heavy-duty diesel trucks, with less than 1% transported by rail and pipelines (Svensson, Odenberger, Johnsson, & Strömberg, 2004). Transporting 1 ton of cargo over 1 km in a heavy-duty diesel truck on average leads to 333 g CO_2 eq. of GHG emissions, which includes emissions from diesel combustion (National Renewable Energy Laboratory, 2012) and the diesel fuel supply chain (*Ecoinvent Database v2.2*, 2010). Table 2.1 lists transportation impacts values per ton-km for all TRACI categories examined.

A CO_2 end-user will typically determine the amount of on-site storage capacity needed for recovered CO_2 based on how critical the service provided by recovered CO_2 is, the rate of CO_2 consumption, the cost of maintaining the CO_2 storage, and the CO_2 transportation costs. Furthermore, the demand for CO_2 may be met by any of the producers closest to the end-user, although the likelihood of a producer supplying CO_2 increases with a decrease in the distance between

the producer and end-user. Together, these factors will determine the total mass of CO_2 transported, the distance traveled during each trip between the producer and the end-user, and the number of trips made by the delivery truck per functional unit of the end-use application. If the CO_2 is transported in bulk in a heavy-duty truck, the impact factors per unit mass per unit distance over which the CO_2 is transported shown in Table 2.1 can be used to calculate the transportation impacts. These impacts include upstream emissions from the diesel fuel supply chain (*Ecoinvent Database v2.2*, 2010) and the tailpipe and fugitive emissions from heavy-duty truck transportation. National Renewable Energy Laboratory, 2012).

Table 2.1. Impacts of transporting 1 metric ton of recovered CO_2 over a distance of 1 km using a heavy-duty diesel truck.

Impact Category	Value	Unit
GWP	3.33×10^{-1}	kg CO_2 eq.
SMOG	4.38×10^{-2}	kg O_3 eq.
ACIDP	7.59×10^{-2}	mol H^+ eq.
EUTP	8.21×10^{-5}	kg N eq.
RESP	3.28×10^{-4}	kg PM10 eq.
ECOTX	1.75×10^{-1}	CTUe
ENER	7.98×10^{-1}	MJ
WATER	5.11×10^{-2}	kg

For example, let us assume that a certain end-use application requires a supply of 5,000 gallons of CO_2 every month from the nearest supplier located 250 km away. The recovered CO_2 is at 20 bar pressure and -22 °C temperature. At this temperature and pressure, 5,000 gallons of CO_2 weighs about 19,700 kg, and so the supplier is likely to transport the recovered CO_2 in a 20 ton. Assuming an empty back-haul of the tanker from end-user to the supplier facility, and the worst-case scenario of

identical fuel consumption during front-haul and back-haul, the transportation emissions can be calculated using the following equation.

$$\text{Transportation Emissions} = \left\{2 \times e_{unit} \times D \times M_{CO_2}\right\} \times N$$

.....Equation 2.1

Here, e_{unit} is the emission or impact per tkm of transportation, D is the one-way distance from the supplier to the end-user in km, M_{CO_2} is the mass of CO_2 transported in tons, and N is the number of trips per functional unit of the end-use application. It should be noted that the emission factors in Table 2.1 are for one-way freight transportation, and account for the gross weight of the tanker and the vehicle. Applying Equation 2.1 to the example above and using impact per ton per km values from Table 2.1, the global warming impact over a year from the transportation of recovered CO_2 to this particular end user is calculated as follows.

$$2 \times 0.333 \frac{\text{kg } CO_2 \text{ eq.}}{\text{tkm}} \times \frac{250 \text{ km} \times 19.7 \text{ tons}}{\text{trip}} \times 12 \text{ trips} = 39{,}361 \text{ kg } CO_2 \text{ eq.}$$

.....Equation 2.2

Producers that supply the end-user with recovered CO_2 are in most cases likely to be in the proximity of the end-user. However, which specific producer will supply CO_2 to a particular end-user of interest will be determined by the regional availability of CO_2, which in turn will be governed by demand for CO_2 from other end-users and the demand for the primary or determining co-product in the case of byproduct CO_2 sources. Regional supply and demand for CO_2 thus not only influences the transportation distance D, but also the causal emissions from the production of CO_2 due to its demand in a particular end-use application. To quantify this uncertainty in transportation and production (cradle-to-gate) emissions, one can perform a Monte Carlo analysis. Such an analysis

would need to estimate or assume the selection probability for all CO_2 producers in the regional supply chain of the CO_2 end-user of interest.

Since the supply of merchant CO_2 has developed around centers of demand, most CO_2 end-users have access to a CO_2 supplier within 200 miles of their location. However, transportation distances in capacity constrained areas may be as high as 800 miles, in which case GWP, SMOG, and RESP impacts from transporting 1 ton of CO_2 are higher than producing it by a factor of over two, eight, and two, respectively. Further, consumers can choose to work with their CO_2 suppliers to source their CO_2 from a specific location for a higher price. There is already precedent for this in the use of high purity CO_2 in applications such as supercritical fluid chromatography and nuclear reactor cooling (purity requirement ≥ 99.998%). These high purity sources are typically ammonia production or natural gas processing plants, or natural CO_2 wells due to a significantly lower concentration of heavier hydrocarbons in the raw gas, which are difficult and expensive to remove. This 'preferred source' may be located outside the regional supply network. We thus recommend examining *both* the regional CO_2 supply network, and any application-specific quality requirements to estimate the production and transportation emissions of merchant CO_2 in a particular end-use application.

2.7 CONCLUSIONS

We recommend that the prevalent practice of ascribing just one set of impact values to all commercially available CO_2 based on attributional allocation methods be replaced with a consequential approach that takes into account the market and product quality factors as discussed in this article. Furthermore, to estimate the cradle-to-grave impacts of recovered CO_2 in a new or existing end-use application, we recommend examining the existing regional CO_2 market and any special CO_2

sourcing requirements related to quality or other factors, as well as any product substitutions that may occur within the life cycle of interest. As researchers, businesses, and governments continue exploring the viability of CO_2 recovery for sequestration, chemical synthesis, and industrial pollution prevention, it will become increasingly important to produce more accurate estimates for causal environmental emissions associated with CO_2 production using market-based allocation methods and accounting distinctions between generation and emission.

CHAPTER 3

CASE STUDIES ON RECOVERED CARBON DIOXIDE IN POLLUTION PREVENTION APPLICATIONS

3.1 SUPERCRITICAL CO_2 METALWORKING FLUIDS IN MACRO-SCALE MACHINING

Metalworking fluids (MWFs) are essential coolants and lubricants used in material removal and deformation processes to improve manufacturing productivity by increasing process throughput and tool life. MWFs are ubiquitous in the machine tool industry, with estimates of world-wide annual consumption reported by Cheng, Phipps, & Alkhaddar (2005) to be in the billions of liters. Typically formulated as either as straight-lubricants, or more typically as aqueous (water-based) emulsions/solutions, MWFs have high life cycle costs from their acquisition, maintenance, and disposal, with estimates ranging between 10 and 17% of total metals manufacturing costs as reported in Klocke & Eisenblätter (1997). Straight-lubricants, such as mineral oils, fatty oils, esters, chlorinated paraffins or a combination of two or more of these compounds, are generally used in friction dominated processes such as grinding, forming and thread tapping.

Aqueous MWFs can contain over a dozen chemicals such as extreme pressure (EP) additives, surfactants, biocides and defoaming agents. Aqueous MWFs are widely used in chip forming processes such as turning, milling and drilling. They are highly effective in transporting chips out of the cutting zone and dissipating heat from the bulk of the workpiece and tool. However, aqueous MWFs create

health risks for workers, such as dermatitis, infection, and cancer. Biological growth within MWFs, along with the buildup of metal particles and oils, deteriorates manufacturing performance and ultimately necessitates disposal. Disposal of untreated MWFs can lead to significant oxygen depletion and nutrient loading in surface waters, further posing environmental risks. Aqueous wastes can also carry heavy metals from manufacturing (e.g., cobalt and lead) into the environment.

Recent research has sought to develop environmentally-benign MWFs with higher performance in manufacturing, thus enabling faster machining without undermining part quality and tool life. Substitutes to aqueous MWFs have been investigated over the past two decades. Minimum quantity lubrication (MQL) technology is one of the most prominent alternatives to conventional MWFs. MQL delivers sprays of lubricants or emulsions in compressed air at about 0.6 to 1 MPa pressure. Developed in the 1990s, MQL has since been researched as a feasible means to deliver lubrication to a variety of machining operations on a number of engineering materials as discussed in a comprehensive review of the technology provided by Weinert, Inasaki, Sutherland, & Wakabayashi (2004). In practice, oil-in-air MQL has largely found acceptance in automotive applications such as crankshaft oil-hole drilling and machining of aluminum engine and transmission prismatics. However, because of its limited capability to remove heat, its adoption in processes such as rough turning and milling, grinding and deep-hole drilling is limited. From an environmental standpoint, MQL has been shown to have lower environmental impact than aqueous MWFs in a comparative life cycle assessment by Fratila (2010).

Liquid nitrogen (LN_2) has been researched as another alternative to aqueous MWFs in applications involving high heat generation and high cutting temperatures. Despite its limited lubrication potential LN_2 has demonstrated the potential for reduced tool wear and improved surface finish relative to aqueous MWFs as reported by Wang & Rajurkar (2000), and relative to MQL as demonstrated by Pusavec, Hamdi, Kopac, & Jawahir (2011) in the machining of recalcitrant materials such as titanium alloys that have poor thermal diffusivities. However, insufficient heat removal at the tool-workpiece interface (due to poor cutting zone penetration) arising from rapid vaporization of LN_2 as reported by Nguyen, Zarudi, & Zhang (2007), and thermal warping from non-uniform cooling of the workpiece have restricted use of LN_2 to certain specific material-process combinations in the industry. Although using larger flow rates of LN_2 can alleviate warping, large flows may be an impractical solution for large components due to high supply costs and high environmental impacts associated with separating and liquefying nitrogen which are outlined in Li & Chou (2010). Further, machining of certain materials such as nickel alloys with LN_2 may require an auxiliary oil line to be added to provide sufficient lubrication. Due to these limitations, LN_2 MWF systems have been limited to pilot scale implementations and are yet to be adopted in production operations in the machining industry.

El Baradie (1996) showed that high-pressure gases could be effective coolants and since then alternative MWFs such as carbon dioxide gas, cooled compressed air, and oxygen have been explored in research. However, these alternatives have found relevance only in certain niche applications and cannot be extended to real-world production-line manufacturing. Considering the limited market adoption of MQL (an excellent lubricant system) and LN_2 (an excellent cooling system), it can be hypothesized that a widespread alternative to conventional MWFs will need to serve *both* as a heat

removal agent and as a lubricating agent, without a trade-off between those two functions. Presently, only flood application of aqueous MWFs at high flow rates has the capability to deliver both cooling and lubrication to a satisfactory level, which is why their use in the industry remains widespread despite their costs and adverse health and environmental effects.

Clarens, Hayes, & Skerlos (2006) proposed an alternative MWF based on supercritical carbon dioxide ($scCO_2$). Carbon dioxide is a reclaimed material that is non-toxic and has excellent solubility for aliphatic and most aromatic hydrocarbons such as vegetable oils above its critical point (critical temperature = 31.2 °C, critical pressure = 7.38 MPa) as shown by Hyatt (1984). It allows for precise control of solvent concentration through pressure and temperature control and, as such, $scCO_2$ has been utilized as a solvent in pharmaceutical and polymer industries, dry-cleaning, semiconductor devices cleaning and automotive component coating as discussed in DeSimone, (2002). Tom & Debenedetti (1991) show that the rapidly propagating mechanical perturbation resulting from the rapid expansion of $scCO_2$ and oil produces a homogenous and finely dispersed spray of dry ice and frozen oil particles a few microns in size. As a result it can be hypothesized that $scCO_2$-MWF sprays can provide sufficient heat removal *and* lubrication to replace conventional MWFs in a greater variety of machining operations than MQL or LN_2.

In this paper we examine the efficacy of $scCO_2$-MWFs over a wide range of metalworking processes to assess their candidacy as an alternative to conventional MWFs. We first hypothesize that $scCO_2$-MWFs perform as well as or better than conventional MWFs in the heat removal function. To test this hypothesis, we perform titanium turning, compacted graphite iron (CGI) milling and A390

aluminum drilling experiments to evaluate flank wear. Arsecularatne, Zhang, & Montross (2006) establish flank wear to be determined by temperature-based phenomena, such as diffusion, adhesion and delamination, and thus flank wear serves as a pragmatic measure to evaluate the heat removal efficacy of MWFs in the tool-workpiece combination examined in this study. Second, we hypothesize that $scCO_2$-MWFs can produce a better lubricating medium than straight lubricants or aqueous MWFs. To test this hypothesis, we perform thread cutting and thread forming experiments on 1018 steel and 2024 aluminum, respectively. Thread cutting and thread forming have been chosen because they are friction dominated and cannot be performed without a good lubricant such as straight oil.

In section 3.1.1, we describe the experimental setup and materials used in this research. Section 3.1.2 discusses the experimental results and their relationship to the hypotheses listed above. Section 3.1.3 concludes with a summary of the key findings regarding $scCO_2$-MWFs as a potential alternative to aqueous MWFs.

3.1.1 Experimental Investigations: Methods and Materials

3.1.1.1 Supercritical CO_2 MWF Delivery

Supercritical CO_2-MWFs can be delivered as a rapidly expanding solution of either $scCO_2$ and a lubricant, or only $scCO_2$. Figure 3.1 shows the solubility curve for CO_2 and soybean oil. The shaded area on the right indicates the phase with $scCO_2$ containing dissolved lubricant ($scCO_2$-DL) and the shaded area on the left indicates the phase where $scCO_2$ is dissolved in the lubricant ($scCO_2$-XL). Table 3.1 lists the characteristics of these two phases as applied in this research, along with the possibility of not including oil in the supercritical carbon dioxide ($scCO_2$-NDL). In this research the lubricant used is a vegetable oil (soybean or canola). Figure 3.2 shows images of the $scCO_2$-DL (left)

and $scCO_2$-XL (right) sprays being expanded at identical pressures through nozzles of same diameter. The notable difference in quantity of oil in $scCO_2$-DL and $scCO_2$-DL phases can be seen from the difference in spray lengths, where a longer spray indicates higher oil content leading to a larger number of agglomerates of frozen oil and dry ice.

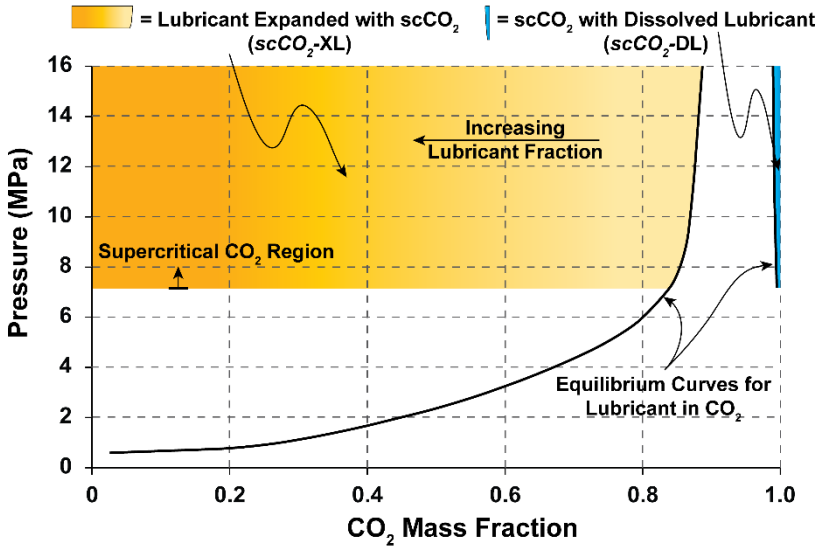

Figure 3.1. Solubility curve for soybean oil in CO_2 at 35 °C (adapted from Ndiaye et al. (2006) and Clarens, MacLean, Hayes, Park, & Skerlos (2009)) showing the two phases of $scCO_2$-MWF delivery when a lubricant is present in $scCO_2$.

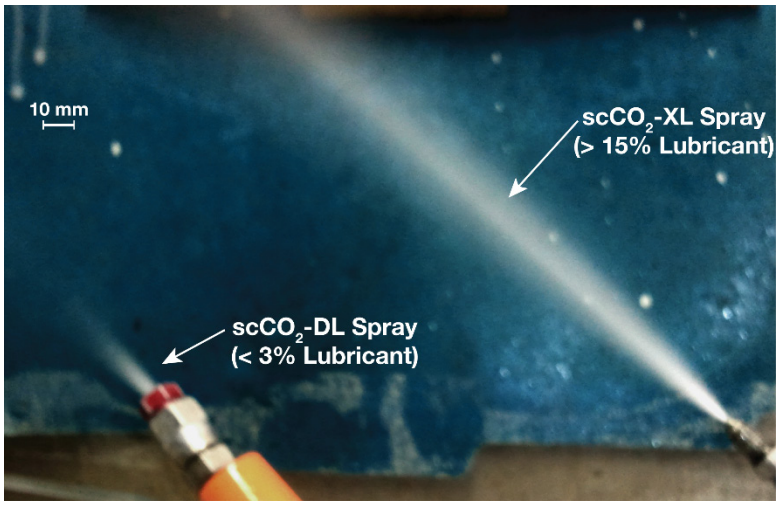

Figure 3.2. Images of $scCO_2$-DL (left nozzle) and $scCO_2$-XL (right nozzle) sprays being expanded from identical pressure and temperature conditions from nozzles of identical orifice size.

Table 3.1. Different forms of $scCO_2$-MWFs with attributes as applied in this research.

$scCO_2$-MWF Form	**Abbreviation**	**Draw Tube**	**Oil Fraction (w/w)***	**Oil Flow Rate (ml/hour)****	**CO_2 Flow Rate (kg/hour)**
No Dissolved Lubricant	NDL	Any	None	None	19
Dissolved Lubricant in $scCO_2$	DL	Top	Up to 2%	4 – 40	19
Lubricant Expanded with $scCO_2$	XL	Bottom	15% or greater	690 – 750	26

* This includes only the amount of oil *dissolved* in $scCO_2$.
** This includes the amount of oil dissolved in $scCO_2$ plus the mass transport of oil through nozzle.

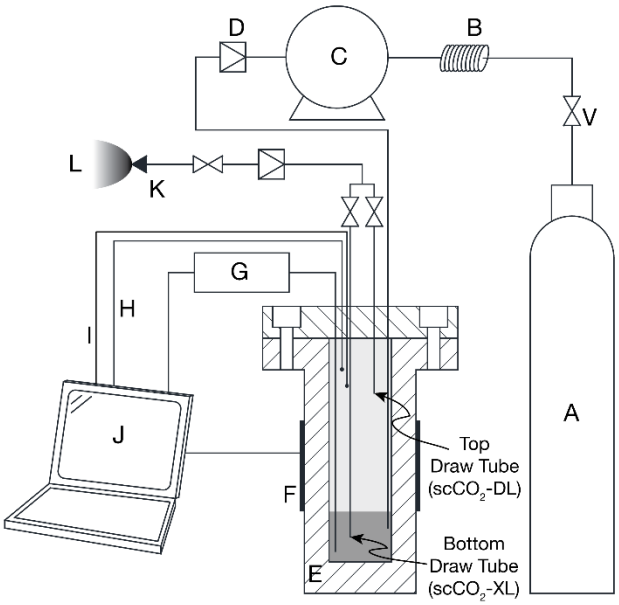

Figure 3.3. Schematic of $scCO_2$-MWF delivery system. A) cylinder of food-grade CO_2, B) cooling unit, C) pump, D) check valve, E) high pressure vessel, F) heating element, G) soybean oil sump, H) pressure transducer, I) thermocouple, J) computer, K) nozzle, L) $scCO_2$-MWF spray, V) on/off valve.

The custom-built apparatus shown in Figure 3.3 was used for the delivery of $scCO_2$-MWFs. Food-grade CO_2 from a commercially available compressed CO_2 cylinder was further pressurized above its critical pressure using a pump, and heated to a specified supercritical temperature using a heating coil. It was then sent to a high-pressure vessel where it was bubbled up through liquid vegetable oil present at the bottom of the vessel. For $scCO_2$-NDL, the high-pressure chamber contains no oil. A nozzle at the end of the outlet line is then used to rapidly expand and direct the $scCO_2$-MWF to the metalworking process as shown in Figure 3.2.

3.1.1.2 Heat Removal Experiments

In this work we define heat removal potential (HRP) as the capacity of a MWF to remove heat from a continuously heated finite flat surface. HRP captures thermal properties of the MWF such as specific heat capacity and thermal conductivity. In this work, HRP was measured using a custom-built

12.5 mm diameter copper rod (99.9% purity) with the 20 mm side cut down to a 3 mm diameter, as illustrated in Figure 3.4.

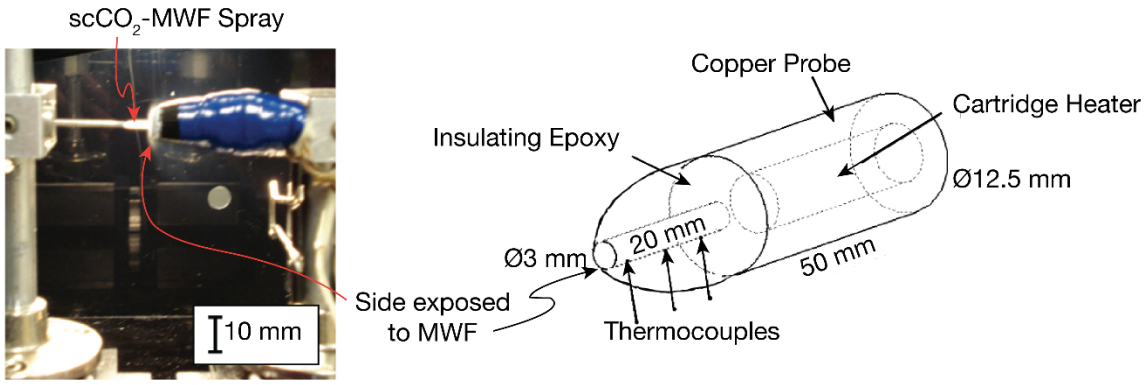

Figure 3.4. Image and schematic of probe used to measure heat removal potential of MWF sprays.

The 12.5 mm side was kept at a constant temperature using a cartridge heater (Tempco, Wood Dale, IL). The 3 mm side was fitted with three K-type thermocouples (Omega, Stamford, CT) and encased in high temperature thermal shock epoxy (Epoxies, Etc. Cranston, RI). The 3 mm diameter tip of the copper rod was placed in the flow field of MWF sprays, and the temperature drop across the thermocouples was recorded using a data acquisition device (National Instruments, Austin, TX). The heat flux was calculated by $\dot{q} = k\Delta T/\Delta x$ and used as a metric of HRP, where $\dot{q}$ is the heat flux, k is the thermal conductivity of copper, and ΔT and Δx are the temperature difference and distance between the thermocouples, respectively. Distance of the nozzle from the surface is also a significant factor in determining the HRP of the spray (Clarens, Park, et al., 2009). Thus, the distance of the MWF nozzle from the flat plate was kept constant for the HRP measurement experiments.

HRP may not fully account for the performance of a MWF in machining since other factors, such

as viscosity, flash point (for oil-based MWFs), molecular density, spray velocity, and cutting zone geometry, also contribute to heat removal. Many of these factors relate directly to the extent of cutting zone penetration the MWF can achieve. To account for thermal, fluid, and geometric characteristics of the MWF delivery process, we operationally define heat removal efficacy (HRE) as the ability to control cutting tool temperature during machining. Depending on the workpiece and tool material, the temperature of the cutting tool can be indicated by phenomena such as flank wear, nose wear, pitting/galling, and localized welding of workpiece material. In this paper, tool flank wear is treated an indicator of HRE in turning of Ti6Al4V and milling of CGI based on the predominant diffusion wear phenomenon observed at high cutting zone temperatures in these processes. To further verify the HRE results, oil-hole drilling experiments were conducted with A390 aluminum in which rapid flank wear is again observed at high tool temperatures.

Ti6Al4V (15.24 cm diameter round) workpieces for turning were supplied by Metal Shorts Incorporated (Seattle, WA) and cut using a Kennametal #MCGN R 164D tool holder equipped with CNGP432FS Grade K313 inserts. The turning operation was conducted with a speed of 46 m/min, feed rate of 0.2 mm/rev, and cut depth of 0.127 mm. Images of the tool wear were taken using an OPTEM International (Fairport, NY) 100X zoom digital camera. Wear measurements were made at the deepest point on the worn flank using Euro-Tech PG1000 v1.0 software. All experiments were performed in triplicate. Measurements were made on a workpiece with a continually changing diameter but constant cutting speed. Time between measurements was kept approximately the same to capture different wear regimes properly.

For milling, an Ingersoll end-mill (Ingersoll Cutting Tools, Rockford, IL) with 5 uncoated carbide inserts was used on CGI workpieces. MWFs were delivered directly through the mill and discharged onto each insert using a high-pressure capacity collar tool holder. The depth of cut was 0.5 mm for each pass, and a total of 300 passes were made with each MWF. Cutting speeds of 150 m/min and 225 m/min were tested, along with feed rates of 0.150 mm/rev and 0.750 mm/rev. Experiments were performed in duplicate. Aqueous MWF used in turning as well as milling experiments was a 5% solution of Castrol 9913 synthetic lubricant (Naperville, IL) with manufacturer reported pH of 7.8 at 5% concentration.

Drilling tests were conducted on a Fadal VMC 4020 vertical machining center. The spindle was fitted with a Lightning Cool through-spindle water-based coolant system (operating pressure 2.06 MPa) with a GAT (Geisenheim, Germany) rotary union at the back of the spindle used to facilitate switching between through-tool aqueous and $scCO_2$-MWF. The aqueous MWF was formulated as a 5% solution of Cimtech 310 synthetic lubricant (Cincinnati, OH) with a manufacturer reported pH of 7.8 at 5% concentration. High Speed Steel (HSS) drills of 8 mm diameter (Guhring 12033869 00390-8.00) were used to drill holes 25 mm deep in an A390 cast aluminum waffle plate. In an accelerated wear study, holes were drilled using each MWF until tool failure occurred as indicated by the distinct vibration of drill. $scCO_2$-MWF was delivered through two orifices, which were custom-fabricated by plugging the existing coolant holes in the drill with epoxy and then drilling 200 μm diameter through holes. Drilling torque was measured using a Kistler 9272 four-component piezoelectric drilling dynamometer. Flank wear was measured on the outer corner of the drill on both flutes, and the mean of these values was reported as the wear value for a given condition. Flank wear

in drilling of Aluminum also has a lubrication component as it is caused by mechanisms such as delamination and oxidation that are closely related with the coefficient of friction at the tool-chip and tool-workpiece interfaces as discussed by Y. Liu, Asthana, & Rohatgi (1991).

3.1.1.3 Lubrication Experiments

To evaluate the performance of a MWF with respect to its lubrication function, we operationally define lubrication efficacy (LE) as the ability to reduce friction at the tool-workpiece interface. In this paper, we use reduction in the machining torque observed relative to a reference MWF in friction-dominated processes as an indicator of LE. Thread cutting and forming were selected due to their friction intensity, and their need for appropriate lubrication often supplied by straight oils. Thread cutting tests were carried out on a MicroTap Mega G8 machine tool (Rochester Hills, MI). ANSI 1018 cold rolled steel workpieces (10 mm thick) were pre-drilled and pre-reamed with 175 holes of 5.6 mm diameter. High-speed steel (HSS) M6 taps were used with 60˚ pitch and 3 straight flutes. For each fluid, 25 replicates were performed on 25 holes and for each hole a torque versus tap traveling distance curve was obtained. The tapping torque efficiency was calculated by normalizing the average torque measured. A detailed description of the tapping torque test methodology is provided by Zimmerman, Takahashi, Hayes, & Skerlos (2003); this method is a modified version of ASTM D 5619 and was designed for increased experimental consistency and rigorous statistical calculation of confidence intervals.

Thread forming tests were conducted on a Cincinnati HMC-400EP high-speed horizontal machining center in accordance with the modified ASTM D 5619 standard. Walter Prototype DP2061705 M6 thread forming taps made from cobalt enriched HSS and coated with titanium

nitride were used. The workpiece material was 2024 T-351 aluminum and the tapping torque was measured using a Kistler 9272 four-component piezoelectric dynamometer. For baseline tests, a UNIST model 9950 external one-channel MQL system was used. UNIST 2210 oil was used for the MQL baseline. The lubricant used in the MQL spray was a vegetable-based oil with no chlorine, sulfur, or silicon additives, as recommended for nonferrous machining by the manufacturer. MQL delivery was performed through a nozzle fixed to the spindle housing. For each test condition, sixteen holes were tapped in the workpiece.

3.1.2 Results and Discussion

3.1.2.1 Heat Removal Potential and Heat Removal Efficacy

The observed HRP values for the various MWFs listed in Table 3.2 are shown in Figure 3.5. Aqueous flood emulsion MWF is seen to have the highest HRP. This is due to the high flow rate, excellent thermal diffusivity of liquid water, and additional heat removal ability created by the phase change of water from liquid to vapor. For the same reasons, the MQL spray of aqueous emulsion features a HRP value that is more than double that observed for the MQL spray of lubricant.

Table 3.2. MWFs used in this study and their delivery conditions.

MWF	Lubricant & Flow rate	Coolant & Flow rate
Emulsion Flood	Petroleum semi-synthetic emulsion (0.05 g/s)	Water (1 g/s)
Lubricant Spray	Soybean oil (0.01 g/s)	Air at 0.6 MPa (1 g/s)
Emulsion Spray	Petroleum semi-synthetic emulsion (0.05 g/s)	Air at 0.6 MPa + Water (1 g/s)
$scCO_2$-DL Spray	Soybean oil (0.001 g/s)	CO_2 at 13 MPa (1 g/s)
$scCO_2$-XL Spray	Soybean oil (0.2 g/s)	CO_2 at 6 or 9 MPa (7 g/s)
N_2 Spray	None	N_2 at 15 MPa (1 g/s)
Argon Spray	None	Ar at 13.5 MPa (1 g/s)

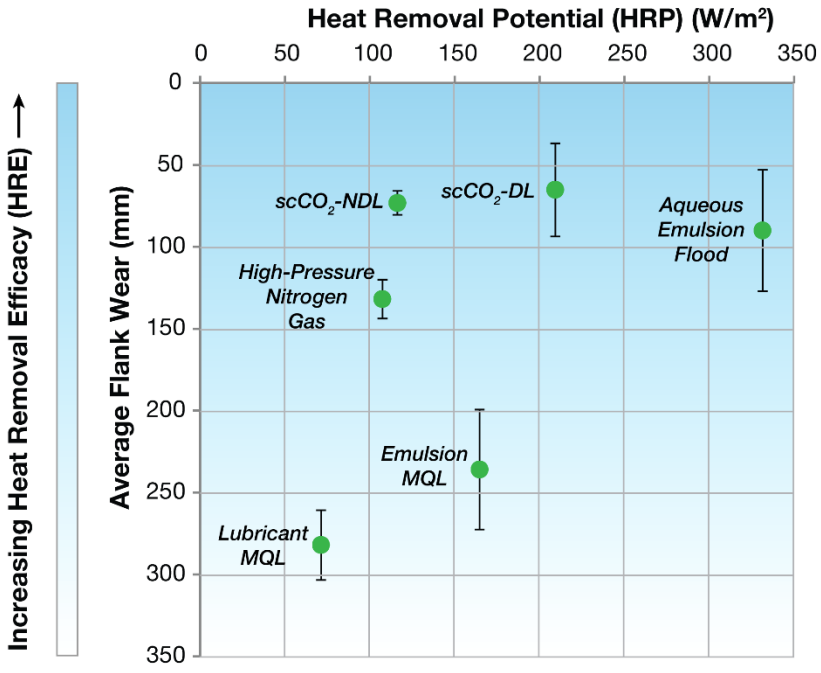

Figure 3.5. HRP and HRE observed for various MWFs examined in turning of Ti6Al4V shows that higher HRP does not necessarily result in higher HRE. Flank wear is used as a surrogate metric for HRE.

$scCO_2$-DL is observed to have the second highest HRP of the tested MWFs while the HRP values observed for the other gas-based MWFs are in the range of the MQL formulations. However, if the cooling ability of a MWF were solely determined by its HRP, the flank wear observed in the turning of titanium would follow the inverse trend of the HRP values. In other words, the tool life observed in titanium turning would follow this sequence: Aqueous emulsion flood > $scCO_2$-DL > Emulsion MQL > $scCO_2$-NDL > High-Pressure Nitrogen Gas > Lubricant MQL. Figure 3.5 shows that this trend is not followed. For instance, although the HRP of the emulsion-based MQL is greater than the HRP of $scCO_2$-NDL by a factor of about 1.5, the HRE of the emulsion-based MQL is two to three times lower.

The HRE data presented here thus provide evidence that cutting zone geometry and a MWF's penetration into the cutting zone are as important as thermal properties in determining the effectiveness of a MWF. This is consistent with the hypothesis of S. Wang & Clarens (2013), who have developed an analytical model for the penetration of aqueous emulsions and various gases based on an orthogonal cutting geometry. They use the Navier-Stokes and Reynolds lubrication equations to compute MWF penetration to the cutting zone and find that gas-based MWFs exhibit nearly 100% penetration to the cutting zone whereas the more viscous emulsion flood and straight-lubricant MWFs have penetration levels at 30% or less at conventional delivery pressures. It therefore can be suggested that high-pressure gas based MWFs, such as $scCO_2$-MWF and compressed nitrogen, are effective in removing heat from the cutting zone because they are better at reaching the heat generation region. The reduction in tool wear associated with the use of nitrogen gas instead of aqueous MWFs is consistent with the findings of Sun, Brandt, & Dargusch (2010) in their work on Ti6Al4V milling.

It is interesting that a higher HRE is observed for high-pressure nitrogen gas and $scCO_2$-NDL than for MQL sprays, despite the fact that the gas-based MWFs have a lower average molecular density and specific heat capacity. This observation is in part due to the Joule-Thomson effect, which is the phenomenon where a gas undergoing adiabatic expansion experiences a drop in its internal energy and consequently its temperature. This drop in internal energy is often expressed in terms of the Joule-Thomson coefficient (μ_{JT}). μ_{JT} is defined as the partial derivative of temperature with respect to pressure under constant enthalpy. The μ_{JT} for nitrogen, carbon dioxide and argon, at pressures and temperatures expected at the nozzle exit, are shown in Table 3.3. The μ_{JT} value for carbon dioxide is approximately five times higher than nitrogen's coefficient and thus at the pressures that would exist

during the expansion out of a nozzle, carbon dioxide will enter the cutting zone at a much lower temperature than nitrogen.

Table 3.3. Joule-Thomson coefficients for high-pressure gas MWFs used in this study (National Institute of Standards and Technology, 2011)

Gas	Pressure (MPa)	Temperature (˚C)	μ_{JT} (˚C/MPa)
Nitrogen	0.1	25	2.1485
Carbon Dioxide	0.1	35	10.0530
Argon	0.1	25	3.6576

Carbon dioxide has additional heat removal capability arising from the sublimation of dry ice particles that are formed during rapid expansion. This sublimation does not occur for nitrogen or argon delivered at the similar pressures. Taken together these factors explain the higher HRP and HRE values observed with $scCO_2$-NDL as compared with nitrogen and argon (note: the tool wear with argon is 125 μm, and it is not shown in Figure 3.5 due to an unavailable HRP value). Figure 3.5 also shows that $scCO_2$-DL has a higher a HRP and HRE than $scCO_2$-NDL. This can be attributed to the presence of oil in the $scCO_2$-DL, which increases the average molecular density and therefore the thermal diffusivity of the spray without a trade-off in cutting zone penetration.

Based on the observations above, it was hypothesized that increasing pressure could increase the HRE of $scCO_2$-DL. To test this hypothesis, $scCO_2$-DL was used at three different pressures and flank wear in turning was compared. Figure 3.6 shows that an increase in pressure of $scCO_2$-DL leads to less wear and thus higher HRE. The lower wear observed at higher operating pressure is due to higher flow rate and greater solubility of lubricant (serving as a heat transfer medium) in $scCO_2$ as its pressure increases. A larger pressure drop during the adiabatic expansion also leads to lower spray temperatures

and thus larger heat transfer rates. Finally as the spray velocity increases due to the larger pressure drop, a higher mass flow rate is achieved along with a greater penetration of spray particles into the cutting zone.

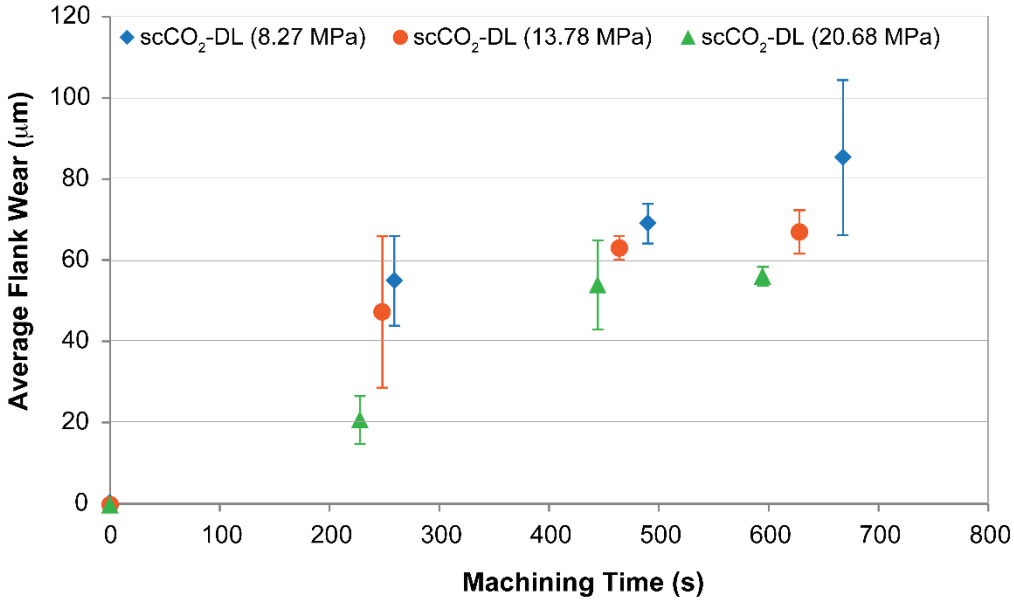

Figure 3.6. Flank wear (indicator of HRE) progression in turning of Ti6Al4V with $scCO_2$-DL at different pressures. Wear with $scCO_2$-DL reduces with increase in its pre-rapid-expansion pressure.

The above data suggest that the Joule-Thomson effect, phase change, and higher cutting zone penetration allow $scCO_2$-NDL as well as $scCO_2$-DL to have higher HRE values relative to conventionally applied aqueous MWFs. To independently confirm this result, $scCO_2$-DL was compared with an aqueous emulsion flood MWF in milling at a material removal rate (MRR) of 150 m/min. Figure 3.7 shows the average flank wear with $scCO_2$-DL is roughly 125 μm after 300 seconds of machining time. This wear value is significantly lower than the flank wear value of 250 μm observed after 250 seconds of milling time with the aqueous flood MWF as currently applied in production operations. Given the higher HRE of $scCO_2$-DL in milling, we hypothesized that it should be possible

to achieve a higher MRR than aqueous emulsion MWF with equivalent tool life. This hypothesis was tested by increasing the MRR in milling from 150 m/min to 225 m/min. Figure 3.7 shows that the average flank wear with $scCO_2$-DL at the higher MRR is lower than that with emulsion flood at the lower MRR. This introduces the possibility of reducing machining time, thereby improving machining productivity via changes in MWF system design.

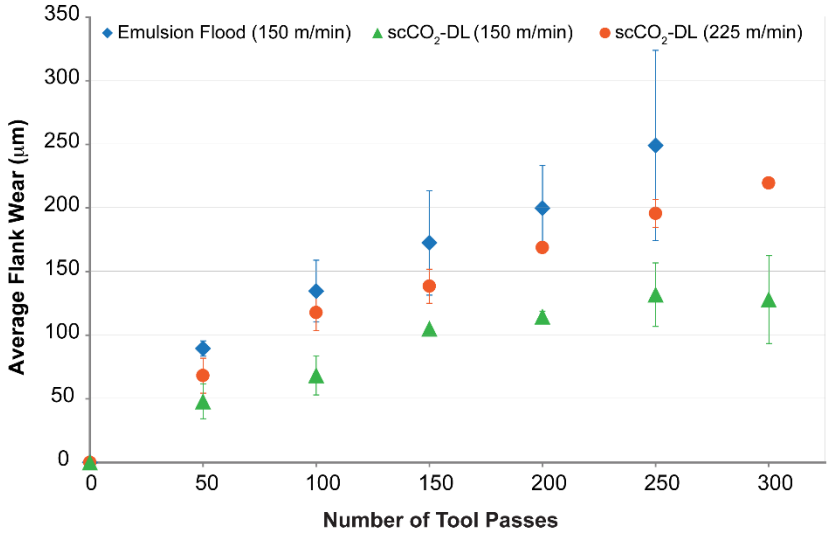

Figure 3.7. Flank wear (indicator of HRE) progression in milling of CGI with aqueous MWF and $scCO_2$-DL. Increasing $scCO_2$-DL pressure allows for higher material removal rates than permitted by aqueous MWFs for a given value of tool wear.

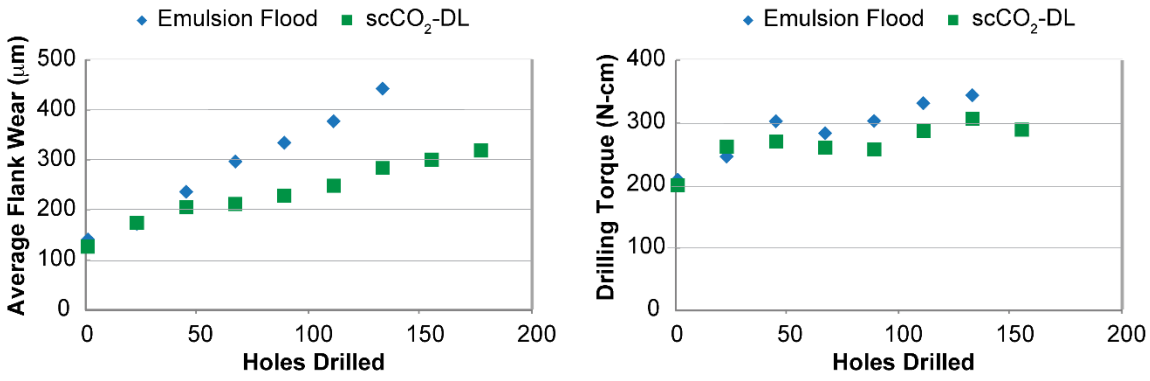

Figure 3.8. Flank wear (a) and torque (b) in drilling using scCO2-DL and aqueous MWFs.

Similar results were observed with oil-hole drilling of CGI engine blocks. Figure 3.8 (left) shows that the tool wear observed with $scCO_2$-DL is significantly lower than that observed with the aqueous MWF currently used in production operations. Figure 3.8 (right) shows only a modest reduction in torque with $scCO_2$-DL over conventional application of aqueous MWF, suggesting that the reduced wear arises from better heat removal rather than improved lubrication.

3.1.2.2 Lubrication Efficacy

Previous work by Clarens et al. (2006) has shown that $scCO_2$-NDL has lubrication efficacy (LE) comparable with semi-synthetic MWFs. The LE of $scCO_2$-NDL can be increased considerably by drawing from the $scCO_2$-XL phase of the $scCO_2$ delivery system. Figure 3.9 shows the performance of $scCO_2$-XL in thread tapping operations expressed as tapping torque efficiency. Tapping torque efficiency is the ratio of a MWF's thread tapping torque compared to the thread tapping torque of a reference MWF. Thus an efficiency of more than 100% for a MWF means that lower torque is needed for a tapping operation when using that MWF compared to the reference MWF. Figure 3.9 (left)

shows that $scCO_2$-XL gives a tapping torque efficiency of 117 % when compared with straight soybean oil as the reference fluid in thread cutting.

MQL is known to have higher LE than aqueous MWFs and as a result MQL is widely used in thread tapping operations, particularly for aluminum. Therefore, $scCO_2$-XL spray is compared with MQL in thread forming experiments. Figure 3.9 (right) shows that $scCO_2$-XL gives a tapping torque efficiency of 117% (coincidentally) when compared with MQL as the reference fluid in thread forming. The reduction in torque observed with $scCO_2$-XL can be attributed to a reduction in friction. This improved LE outcome is a likely result of better penetration into the working zone due to higher velocities (and pressures) found in $scCO_2$-MWF systems relative to MQL systems. Exclusion of oxygen from the working surface is also a possible working mechanism for the $scCO_2$-MWF systems, especially in aluminum machining, since high friction coefficients can arise due to oxide formation on freshly cut aluminum surfaces. Since $scCO_2$-XL is delivered at high spray velocities and high CO_2 flow rates, it has the potential to keep oxygen locally out of the cutting zone whereas MQL is delivered in air and thus cannot exclude oxygen from the cutting zone.

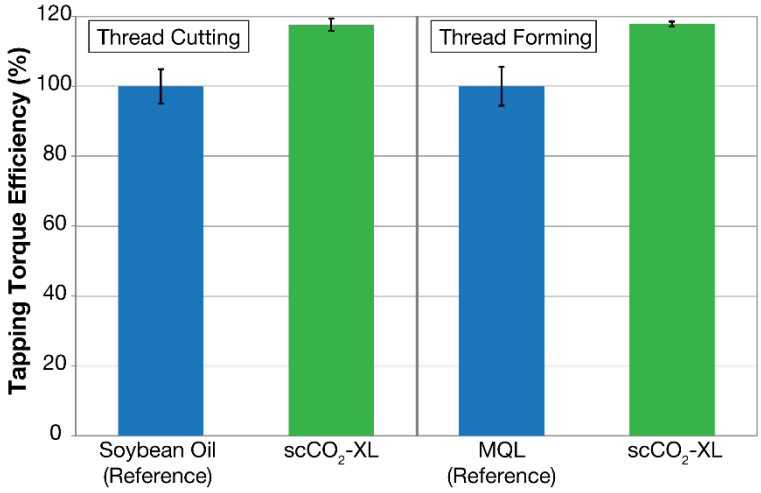

Figure 3.9. Tapping torque efficiencies (indicator of LE) for $scCO_2$-XL in thread cutting and forming.

3.1.2.3 Environmental Performance

A life cycle assessment of environmentally adapted gas-based MWFs performed by Clarens et al. (2008) shows a lower overall environmental impact for $scCO_2$ MWF than aqueous MWFs and MQL. As a result, it can be shown that $scCO_2$ MWFs eliminate key environmental and health hazards associated with MWF use while in common cases reducing the carbon footprint of MWF systems. Even so, they overestimate global warming potential (GWP) contribution from $scCO_2$ MWF sprays because their approach uses a price-based allocation for CO_2. The marginal impacts of recovered CO_2-based MWFs using the production emissions inventory and market-based allocation method formulated for recovered CO_2 in this dissertation are discussed in detail in section 3.3.

3.1.3 Conclusions

This work has established the versatility of $scCO_2$-MWFs to be applied with success in a diverse set of manufacturing operations including turning, milling, drilling, and tapping. These operations are inclusive of three intense heat generation machining processes and two intense friction machining

processes. It was found in all cases that $scCO_2$-MWFs provide better cooling and lubrication than aqueous MWFs, straight lubricants, or MQL formulations as applied under production conditions. Therefore it is concluded that a MWF's potential for heat removal or lubrication based on its physical properties alone does not necessarily correlate with the efficacy with which it removes heat or lubricates in a real machining process. Cutting zone penetration of a MWF is also important in determining its functional efficacy as a metalworking coolant or a lubricant.

This work has also established the following properties of $scCO_2$-MWFs:

1. $scCO_2$-MWFs can be delivered as rapidly expanding sprays of i) $scCO_2$ with no dissolved lubricant (NDL), ii) $scCO_2$ with dissolved lubricant (DL), or iii) Lubricant expanded with $scCO_2$ (XL).
2. For the processes studied in this work, $scCO_2$-NDL has a higher heat removal efficacy than conventional aqueous flood MWF, despite $scCO_2$-NDL having a lower heat removal potential. This is likely a consequence of better cutting zone penetration of $scCO_2$-NDL relative to aqueous MWF.
3. The presence of lubricants, such as vegetable oil, in $scCO_2$ increases both heat removal efficacy and lubrication efficacy, whereas increased percentage of lubricant in MQL as well as aqueous MWFs reduces their heat removal efficacy.
4. The heat removal efficacy of $scCO_2$-DL increases with increasing pressure of the supercritical solution. This is likely due to higher lubricant solubility, lower spray temperatures arising from to the Joule-Thompson effect, higher spray velocities, and higher mass flow rate of CO_2 and lubricant.

5. $scCO_2$ can dissolve lubricants unlike high pressure nitrogen or argon, while leading to colder sprays with higher heat removal potential and efficacy.
6. $scCO_2$-DL can increase tool life or enable higher material removal rates, thus creating an opportunity for increasing manufacturing productivity while reducing environmental and health concerns associated with aqueous MWFs.
7. $scCO_2$-DL can provide better lubrication efficacy than straight oils and oil-in-air MQL.

From these observations, it is concluded that $scCO_2$-MWFs can be both better coolants and better lubricants than conventional MWFs. Since the delivery mode of $scCO_2$ can be switched between NDL, DL and XL by simple valve control, $scCO_2$ provides a versatile MWF platform that can operate over a broad range of metalworking processes in industrial practice.

3.2 SUPERCRITICAL CO_2 METALWORKING FLUIDS IN MICRO-SCALE MACHINING

3.2.1 Introduction

Mechanical micro-manufacturing is receiving increasing attention due to its ability to create truly three-dimensional (3D) features in multiple length scales and its compatibility with a broad range of engineering materials. As such, mechanical micro-manufacturing processes provide capabilities that are complementary to lithographic processes used in MEMS fabrication (Dornfeld, Min, & Takeuchi, 2006; Liow, 2009) in terms of materials, geometries, and dimensions (Ehmann et al., 2005). In particular, micromachining, which uses micro-scale milling and drilling tools within high precision machining environments, has the potential to become an effective and widespread technique for creating 3D structures and devices (Dornfeld et al., 2006; Filiz, Xie, Weiss, & Ozdoganlar, 2008; Liow, 2009; Wilson et al., 2011).

While having similar process kinematics, the mechanics of material removal in micromachining differs significantly from macroscale machining (C.-J. Kim, Mayor, & Ni, 2004; X. Liu, DeVor, & Kapoor, 2006; X. Liu, DeVor, Kapoor, & Ehmann, 2004; Lucca, Seo, & Komanduri, 1993; Vogler, Kapoor, & DeVor, 2004). This difference in process mechanics brings fundamental changes to the forces, surface and dimensional quality, and tool wear characteristics experienced during micromachining (Filiz, Conley, Wasserman, & Ozdoganlar, 2007; X. Liu et al., 2004). Although recent investigations of various engineering materials have provided some basic understanding of micromachinability, there is still a significant need for innovative approaches that will address contemporary challenges in micro- machining (Arif, Rahman, & San, 2011; Bissacco, Hansen, & De Chiffre, 2005; Egashira & Mizutani, 2002; Kakinuma, Yasuda, & Aoyama, 2008; Lee & Dornfeld,

2002; Ng, Melkote, Rahman, & Senthil Kumar, 2006; Weinert & Petzoldt, 2008). One approach to improve micromachinability is to use metal- working fluids [2]. MWFs are proven to improve machinability and part finish at the macroscale by providing lubrication and cooling, as well as by facilitating chip evacuation. To date, only few studies have investigated the use of MWFs in micromachining. Jun, Joshi, DeVor, & Kapoor (2008) used a minimum quantity lubrication (MQL) MWF system in the micromilling of aluminum 7075 and 1018 carbon steel, and reported reduced peak to valley forces, lower cutting zone temperatures and better surface finish compared to dry micromachining or micromachining with conventional aqueous cutting fluids. The work by Li & Chou (2010) with MQL- assisted micromilling of SKD-61 tool steel showed reduced tool wear and low surface roughness values, both remaining stable under increasing length of cut, using MQL versus dry conditions. Machining in a cryogenic or low temperature MWF environment has been shown to improve surface finish and machinability at the macroscale (Pusavec et al., 2011; Su, He, Li, & Li, 2006; Z. Y. Wang & Rajurkar, 2000). Supercritical carbon dioxide ($scCO_2$) MWF is one such low temperature MWF which has been shown to improve tool life and surface finish, particularly at high material removal or deformation rates, on materials ranging from carbon steels to titanium and compacted graphite iron in macro- scale machining and forming applications (Clarens et al., 2006; Clarens, MacLean, et al., 2009; Clarens, Park, et al., 2009; D. J. MacLean et al., 2009). This paper presents a preliminary study that explores the feasibility of productively utilizing scCO2 MWFs in the micromachining of metals.

While having similar process kinematics, the mechanics of material removal in micromachining differs significantly from macro-scale machining (C.-J. Kim et al., 2004; X. Liu et al., 2006, 2004;

Lucca et al., 1993; Vogler et al., 2004). This difference in process mechanics brings fundamental changes to the forces, surface and dimensional quality, and tool wear characteristics experienced during micromachining (Filiz et al., 2007; X. Liu et al., 2004). Although recent investigations of various engineering materials have provided some basic understanding of micro-machinability, there is still a significant need for innovative approaches that will address contemporary challenges in micromachining (Arif et al., 2011; Bissacco et al., 2005; Egashira & Mizutani, 2002; Kakinuma et al., 2008; Lee & Dornfeld, 2002; Ng et al., 2006; Weinert & Petzoldt, 2008). This paper presents a preliminary study that explores the feasibility of productively utilizing $scCO_2$ MWFs in the micromachining of metals.

3.2.2 Experimental Methods

3.2.2.1 Experimental Setup

Micromachining experiments were performed on the high-precision miniature machine tool (MMT) shown in Figure 3.10. The MMT includes a 160,000 rpm air turbine, air bearing miniature ultra-high-speed spindle equipped with a 3.125 mm (1/8 in.) precision collet. The feed motions are provided by three-axis slides (Aerotech® ALS130-XYZ) with a 10 nm resolution and a maximum linear (feed) speed of 250 mm/s. To facilitate the measurement of micromachining forces, the workpiece is mounted on a dynamometer (Kistler 9256C1), which in turn is attached to the three-axis slides. A stereomicroscope with 95X magnification is used to view the workpiece surface during the initial tool approach.

The $scCO_2$ MWF system employed for this study is shown in Figure 3.11. Commercially available food grade CO_2 is compressed above its critical pressure (7.32 MPa) and sent to a high pressure mixing

chamber, where it passes through vegetable oil present at the bottom of the chamber. The resulting solution of $scCO_2$ and vegetable oil is maintained at a specified temperature above the critical temperature of CO_2 (31.1˚C) using a temperature sensor and heating coil apparatus controlled by a central PLC unit. A 150 µm orifice nozzle is used to rapidly expand the solution of lubricant in $scCO_2$ as a high velocity spray directed to the tool/workpiece interface. Under these delivery conditions, the flow rate of oil is about 22 ml/hour and the flow rate of CO_2 is about 19 kg/hour. The average temperature of the $scCO_2$ MWF spray measured at the nozzle exit is about -66 ˚C.

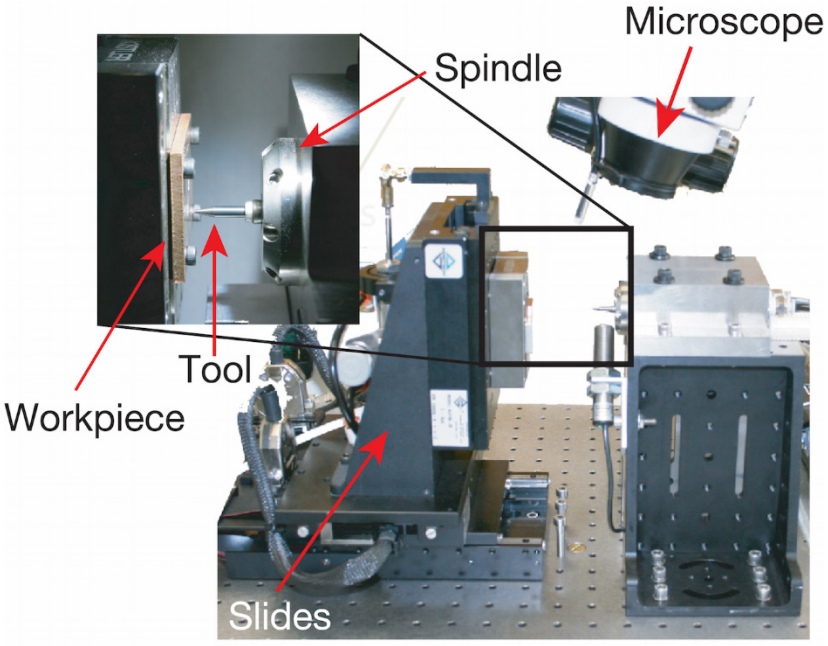

Figure 3.10. High-precision miniature machine tool (MMT) system

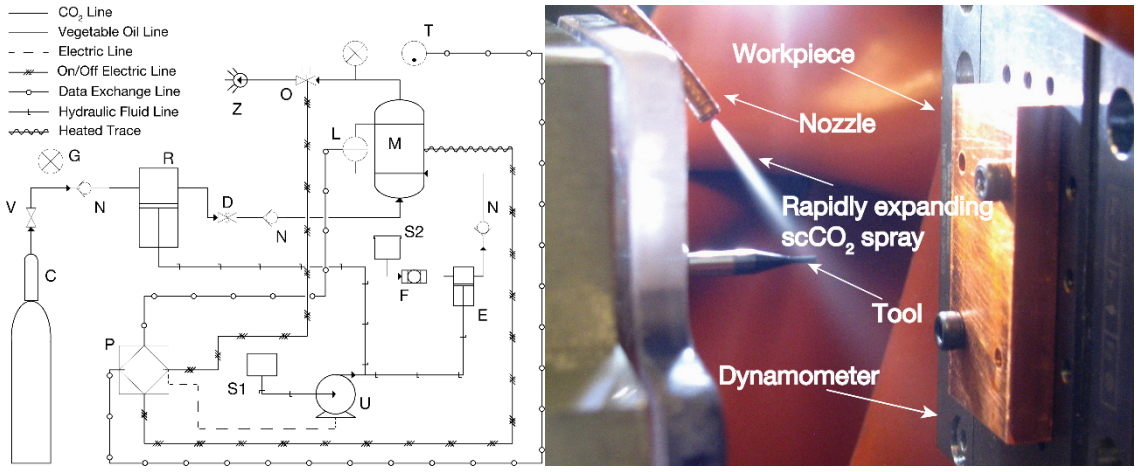

Figure 3.11. $scCO_2$ MWF delivery system: C. Tank of food-grade carbon dioxide; V. Gate Valve; G. Pressure gauge; N. Check valve; R. CO_2 compression pump; D. Burst Disc; P. PLC; S1. Hydraulic oil sump; U. Hydraulic oil pump; S2. Vegetable oil reservoir; F. Oil filter; E. Oil pump; M. High pressure mixing chamber; L. Oil level sensor; T. Temperature sensor; O. Solenoid valve; Z. Spray Nozzle delivering rapidly expanding $scCO_2$ + oil mixture.

3.2.2.2 Design of Experiments

AISI 304 grade Austenitic stainless steel and Oxygen Free High Conductivity (OFHC) 101 grade copper were chosen as workpiece materials. AISI 304 is a difficult material to machine due to high tool-wear rates, high cutting-zone temperatures, work-hardening, and built up edge formation. Cu-101 is a ductile material that creates challenges in achieving sufficient surface finish and form accuracy. Micromilling of these materials was performed using surface roughness, burr formation, average specific cutting energy, and tool wear as metrics of machinability following Filiz et al. (2007) and Stephenson & Agapiou (2005).

A two level half-factorial design of experiments was conducted with three factors: feed per tooth (f_z), axial depth of cut (a_p) and cutting velocity (v_c). As shown in Table 3.4, all four machining conditions were employed with $scCO_2$ MWF and dry cutting conditions on both AISI 304 (experiments 1-8) and OFHC Cu-101 (experiments 9-16). For each experimental condition, seven

channels (25 mm long) per condition were slot-milled with each channel separated by 0.7 mm. Channels on both materials were cut using 254 μm diameter two-fluted tungsten carbide micro-endmills with a helix angle of 30°. A fresh tool was used for each experiment. The eight experiments for each material were distributed over three workpieces. Prior to each experiment, the surface of the workpiece was cleaned using a 500 μm diameter micro-endmill. $ScCO_2$ MWF was expanded from a pressure of 10.3 MPa and temperature of 34°C.

Table 3.4. Design of experiments.

Levels of factors in the experiment						
	Steel			**Copper**		
Level	f_z (μm/tooth)	a_p (μm)	v_c (m/min)	f_z (μm/tooth)	a_p (μm)	v_c (m/min)
-	0.75	12	80	0.75	25	80
+	3	22	100	3	40	100

Design of Experiments			
Machining Conditions	f_z	a_p	v_c
1 (Ex. 1, 5, 9, 13)	-	-	+
2 (Ex. 2, 6, 10, 14)	+	-	-
3 (Ex. 3, 7, 11, 15)	-	+	-
4 (Ex. 4, 8, 12, 16)	+	+	+

3.2.2.3 Metrics and Measurements

Burr formation was analyzed qualitatively using a burr chart created from SEM images of the micromilled channels, as introduced in Filiz et al. (2007) . For stainless steel, only the images from the first channel were used for each machining condition to eliminate the effect of tool wear. For copper, given low wear rates, the images from either the first or the second channel were used. A 3D optical surface profilometer (Zygo NewView 7300) with sub-nanometer out-of-plane resolution and 2.2 μm in-plane resolution (with the 10X objective) was used for measuring surface roughness. The roughness

values (R_a) from four areas sized 0.8 mm x 0.2 mm on the bottom surface of the first channel were measured. Both the average and the standard deviation of Ra values were then calculated.

Cutting forces were measured using a three-axis dynamometer (Kistler 9256C1, 2mN noise threshold with linearity and hysteresis less than 0.5% of the measurement range), a charge amplifier (Kistler Type 5010 Charge Amplifier), and a data acquisition sys- tem (NI PXI-6115). To eliminate the electrical and environmental noise from the measured forces, the data were post processed using a zero-phase-shift band-pass filter such that only those force components within a narrow band (6Dx) at the spindle frequency and its harmonics were retained. Force data were compensated to eliminate the effect of dynamometer dynamics. Impact hammer tests up to 15kHz frequency were conducted to obtain frequency response functions (FRFs) in the three measurement axes. The resulting 3-by-3 matrix of FRFs was curve-fitted as a complex function of frequency, and inverted and multiplied with measured forces to calculate their compensated values. The effect of $scCO_2$ MWF on micromilling may be obtained by determining the average specific cutting energy for each experiment considering the kinematics of the milling process. The specific cutting energy, also referred to as specific cutting force or specific cutting power in the literature, is calculated by dividing the average peak-to-valley tangential cutting force for each revolution by the average (uncut) chip area obtained by multiplying the average feed (f/2p) with axial depth of cut. Averaging the cut- ting forces per revolution rather than per tooth pass eliminates the effect of tool-tip runout on the forces. To remove the effect of tool wear, only the forces from the first channel in each experiment were used. These forces were averaged over 500 revolutions to determine both the averages and the standard deviations. Reported error bars

for surface roughness and specific cutting energy represent 95% confidence for these measurements, though they do not include variation between channels.

Tool wear was assessed based on the reduction of the tool diameter with increased length of cut, as evidenced from the observed changes in the channel widths, as outlined in Filiz et al. (2007). The wear analysis was completed only for Cu-101 due to the observed chipping of the tools for certain cases during machining of AISI 304. In order to facilitate better measurement of channel widths, replicas of the channels were fabricated through elastomer molding. Optical profilometer measurements of the molded features were then obtained, and the measured profiles were post-processed to determine the average channel widths. The channel widths were defined as the parallel distance between feature sidewalls in a plane that is 1 μm below their top surfaces.

3.2.3 Results and Discussion

3.2.3.1 Specific Cutting Energy

Figure 3.12 shows the X, Y and Z components of the machining force for condition 4 (copper) when using $scCO_2$ MWF. The dotted lines represent one revolution of the tool. A slight tool runout can be observed in the forces. The average specific cutting energies for all experiments are provided in Figure 3.13. It is observed that the specific cutting energy in condition 1 (low chip load and low axial depth of cut) is significantly higher than the other three conditions in both dry and $scCO_2$ MWF conditions in both materials, which is most likely due to the size effect that becomes prominent when the ratio of uncut chip thickness to tool nose radius drops below 1 as observed in studies in the literature (Aramcharoen & Mativenga, 2009; Filiz et al., 2007; Lucca et al., 1993; Ng et al., 2006).

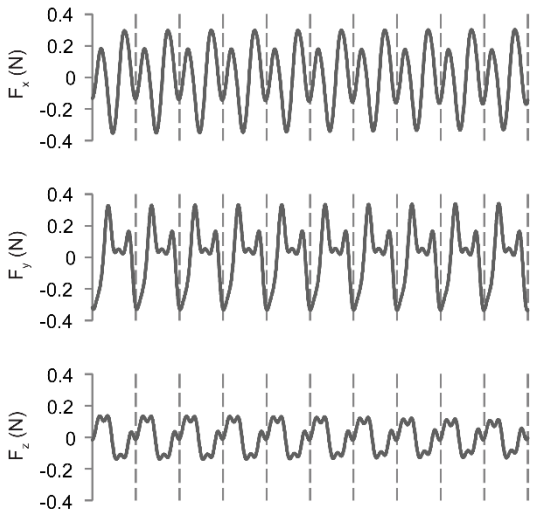

Figure 3.12. Cutting forces for Cu-101 when machining with $scCO_2$ MWF at 3 μm/tooth chip load, 40 μm axial depth of cut and 100 m/min cutting speed.

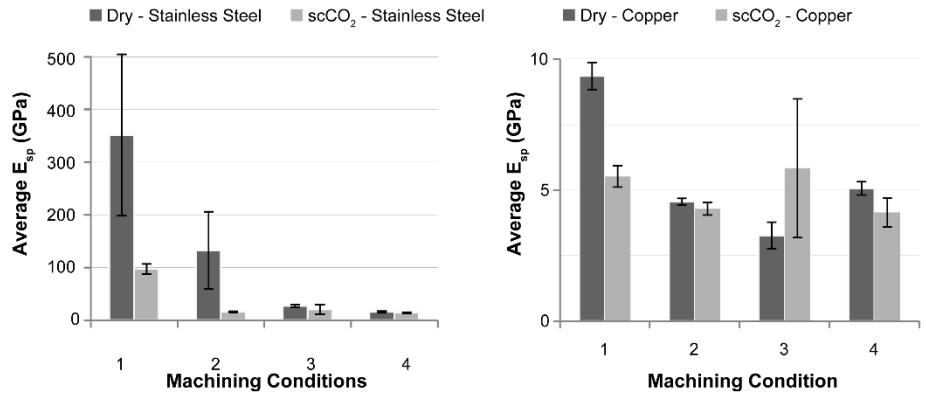

Figure 3.13. Average specific cutting energies for AISI 304 stainless steel (left) and Cu-101 (right) with and without $scCO_2$ MWF under all four machining conditions examined.

Specific cutting energy is reduced for condition 1 when using $scCO_2$ MWF compared with dry machining, and is statistically indistinguishable for the other conditions. The reduction in specific cutting energy from the use of $scCO_2$ MWF could be a consequence of a local increase in material hardness and a reduction in minimum chip thickness resulting from exposure to the low-temperature

spray. A similar reduction in specific cutting energy with low temperature MWFs was observed by Pušavec, Govekar, Kopač, & Jawahir (2011), who attributed the reduction to an increased brittleness from low temperatures in the cutting zone. They hypothesize that the brittleness reduces plastic deformation or "ploughing" near the nose of the cutting tool where negative rake angles are generally observed even at the macrolevel.

3.2.3.2 Tool Wear

Figure 3.14 shows the percentage reduction in channel width and SEM images of cutting tool nose when machining copper under condition 2 for both dry and $scCO_2$ MWF cases. No discernable tool wear is observed with $scCO_2$ MWF, whereas an average wear rate of 3.39 μm/channel is observed for dry machining in condition. Condition 4 (not shown in Figure 3.14) showed an average wear rate of 6.02 μm/channel. The reduction in tool wear observed under $scCO_2$ application may be an outcome of improved lubrication, increased heat removal, increase in material hardness and machinability, or a combination of these factors.

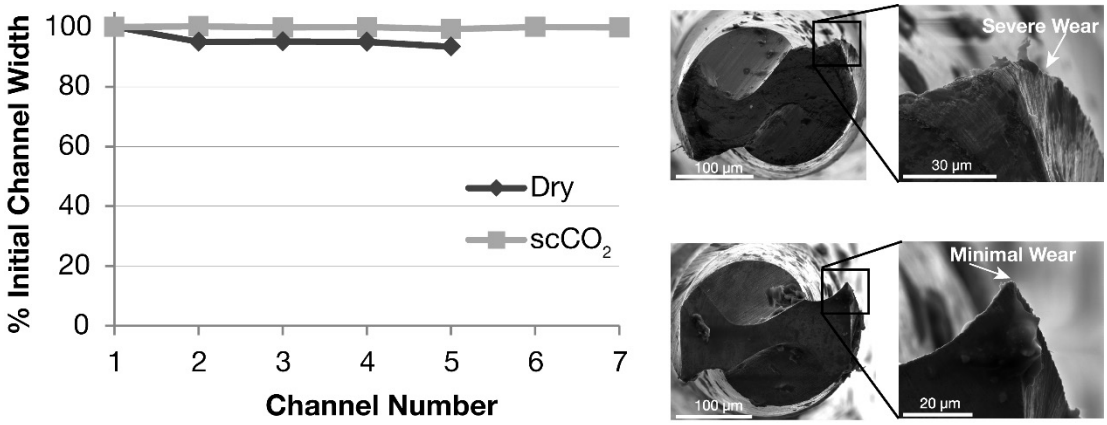

Figure 3.14. Wear progression (left) and SEM images (right) of tool nose wear in dry and $scCO_2$ assisted machining of Cu-101.

For conditions 1 and 3, the tool wear was seen to be comparable for dry and $scCO_2$ MWF cases. It should be noted that width data for the last two channels of dry machining in condition 2 (Figure 3.14, left) could not be obtained due to excessive burr formation, and SEM images of cutting tools for condition 4 could not be obtained due to tool breakage during handling.

3.2.3.3 Burr Formation and Surface Roughness

Figure 3.15 shows a chart of top surface burrs for both stainless steel and copper. Machining parameters (feed, axial depth of cut and cutting speed) for each condition are indicated in parentheses next to the condition number, and their values for each material are shown in Table 3.4. In general, $scCO_2$ MWF assisted machining gives lower burr formation and thus cleaner channels as compared to dry machining. The most significant improvement was seen in conditions 1 and 3 for stainless steel (low feed conditions), and in condition 4 for copper (high feed and highest material removal rate). In conditions 1 and 4 for stainless steel with $scCO_2$ MWF, the tool chipped, thus yielding two distinct depths of cut as seen in Figure 3.15. Further work will be needed to determine whether the chipping was related to the method of applying $scCO_2$ MWF.

The average surface roughness values are shown in Figure 3.16. Compared to dry machining, $scCO_2$ MWF roughness values are lower by up to 69% in stainless steel and up to 33% in copper. In all cases, the observed surface roughness with $scCO_2$ MWF was either equal to or lower than under dry conditions. Improvement in surface finish from lower roughness or reduced burr formation may be attributed to the same factors that are responsible for lower specific cutting energy and tool wear under application of $scCO_2$ MWF. However, verification of this conjecture would require development of a sophisticated set of experiments designed specifically to investigate underlying

mechanisms of cooling, lubrication, and tool wear in micromachining, which was beyond the scope of the feasibility study presented here.

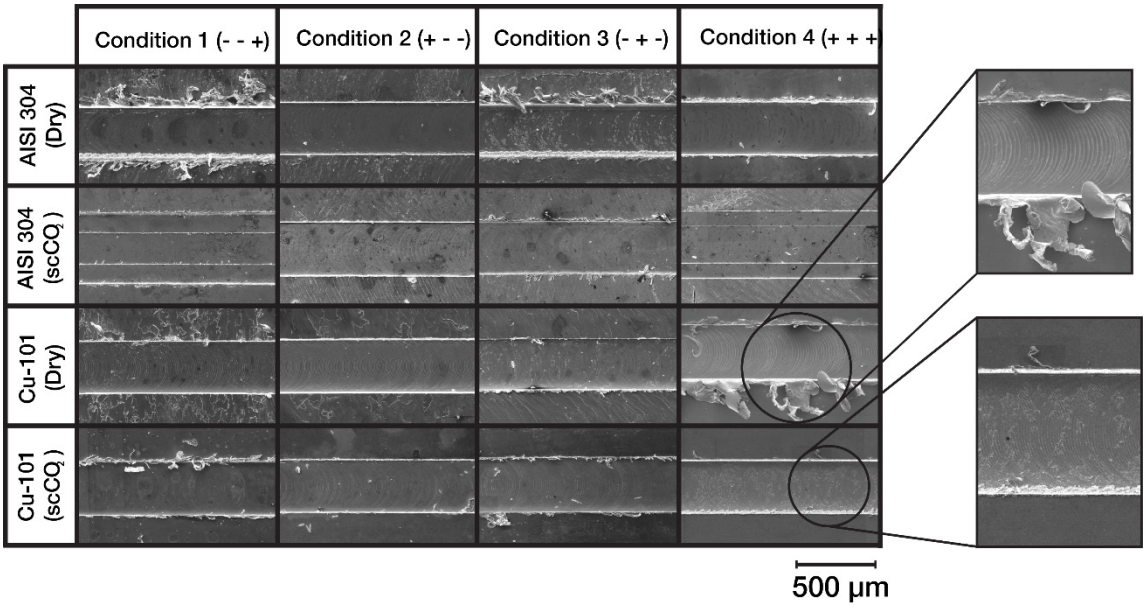

Figure 3.15. Burr formation on AISI 304 and Cu-101 with and without $scCO_2$ MWF for all machining conditions examined where + and – signs in parentheses represent levels of f_z, a_p, and v_c in that order.

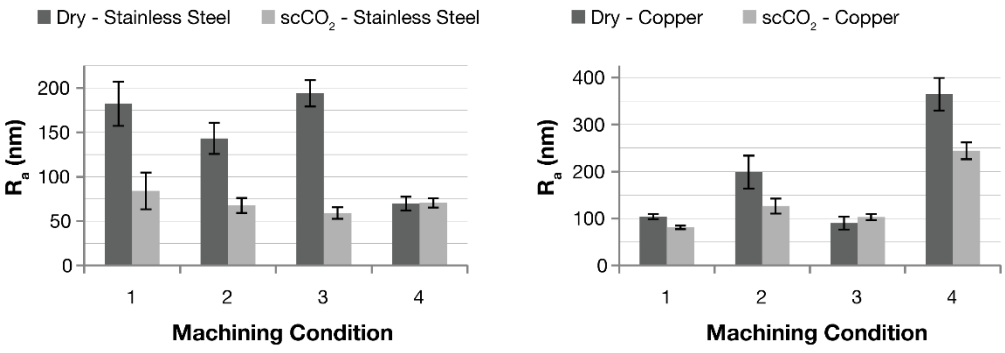

Figure 3.16. Bottom surface roughness (R_a) for AISI 304 (left) and Cu-101 (right) with and without $scCO_2$ MWF for all machining conditions examined

3.2.4 Conclusions

This work investigated the feasibility of using $scCO_2$ based metalworking fluids in the micromilling of stainless steel and copper. Burr formation and surface roughness analyses showed that $scCO_2$ MWFs are effective in improving part quality under most cutting conditions. Average specific cutting energies were also typically observed to be lower when using $scCO_2$ MWF relative to dry conditions. In addition, it was observed that the application of $scCO_2$ MWF reduces tool wear for high feed rate conditions during machining of Cu 101. Based on these results it can be concluded that $scCO_2$ MWFs can be a productive asset to micromachining, and that further research is warranted into its performance relative to other MWFs, as well as into the relative importance of cooling versus lubrication mechanisms in achieving better micro-machinability.

3.3 MARGINAL LIFE CYCLE ENVIRONMENTAL EMISSIONS OF SUPERCTITICAL CO_2 METALWORKING FLUIDS

3.3.1 Goal and Scope of the LCA

To evaluate the life cycle impacts of $scCO_2$ metalworking fluids, we use the life cycle inventory data for beverage grade purity CO_2 obtained from a high purity ammonia or ethanol source, and the allocation methodology for recovered CO_2-based applications presented in CHAPTER 2 of this dissertation. The goal of this life cycle assessment is to estimate the marginal environmental impacts from the use of $scCO_2$ in macro-scale machining to replace aqueous MWFs, and then to compare these marginal impacts with those of competing alternative MWF technologies in the market. Aqueous MWFs are assumed to be a 5% aqueous emulsion of semi-synthetic oil containing surfactants and biocides as per the formulation specified in Byers (2006). System boundaries used in the analysis are shown in Figure 3.17.

Emissions from production of the machine tool and auxiliary machines such as MWF handling systems are excluded from the analysis. Emissions from wastewater treatment were found to be negligible and excluded from the analysis. For all MWFs, cradle-to-gate data on emissions, energy use, and water use were used for each component of the MWF considered in the analysis. Recovered CO_2 source is assumed as ammonia/ethanol production. Environmental impacts were evaluated for the following mid-point categories: 100 year global warming potential, ozone depletion potential, photochemical smog formation potential, acidification potential, eutrophication potential, respiratory effects, ecotoxicity, total energy use, and fresh water use.

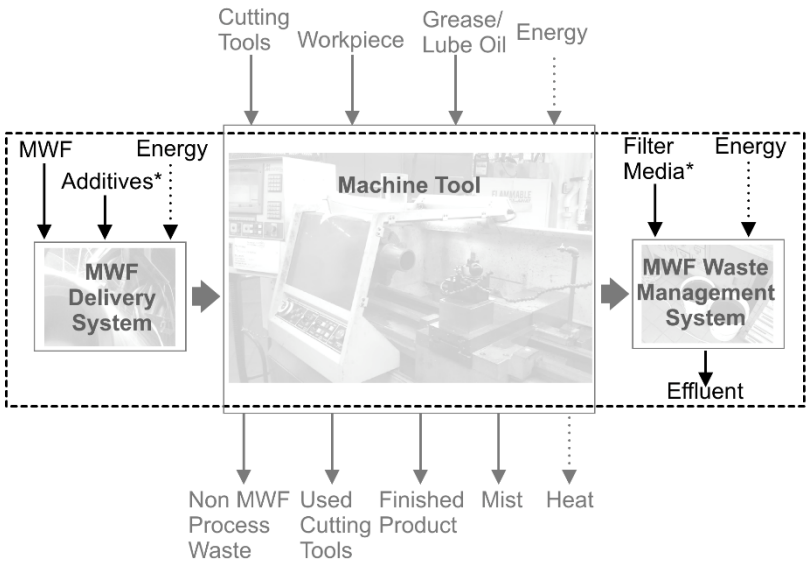

Figure 3.17. System boundaries used in this comparative life cycle assessment of various MWFs.

The functional unit is chosen as the service provided by a MWF system at a machine tool in a medium-size manufacturing facility in Detroit, MI machining Inconel alloy workpieces over a period of one year. Inconel is chosen as the workpiece material because of its recalcitrant machinability, which necessitates the use of MWFs with high heat removal capability (e.g., this rules out traditional minimum quantity lubrication as an option). It is assumed that the machine tool operates for two 8-hour shifts a day for 251 working days in a year with a utilization factor of 60%. The reference flow for the analysis is then the quantity of a MWF used at the facility over a period of one year. Operating conditions used to determine the range of impacts for the various MWFs compared in this study are listed in Table 3.5.

Table 3.5. Operating parameters used for various MWFs to estimate the range of their impacts.

Parameter	Nominal	Low	High	Units
CO2 flowrate	6.0	9.0	19.0	kg/hr
Vegetable oil flowrate	40.0	40.0	500.0	ml/hr
MWF sump replacement frequency	1	2	3	/year
MWF loss from sumps	5%	10%	20%	/day
Water loss rate from cooling (heat exchanger) units	0.50%	2.75%	5.00%	/day
Aq. MWF flowrate	226.8	1134.0	2268.0	kg/hr
HiPr. Aq. MWF flowrate	1200.0	3000.0	3000.0	kg/hr
CO2 Transportation Distance	250	250	1556	km/one way trip
LN2 Transportation Distance	925	925	925	km/one way trip
LN2 flowrate	10.0	20.0	20.0	kg/hr

3.3.2 Results and Discussion

Figure 3.18 shows that a majority of the life cycle environmental impacts of $scCO_2$ MWF are from the recovery of CO_2, which includes energy use for the compression and refrigeration of CO_2 at the ammonia plant. The nominal case in this analysis assumes that the manufacturing facility in Detroit, MI sources its CO_2 from the Lima, OH ammonia plant 250 km away through a local industrial gas supplier. As such, the impacts from transportation of CO_2 to the manufacturing facility contribute only about 25% to the total impacts in most impact categories except smog formation potential where it contributes to 80% of the total impacts.

Impacts in the global warming potential, smog formation potential, acidification potential, and respiratory effects mid point metrics are strongly correlated with the distance of the ammonia plant from which the CO_2 is sourced. CO_2 generated at the ammonia plant in the steam reformer and shift converter counts towards its Scope 1b emissions. The CO_2 in the steam reformer is emitted into the atmosphere at the ammonia plant, and constitutes its Scope 1a emissions. The CO_2 from the shift converter is captured at the ammonia plant, and eventually emitted at the manufacturing facility as spent $scCO_2$ MWF, thus constituting for the manufacturing facility's Scope 1c emissions.

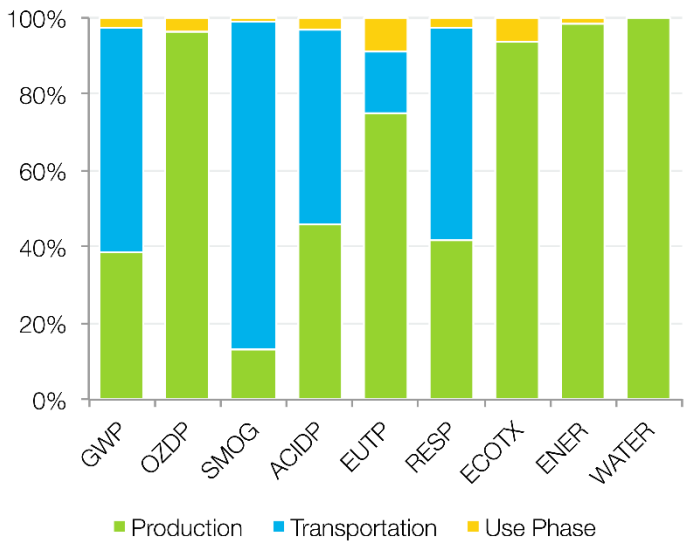

Figure 3.18. Breakdown of $scCO_2$ MWF environmental impacts by various stages in its life cycle. No significant end-of-life impacts observed for $scCO_2$ MWF.

Based on the allocation as well as GHG accounting method proposed in CHAPTER 2, the CO_2 emitted from the manufacturing facility in the form of spent $scCO_2$ MWF is not counted towards the GWP of $scCO_2$ MWF. The GHG emissions in Scopes 1a, 1b, and 1c of the manufacturing facility add up to the GWP potential of $scCO_2$ MWF. Additionally, since spent $scCO_2$ MWF only consists of CO_2 and trace quantities of lubricant, both of which are non-toxic substances requiring no additional treatment, the end-of-life impacts from the use of $scCO_2$ MWF are insignificant.

Figure 3.19 compares the environmental impacts from $scCO_2$ MWF with high pressure aqueous MWF and LN_2 under the nominal operating conditions shown in Table 3.5. It is assumed that the aqueous MWFs are recycled weekly and disposed twice a year after proper primary, secondary and tertiary treatment of the spent MWF. The impacts shown for all MWFs do not include credits from the displaced conventional aqueous MWF end use. Avoided impacts from conventional aqueous MWFs, which are identical for all three MWFs are instead shown separately. These impacts should be

subtracted from the impacts of each substitute MWF to estimate the marginal environmental impacts from the use of that substitute MWF.

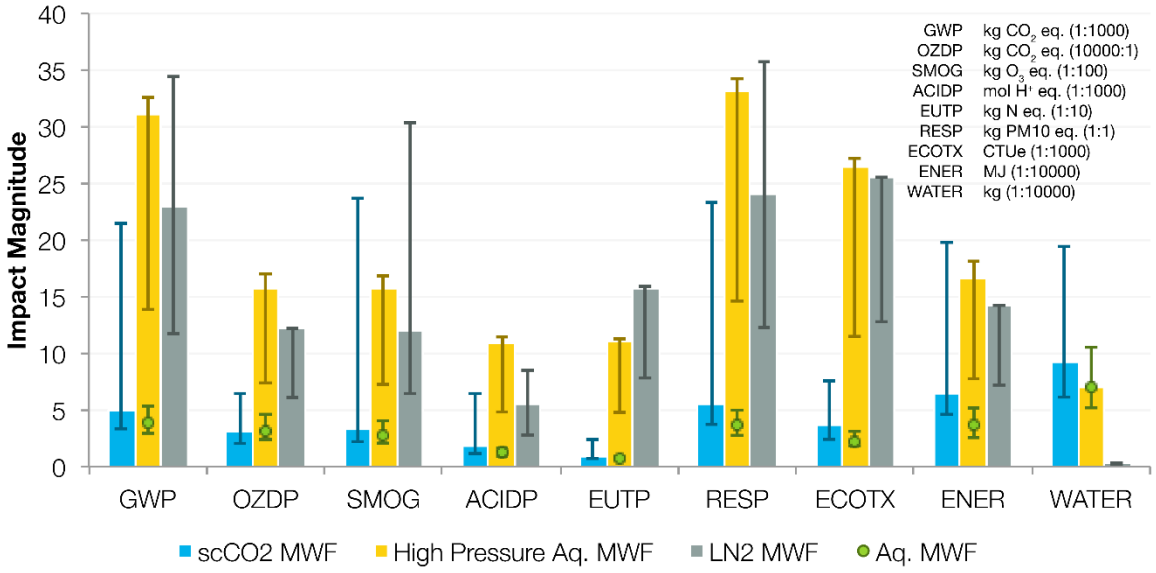

Figure 3.19. Life cycle environmental impacts of $scCO_2$, high pressure aqueous, and liquid nitrogen MWFs without displaced end use credit. Points along the high pressure aqueous MWF data represent values for conventional aqueous MWFs (displaced end use).

It is observed that high pressure aqueous MWF has more than three times the impact of $scCO_2$ MWF in all categories. Most of the increased impact comes from the higher energy required to pressurize the water to about 11 MPa. The equipment, labor, and environmental compliance costs, as well as operator health and safety concerns associated with operating and maintaining conventional aqueous MWF systems still exist for high pressure aqueous MWF as they do for conventional aqueous MWF systems. While the analysis assumes that spent aqueous MWFs are properly treated before being discharged into the environment, this may not always be the case due the lack of specific regulations for MWFs. If untreated spent MWFs are released into the environment, they lead to high level of nutrient loading, human toxicity and ecotoxicity due to the presence of oils, biocides, and heavy

metals. LN_2 is produced using cryogenic air separation, which is an energy intensive process. This leads to higher environmental impacts compared with the other alternative MWFs. Transportation emissions for LN_2 are roughly 35% more than transportation emissions for CO_2, but the overall impacts are dominated by production of LN_2, and are thus strongly correlated with the flow rate of LN_2 MWF. The LN_2 MWF was assumed to be running without a lubricant.

It is important to differentiate and examine the environmental impacts of each MWF system from a qualitative perspective, as well as the quantitative perspective provided in Figure 3.19. For instance, global warming and ozone depletion are global impacts that have an adverse effect on the ecosystems worldwide regardless of the location of the emission source. Smog formation, acidification, eutrophication and ecotoxicity are more regional impacts. Even within each of these regional impacts, there is a qualitative difference between 1kg of pollutant emissions coming from a source such as an ammonia plant or a power plant that may be far away from populous areas, and 1 kg of the same pollutant emission coming from a source such as a transportation truck which causes a more localized impact on the air, water and soil quality. There could thus be a tradeoff between regional air quality and operator health and safety when selecting a MWF system.

The absolute value of the emissions should also be taken into account while assessing the relevance of a particular environmental impact. For instance the GHG emissions from $scCO_2$ MWF are comparable to an average person's annual personal driving GHG emissions, but all of the MWF systems considered here have several hundred times the average person's acidification or photochemical smog footprint. The decision to select a particular alternative MWF system thus has to put the

quantitative LCA results in the context of a qualitative assessment of global, regional and human health impacts relative to the existing levels of pollution. These considerations should be made on a case-by-case basis beginning with the LCA results and approch provided here.

3.3.3 Conclusions

A market based allocation method consistent with consequential life cycle assessment frameworks is proposed for quantifying the market driven emissions associated with the use of recovered carbon dioxide in sustainable manufacturing applications. A greenhouse gas accounting method is also proposed that distinguishes between greenhouse gas generation and emission, thus creating a framework to assess and account for the true environmental impacts associated with utilizing recovered CO_2 to displace manufacturing processes that involve hazardous and energy intensive substances, and, eliminating barriers to the use of recovered CO_2 in such applications owing to previous problems of perception related to the use of mass-based and price-based allocation methods in assessing the environmental burdens of systems based on recovered CO_2 .

The approach is applied to estimate marginal emissions and environmental impacts from using CO_2 generated from an ammonia plant in a supercritical CO_2 metalworking fluid used at a manufacturing facility, while displacing the costly aqueous metalworking fluids that are harmful to operator health. The results indicate significant improvements machining productivity tool life and operator exposures may also come along with significant environmental improvements. Future work should focus on considering other end-use applications as well as understanding the local environmental impacts of recovered CO_2 systems.

3.4 SUPERCRITICAL CARBON DIOXIDE IN MICROELECTRONICS MANUFACTURING

3.4.1 Introduction

The semiconductor devices industry including semiconductor materials, fabrication, and ancillary supply chains is worth nearly $400 billion annually. Increasing demand for consumer electronics in emerging economies, a trend towards integrating CMOS and MEMS systems into a growing number of applications, and advances in data storage and computing point to an annual growth rate of 4.5% to 7.6% over the next four years by some market estimates (KPMG, 2013; Yahoo, 2013). Although semiconductor devices have revolutionized almost every sector within the technosphere, their extremely low-entropy state necessitates high energy and resource consumption (Boyd, 2011; Krishnan, Williams, & Boyd, 2008; Krishnan, Boyd, et al., 2008), and the chemicals used during their manufacture pose significant environmental concerns as well (Lin, Panchangam, & Lo, 2009; Tsai, Chen, & Hsien, 2002). For instance, 1 g of a typical fabricated silicon device using about 41 MJ of energy, 105 L of water, and 280 g of toxic and/or corrosive chemicals (Krishnan, Boyd, et al., 2008). Approximately 50% to 75% of the water consumption at a wafer fabrication facility is from the use of ultrapure water (UPW), which is used as a cleaning agent to wash off photoresist or any other residue that may build up on the wafer surface during the fabrication process. Purification of water to the stringent standards necessitated for this application requires a significant amount of energy, accounting for almost 10% of the fabrication facility's total energy consumption (Hattori, 2011; Mendicino, Mccormack, Gibson, & Covington, 1998).

Besides high water and energy consumption, UPW poses functional challenges too (Hattori, 2011). Cleaning with UPW must be followed by a drying process immediately to prevent the

formation of 'watermarks' on the wafer surface, which can create problems with etching as well growth of subsequent layers particularly for devices with small feature sizes. Water's high surface tension also makes drying small and intricate features more difficult. In some cases, the jet of water (high resistivity) impinging on a spinning wafer can induce an electrostatic charge on the wafer surface causing adhesion of particles post-cleaning. Thus, from an environmental as well as functional perspective, a replacement for UPW would be useful. Researchers have explored several alternatives in the last decade. Out of these alternatives, supercritical carbon dioxide ($scCO_2$) has aroused particular interest. In its supercritical state ($T > T_{crit} = 304.25$ K; $P > Pcrit = 73.1$ bar), CO_2 has the fluidity of a gas, i.e. it has zero surface tension, which allows for wetting of complex features on the wafers. Additionally, CO_2 is acts as a nonpolar solvent for water-insoluble compounds often found in residues or substrates on semiconductor wafer surfaces, which means that surface cleaning can occur through physical mechanisms as well as chemical solubility of impurities.

Although several studies have examined the functional characteristics of $scCO_2$-based wafer cleaning, a comprehensive assessment of its environmental impacts as a substitute for UPW is yet to be performed. The focus of this paper is thus examine the life cycle environmental impacts of using $scCO_2$ as a substitute for UPW as a cleaning agent during the semiconductor wafer fabrication process. A consequential approach is adopted to estimate the marginal emissions from the production of VLSI grade CO_2 needed for use in $scCO_2$-based wafer cleaning.

3.4.2 Methods

Cradle-to-grave life cycle impacts of UPW and $scCO_2$ are compared for their function as cleaning agents. Functional unit for the life cycle assessment is chosen as one cleaning cycle used to clean one

300 mm silicon wafer (1/8" thick) in a cassette of 24 wafers. A monthly production capacity of 50,000 wafers is assumed. Process details for $scCO_2$ and UPW wafer cleaning along with their reference flows are discussed in sections 3.4.2.1 and 3.4.2.2 respectively. Impact assessment is done using the U.S. EPA TRACI 2 method.

3.4.2.1 Life Cycle Inventory of Recovered CO_2

CO_2 used in the wafer cleaning application was assumed to be recovered from an ammonia plant due to its high raw feed gas purity and partial pressure compared to CO_2 recovered from flue gases, as well as fewer trace impurities than other high purity sources such as ammonia and hydrogen plants. The life cycle inventory and allocation method for recovered CO_2-based applications developed in CHAPTER 2 were used for estimating the marginal environmental impacts of the $scCO_2$ wafer cleaning process. The approach allocates impacts to CO_2 recovered as a byproduct or co-product on a causal basis. Thus, only impacts from processes that are affected on the margin due to the demand for recovered CO_2 are attributed to CO_2. The marginal processes for VLSI grade CO_2 used in semiconductor wafer cleaning (≥ 99.995% purity) are those involved in purification, dehydration, liquefaction, and transport of CO_2. Purification steps include the specific processes and materials needed to obtain purity beyond just industrial grade (≥ 99.5% purity) CO_2.

The liquid CO_2 obtained from the recover plant is assumed to be transported in tankers via heavy-duty trucks to the CO_2 end-user. Transportation emissions were allocated per wafer assuming that a 20,000 L capacity tanker delivers CO_2 to a wafer fabrication processing facility producing about 50,000 wafers per month at the delivery frequency necessitated by the CO_2 consumption rate at the facility. Emissions from transporting an empty tanker back to the CO_2 production facility were also

attributed to CO_2. This allocation method is chosen to represent the worst-case scenario for transportation emissions for recovered CO_2. The wafer cleaning facility was assumed to be the University of Michigan Lurie Nanofabrication Laboratory in Ann Arbor, MI, USA, and the CO_2 was assumed sourced from the nearest ethanol-byproduct CO_2 recovery plant located 80 km away in Riga, MI, USA. It should be noted that emissions associated with production and transportation of AC, molsieves, filters and all capital equipment were outside the system boundaries of this LCA.

During the use phase, liquid CO_2 at room temperature is compressed to about 310 bars and cooled to about 338 K to achieve supercritical conditions for required for wafer cleaning. In addition to $scCO_2$, propylene carbonate (PCO3) is used as a co-solvent in a 15% v/v ratio with $scCO_2$. Emissions from PCO3 production were obtained by creating a model of its production process from propylene oxide and carbon dioxide in SimaPro v.7.3.3, (2012) using the Ecoinvent 2.2 database. Assuming stoichiometric conditions and a process yield of 90%, 1.95 kg of propylene oxide is assumed to react with 2.57 kg of supercritical carbon dioxide in an autoclave for 12 hours under constant stirring (Du, Cai, Kong, & He, 2005). The PCO3 was assumed to be sourced from a supplier in Rochester, NY, USA.

The $scCO_2$ wafer cleaning process and data on its energy use, CO_2 consumption, and PCO3 consumption were based on Blowers & Titus (2004), who state that the wafer cleaning operation after any fabrication step involves the following steps: (a) $scCO_2$ system start-up, (b) purging of the cleaning system, (c) cleaning operation, (d) post-cleaning separation of impurities and co-solvent from $scCO_2$ via throttling, and (e) flushing of system with pure CO_2. This sequence of steps is repeated for every

cleaning step during the wafer fabrication process. It is assumed that during the process of separating the impurities from CO_2, all the CO_2 is fully recovered, and all the co-solvent is lost. CO_2 is lost only during the start-up and purging steps, and thus each cleaning cycle requires 1.02 kg of CO_2 and 0.27 kg of PCO3. Reference flows for the $scCO_2$ cleaning system are calculated based on these use phase consumption data for CO_2 and PCO3.

3.4.2.2 Life Cycle Inventory of Ultrapure Water

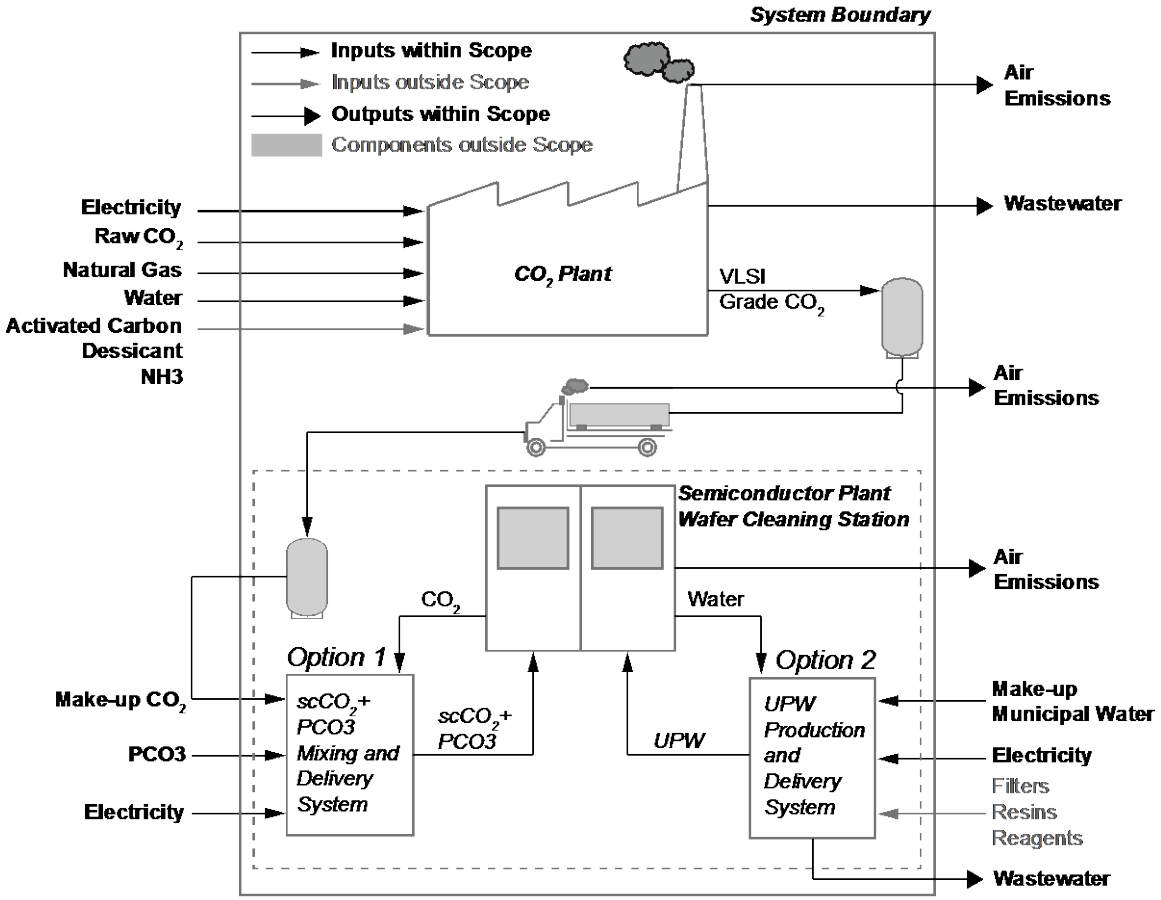

Figure 3.20. System boundaries used in this life cycle assessment.

Production of UPW involves on-site purification of potable municipal water at the wafer fabrication facility involving multi-media filtration, reverse osmosis (RO), vacuum degasification,

mixed-bed demineralization, UV sterilization, and ultrafiltration of the municipal water (Mendicino et al., 1998). Due to the low yield of the RO process, energy intensive regeneration steps, high wattage UV lamps, and high water pressure needed across the ultrafiltration membranes (about 20 bar), the energy consumption of UPW is about 17.5 kJ/kg, which is over five times the specific energy consumption of municipal water. For every kg of UPW produced, 1.5 kg of municipal water is used since a large portion of the municipal water is lost during the RO process (Mendicino et al., 1998). Upstream emissions from energy use at the municipal water plant, and downstream emissions from energy use at the wastewater treatment plant are included in the life cycle inventory. Life cycle impacts of consumables such as filters, resins, and acids are outside the system boundaries. Figure 3.20 shows the system boundaries used for the life cycle assessment (only one wafer cleaning option between $scCO_2$ + PCO3 and UPW is assumed to be used at the facility).

3.4.3 Results and Discussion

3.4.3.1 Production Impacts of VLSI grade CO_2

Recovery, purification, and liquefaction of 1 kg of VLSI grade CO_2 from an ethanol plant requires about 2.69 MJ of energy, 4.23 liters of water, and leads to a global warming potential (GWP) of 163.9 g CO_2 eq. Table 3.6 lists TRACI impact categories and resource consumption metrics examined in this study. These impacts are further broken down by major source in Figure 3.21. Indirect emissions from electricity use at the CO_2 recovery plant account for the majority of impacts in almost all the categories examined. On-site natural gas combustion for generating steam, and heating air and dry CO_2 during regeneration/drying of AC and molsieve beds however, accounts for about 50% of the total (direct + indirect) energy use. CO_2 from natural gas combustion together with fugitive losses of

natural gas contribute to 35% of GWP. Only about 10% of the total water consumption occurs from on-site use is for cooling and steam generation.

Non-combustion contributions to on-site impacts (emissions and energy/water use at the recovery plant) of CO_2 recovery include natural gas fugitive emissions contributing to GWP, once-through scrubbing water contributing to water use, and fugitive ammonia emissions contributing to acidification and eutrophication potential. It should be noted that emission of impurities such as sulfides, alcohols, and ketones that are present in the vent gas of the recovered CO_2 plant are not attributed to the recovered CO_2. This is because these impurities source from feedstock and chemicals used to produce ammonia, and would be emitted to the atmosphere even in the absence of a CO_2 recovery plant. Furthermore, the demand for recovered CO_2 is unlikely to affect the demand for ammonia, and thus it is unlikely that larger quantities of ethanol and thus higher emissions of impurities will be produced due to demand for recovered CO_2.

Table 3.6. Production impacts of 1 kg of CO_2 recovered as a byproduct of ethanol production and purified to VLSI grade.

Impact Category	Abbrev.	Value	Units
Global warming potential	GWP	163.9	g CO2 eq.
Ozone depletion potential	OZDP	13.6	g CFC-11 eq.
Smog potential	SMOG	5.65	g O3 eq.
Acidification potential	ACIDP	61.3	mmol H+ eq.
Eutrophication potential	EUTP	0.38	g N eq.
Respiratory effects	RESP	0.185	g PM10 eq.
Ecotoxicity	ECOTX	0.156	CTUe
Energy use	ENER	2.69	MJ
Water use	WATER	4.23	Liters

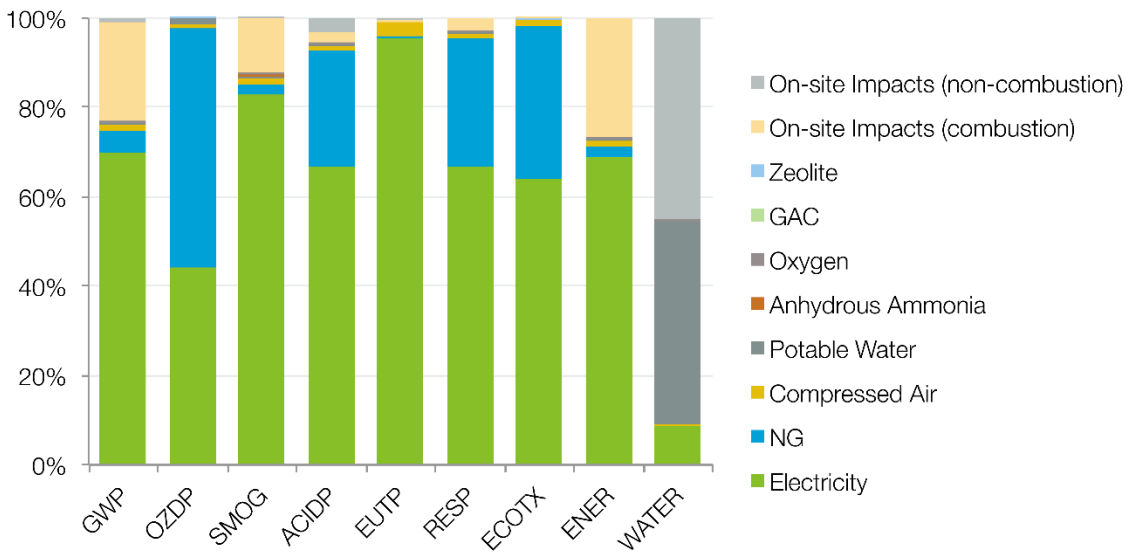

Figure 3.21. Production impacts of 1 kg of VLSI grade CO_2 categorized by source.

Per kg of CO_2 processed in each step, purification steps account for about 60% of the total energy consumption of recovered CO_2. However, when the process yield of AC adsorption, loss of dry CO_2 for molsieve bed regeneration during drying, and reboiler duty for CO_2 distillation is taken into account, only about 52% of the CO_2 feed gas is obtained as the output of the entire recovery and purification process. Upon factoring the cumulative yields of each step in the recovery and purification process, the compressor energy use changes from 294 kJ/kg CO_2 to 566 kJ/kg CO_2 output, and together with refrigeration (540 kJ/kg CO_2 output) accounts for about 90% of total on-site electricity use and 30% of total on-site energy use. The purification steps thus have a profound impact, both directly and indirectly, on the total energy consumption and GWP of recovered CO_2. By comparison, industrial grade CO_2 (> 99.5% purity) requires just 1.8 MJ of on-site energy use per kg of CO_2 output, which is approximately half of the on-site energy use for VLSI grade CO_2.

3.4.3.2 CO_2 Transportation and Use Phase Impacts

Assuming a cassette capacity of 24 wafers, cleaning of one wafer over one cleaning cycle using $scCO_2$-PCO3 solvent mixture requires 41.7 g of CO_2 and 11.3 g of PCO3 along with 51.2 kJ of electricity. Based on this CO_2 usage per wafer, CO_2 transportation emissions per wafer are calculated. Combining the transportation and use phase inventories with the production phase inventory, cradle-to-grave impacts of using $scCO_2$ for semiconductor wafer cleaning are calculated and shown in Table 3.7. A breakdown of these impacts by life cycle stage is illustrated in Figure 3.22.

Table 3.7. Cradle-to-grave impacts of using VLSI grade CO_2 recovered as a byproduct of ethanol production for semiconductor wafer cleaning.

Impact Category	Abbreviation	Value	Units (per wafer)
Global warming potential	GWP	1.19E-01	kg CO2 eq.
Smog potential	SMOG	6.59E-03	kg O3 eq.
Acidification potential	ACIDP	2.81E-02	mol H+ eq.
Eutrophication potential	EUTP	8.58E-04	kg N eq.
Respiratory effects	RESP	1.16E-04	kg PM10 eq.
Ecotoxicity	ECOTX	2.11E-01	CTUe
Energy Use	ENER	4.01E-01	MJ
Water Use	WATER	1.92E+00	kg

Based on the results, it can be observed that upstream processes involved in the production of PCO3 are the most significant contributors to the life cycle impacts of $scCO_2$-based semiconductor wafer cleaning. Propylene oxide, from which PCO3 is synthesized by reaction with liquid carbon dioxide in a pressurized heated vessel, has a large embodied energy due to its use of sodium hydroxide and liquid chlorine which are both highly energy intensive chemicals to produce.

CO_2 transportation emissions per wafer cleaned are found to be negligible due to low the relatively low amount of CO_2 lost per cleaning cycle. Use phase emissions associated with CO_2 alone (i.e.

without including PCO3) in every impact category are found to be lower than production phase emissions. Most of the use phase emissions are from electricity use by the CO_2 compressor, which is required to compress CO_2 to pressures between 60 bars and 310 bars during the various steps involved in a wafer cleaning cycle. In fact, electricity use during use phase is about 1.39 MJ/kg of CO_2, which is slightly higher than the value of 1.25 MJ/kg CO_2 output calculated for the production phase electricity use.

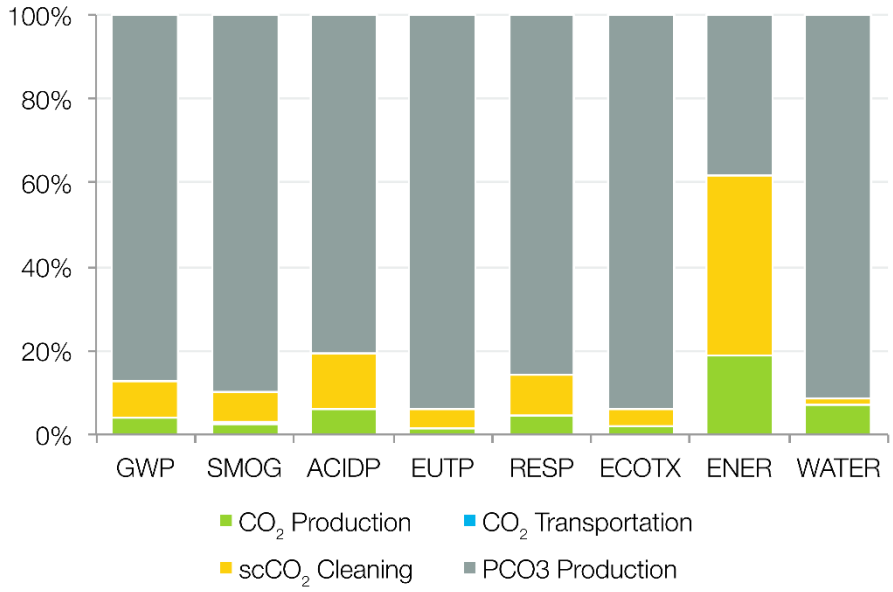

Figure 3.22. Life cycle impacts of VLSI grade CO_2 with PCO3 co-solvent to clean one semiconductor wafer categorized by life cycle phase.

3.4.3.3 Ultrapure Water Impacts

A typical semiconductor wafer fabrication facility uses 5040 liters of UPW, and 198 MJ of electricity per wafer (Mendicino et al., 1998). Furthermore, there are about 130 steps in the fabrication of a wafer that require surface cleaning (Blowers & Titus, 2004). Thus, the direct energy and water use per wafer in one cleaning step is 1.52 MJ and 87.2 liters respectively.

3.4.3.4 Comparison of $scCO_2$ and Ultrapure Water

Assuming that the cleaning performance provided by $scCO_2$ and UPW under the operating conditions assumed in this study is comparable, the life cycle impacts of $scCO_2$ + PCO3 co-solvent are significantly lower than those of UPW in every impact category examined. Figure 3.23 shows life cycle impacts of $scCO_2$ + propylene solvent normalized to UPW impacts. Water consumption of $scCO_2$ + PCO3 is only about 2.5% of UPW's water consumption which is 101 liters. Ecotoxicity of $scCO_2$ + PCO3 as a fraction of UPW's impact is higher than other impact categories due to the high upstream coal-based electricity use in production of PCO3. Additionally, PCO3 itself has an ecotoxicity of about 5.1 CTUe (equivalent to 17.7 g of 2,4-D).

A co-solvent with $scCO_2$ is essential to reduce the bond between photoresist and the wafer surface to facilitate dissolution of the photoresist material into $scCO_2$. Although PCO3 has relatively lower toxicity than other co-solvents such as methylene chloride and methyl chloroform, its contribution to the overall impacts of $scCO_2$-based wafer cleaning is quite significant. One way to reduce this impact is to use a lower concentration of PCO3 in the $scCO_2$ cleaning solution. For instance J. B. Rubin, Davenhall, Barton, Taylor, & Tiefert (1998) used 5% by volume of PCO3 in $scCO_2$ applied in a pulsed manner similar to the one assumed in Blowers & Titus (2004) which is used to characterize the use phase in this paper. By using a 5% PCO3 solution, life cycle impacts of the $scCO_2$ + PCO3 cleaning solution can be within 25% of UPW's life cycle impacts in every impact category examined. Alternate co-solvents such as acetic acid could also be explored.

3.4.3.5 Uncertainty and Sensitivity Analysis

A preliminary uncertainty and sensitivity (sensitivity defined as % change in output per unit % change in input) analysis on $scCO_2$ + PCO3 and UPW use phase operating parameters reveals that energy use as well as impact categories such as GWP, SMOG, ACIDP, EUTP, ECOTX, and RESP that are associated with energy use are highly sensitive to the number of wafers processed per cassette (sensitivity > 2.0 for all categories), and PCO3 concentration (sensitivity > 0.7 for all categories). Impacts are found to be weakly sensitive to flow rate of CO_2 (sensitivity between 0.04 to 0.13 for different categories), thermal efficiency of regeneration steam boiler in the CO_2 recovery process (sensitivity between 0.07 to 0.3 for different categories), and start-up/purge cycle time (sensitivity between 0.1 to 0.6 for different categories). Uncertainty bounds on the relative impact of $scCO_2$ + PCO3 cleaning solution against UPW shown in Figure 3.23 are estimated by running the LCA model with the parameters shown in Table 3.8. The uncertainty analysis indicates that $scCO_2$ + PCO3 shows a reduction in all impact categories even in the worst-case scenario assumed in this study. Although $scCO_2$ + PCO3 shows higher values for EUTP and ECOTX in the worst-case scenario primarily due to the lower number of wafers per cassette, it is likely that a commercial semiconductor manufacturer will try to maximize the number of wafers per cassette is quite low for cost reasons. Thus, the overall impacts of $scCO_2$ + PCO3 are more likely to be around the nominal value shown in Figure 3.23.

Transportation distance has a marginal effect on the life cycle emissions of $scCO_2$ cleaning solution. If the VLSI grade CO_2 is assumed to be sourced from the ethanol CO_2 recovery plant in Lawrenceburg, IN, USA located 391 km away from Ann Arbor, a slight increase in SMOG and RESP is observed due to increased emissions of NOx and particulates from the diesel truck. However, the

contribution of transporation emissions to total life cycle emissions in these impact categories still remains less than 0.5%.

Table 3.8. Values of parameters used for estimating bounds on life cycle impacts of $scCO_2$ + propylene carbonate cleaning solution.

Parameter	Nominal Value	Lower Bound	Upper Bound
Use Phase			
Number of wafers per cassette	24	12	24
PCO3 concentration	15%	5%	15%
Total number of cleaning steps	130	117	143
Flow rate of $scCO_2$ (L/s)	6	6	8
Start-up and purge cycle time (s)	5	5	10
CO_2 Production Phase			
Feed gas impurities (w/w)	3%	1%	5%
Regeneration steam boiler thermal efficiency	90%	80%	95%
Transportation distance (km)	83	83	391

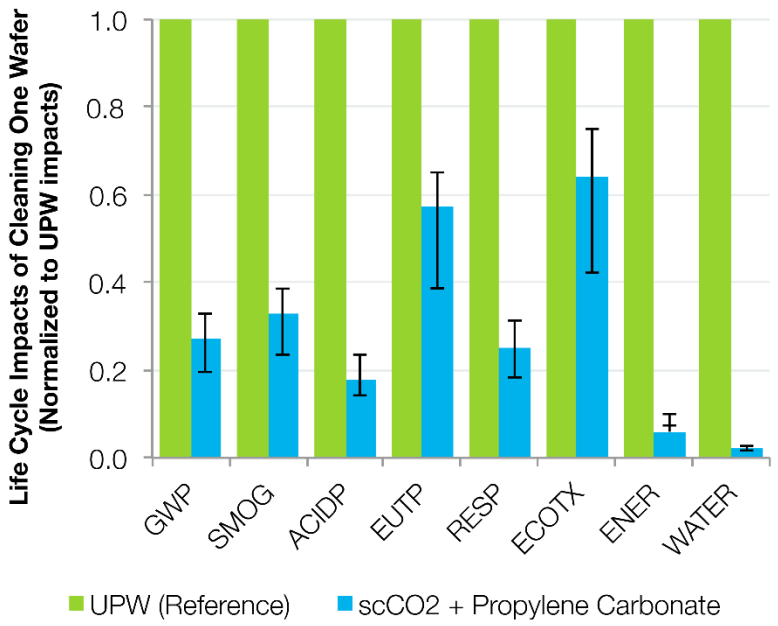

Figure 3.23. Life cycle impacts of $scCO_2$ with PCO3 co-solvent relative to impacts of UPW.

The loss of CO_2 and thus CO_2 consumption rate per cleaning cycle is determined by the duration of the start-up and purging cycles. While these times are assumed to be about 5 s in this study based

on Blowers & Titus (2004), it is possible that higher cycle times or larger CO_2 flow rates can be employed during these steps. A ten-fold increase in CO_2 consumption due to either an increase in cycle time, flow rate, or a combination of both will still result in lower life cycle impacts than UPW in all impact categories examined under the nominal operating conditions. Under this ten-fold CO_2 consumption increase scenario, more than 40% of life cycle impacts in all categories are from the production of VLSI grade CO_2.

3.4.4 Conclusions

This work presented a process-based consequential life cycle inventory of VLSI grade CO_2 used together with propylene carbonate as a cleaning agent during semiconductor wafer fabrication processes. The life cycle impacts of supercritical CO_2-based wafer cleaning were compared with those of ultrapure water. It was found that $scCO_2$-based cleaning system has a lower life cycle impact than UPW under the impact categories examined in the study. Impacts of recovered CO_2 were largely from energy intensive and low yield purification steps that are necessary to remove trance impurities and water vapor to achieve greater than 99.998% v/v purity of VLSI grade CO_2. However, the majority of life cycle impacts of $scCO_2$-based cleaning systems were found to be primarily from PCO3 (co-solvent) use.

Semiconductor manufacturers aim to maximize throughput without affecting process yield as indicated by readily available commercial wafer cassettes with capacities of 24 wafers or higher as assumed in this study. Furthermore, the combined mechanical and solvent-based cleaning action of $scCO_2$ + PCO3 means that it can likely achieve effective cleaning at flow rates of about 6-8 L/min as assumed in this study. Thus, based on a consequential approach, $scCO_2$-based cleaning systems can

lead to a net reduction in environmental emissions, energy use, and as much as 90% reduction in water use. The results from this study thus warrant further development of $scCO_2$-based technology to replace ultrapure water in semiconductor wafer cleaning applications.

CHAPTER 4

LEAST-COST STRATEGIES FOR CARBON DIOXIDE ABATEMENT IN THE ELECTRIC AND AUTOMOTIVE SECTORS

4.1 INTRODUCTION

Unmitigated emission of greenhouse gases (GHGs) is concerning for a number of social, environmental and economic reasons, many of which are caused by the projected global temperature increase. Despite the recent global economic recession, GHG emissions have continued to increase globally. Under business-as-usual conditions, these emissions are projected to continue to increase at a rapid pace. In their Fourth Assessment Report (AR4), the Intergovernmental Panel on Climate Change (IPCC) has tested a number of scenarios ranging from low to high emission activity under current climate action policies, and all the scenarios project an increase in global temperature (Intergovernmental Panel on Climate Change, 2007). Scenarios leading to emission stabilization curves through 2100 will have to rely on currently available technologies as well as technologies with potential commercial viability in order to achieve the requisite emission reductions. The AR4 report also emphasizes the significance of emission reduction efforts over the next three decades in achieving long-term CO_2 stabilization levels.

These technology-related conclusions in AR4 hold significant implications for the United States (U.S.) automotive and electric power sectors. According to 2008 statistics, the U.S., which accounted

for about 4.5% of the world's population, contributed about 21% of the world's GHG emissions (U.S. DoE/EIA, 2011). Figure 1.1, which shows the breakdown of these GHG emissions by sector, indicates that about 60% of the total U.S. GHG emissions come from the transportation and electric power generation sectors. As such, a large proportion of emission reduction strategies should be focused on these two sectors. This conclusion is corroborated by the IPCC's study of emission mitigation potentials over the next three decades (Intergovernmental Panel on Climate Change, 2007). Use phase emissions (emissions from combustion of fuels) from light duty vehicles (i.e. passenger cars and light trucks), and electricity generation accounts for roughly 80% of the transportation and power sector emissions, and are thus treated as the focus of the emission mitigation strategies and technologies presented in this work.

The IPCC's TAR (IPCC, 2001) and AR4 (Intergovernmental Panel on Climate Change, 2007) reports suggest that to keep the global mean temperature rise (compared to pre-industrial times) at stabilization in the range of 2.0 - 2.4 °C, a reduction of 85-50% is required in global GHG emissions by 2050. Although technologies exist to achieve such an emission reduction target by 2050, economically meeting the mobility and electricity needs of society while drastically reducing associated GHG emissions depends not just on the mere existence of a carbon-neutral technology, but critically on the diffusion of such technologies into the market. For instance, successful automotive sector emission reduction through the displacement of internal combustion engine (ICE) vehicles by advanced electrification technology depends on sufficient market adoption, and the accessibility to low-carbon electricity sources.

Cutting edge research on alternative fuels and technologies has lead to significant improvements in the fuel consumption of vehicles and power plants in the last two decades, and advances in this research continue to project an optimistic outlook for eventually moving towards a low-carbon economy. However, the social cost of carbon emissions, which includes damages to ecosystems, loss in economic output, and adaptation measures, increases with every year of delay in climate action; that is, a unit of CO_2 emitted in the future has the potential to cause more environmental and social damage than a unit emitted today (Stern, 2008; United States Government, 2013). By extension, avoiding a unit of CO_2 emission today will have a higher potential to mitigate environmental and social damages than a unit of CO_2 emission in the future. There may, however, be a trade-off in terms of the technological and social costs of cutting a unit of CO_2 emission today versus in the future due to the anticipated improvements in carbon abatement technologies and their associated costs.

A significant body of literature has evaluated the costs of climate inaction, and unequivocally suggests that inaction only stands to increase the *overall* societal costs associated with climate change mitigation and adaptation (Butler, Reed, Fisher-Vanden, Keller, & Wagener, 2014; Rogelj, McCollum, Reisinger, Meinshausen, & Riahi, 2013; Stern, 2008). However, in the absence of formally implemented and committed carbon emission constraining measures such as carbon taxes or permits across the world's largest GHG emitters, it is highly unlikely that the economic externalities of climate inaction will be internalized and reflected in energy services production and consumption. As such, the visible costs of carbon abatement for producers, consumers, and governments, collectively called "the society" in the context of this work, are those associated with producing/buying, operating, maintaining, and scrapping technologies that provide energy services, both in the present and future.

An analysis that focuses on only the technological costs of climate action delay, specifically in the U.S., is absent from the literature, and knowledge this gap serves as the motivation for this work.

The overarching goals of the study are thus to (1) quantify the technological costs of climate action delay in the U.S. electricity and automotive sectors, and (2) identify technology pathways for both sectors to achieve at least 60% reduction in emissions compared to 1990 levels at least cost relative to the business-as-usual (BAU) case. The mathematical formulation, input data, and a description of various technology and regulation scenarios investigated in the study are first discussed, followed by a detailed discussion of the results and their policy implications.

4.2 MODEL FRAMEWORK AND MATHEMATICAL FORMULATION

This study develops a bottom-up model of the light duty vehicle (LDV) and electricity utility power generation (electric utility) fleets by considering various technologies currently available in these two sectors. Light duty vehicles, which include passenger cars and light trucks, are chosen here for analysis since they collectively contribute to nearly 60% of the total transportation sector emissions in the U.S. *Technology* is defined in this study at a high level as a type of vehicle or generator (e.g. hybrid electrics, coal powered generator), and each vehicle or generator capacity is called a *unit*. Cost and emission characteristics of technology units are used to determine their total lifetime cost and CO_2 emissions. A stock-and-flow model of fleets, representing stocks of existing units and flows of new units, is developed on a yearly scale, meaning all capital and operating costs associated with each unit are incurred on the first day of the year. We also assume that technologies used to meet the demand for mobility (vehicle miles travelled) or electricity (MWh of electricity generated) in a given year will be selected such that the total lifetime cost of purchasing and operating a unit of the technology are

minimized. As a result of this assumption, we apply a design optimization framework to the stock-and-flow model of fleets to minimize the net present value of lifetime costs over a known time horizon. The framework allows imposition of emission, fleet population, and market constraints Figure 4.1 shows a graphical representation of the model. Elements of the stock-and-flow fleet model and optimization framework are discussed in detail in the following sub-sections.

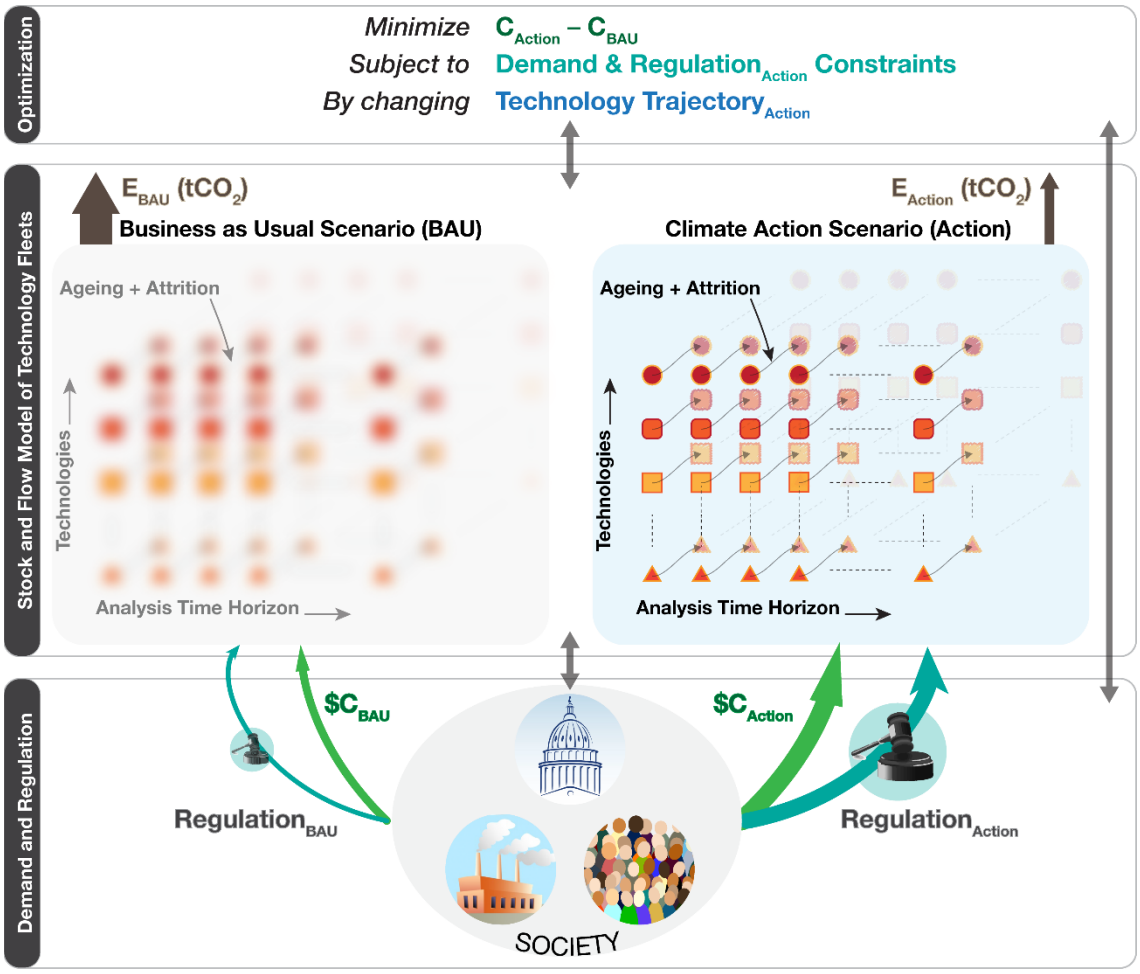

Figure 4.1. Framework and information exchanges in the stock-and-flow optimization model for the U.S. automotive and electricity generation fleets.

4.2.1 Technologies, Assumptions, and Data Sources

4.2.1.1 Light Duty Vehicle Sector

The technologies considered in the LDV (auto) sector are (1) conventional fossil fuel-driven vehicles (CV), (2) hybrid electric vehicles that operate partially on fossil fuels (HEV), (3) battery electric vehicles (BEV), and (4) plug-in hybrid electric vehicles (PHEVs). For tractability, all vehicle segments within each technology type such as compact, mid-side sedan, SUVs, and light trucks are treated as one representative vehicle. Fuel economy and price each representative vehicle is calculated as a sales-weighted average value for the year 2011 based on EIA data (U.S. Energy Information Administration, 2011), and shown in Table 4.1. The time horizon of interest for this study is 2011 to 2050, i.e. forty years. However, operating costs beyond 2050 for units deployed before 2050 also need to be included in the NPV calculation of lifetime costs. To achieve this, the cost-minimization model for the LDV and utility sectors is run for sixty and eighty years respectively, although technology trajectories and costs are presented and discussed only for the period from 2011 to 2050. Annual costs and emissions for each unit of a given technology type are based on various data sources and assumptions discussed in detail below.

Table 4.1. Sales-weighted fuel economies and prices of representative vehicles for various technologies in the light duty vehicle sector. Prices of electric vehicles do not include subsidies since the model calculates total cost to society.

Representative Vehicle	Sales-Weighted MPG	Sales-Weighted Price
CV	21.9	$25,754
HEV	40.3	$29,210
BEV	145.3	$96,200
PHEV	55.2	$40,832

Deployment (sales) costs of new vehicles are based on the average 2011 sales prices of the basic versions of each vehicle technology. Annual maintenance cost for CVs is assumed to be $400 and $600 for the remaining battery-based technologies. The model allows retirement of units before their designed service (critical) life, which in the case of LDVs is assumed as 20 years for all four technologies. All vehicles are assumed to be scrapped after their critical age. Retiring vehicles in operation before they reach their critical life (forced retirement) incurs a penalty due to a shortened operating life, and increases deployment requirements allowing for technology replacement. The newer the vehicle is, the higher the penalty. Scrappage values for various technologies are obtained from Allgemeiner Deutscher Automobil-Club e.v. (2014) based on the average loss in value of vehicles with age, and the retirement cost of a unit of a specific technology type and age is assumed to be equal to its value.

Fuel economies (mpg) of vehicles before 2010 are assumed to align with the Corporate Average Fuel Economy (CAFE) standards for the year of manufacture of the vehicle. For vehicles sold after 2010, fuel economies for each technology type are assumed to increase at a constant rate of 1-2%, until 2030, and at 0.5-1% thereafter (see Appendix H and Appendix I). This assumption is made based on the recent trend towards increased fuel economy due to stricter CAFE standards. The assumed fuel economy improvements lead to CV fuel economies that are between 70% and 90% of the CAFE standard, but fuel economies of HEVs are higher than the CAFE standard in most years. For this study, the 2010 data compiled by the U.S. Department of Transportation – National Highway Traffic Safety Administration regarding vehicle registrations (U.S. Department of

Transportation (FHWA), 2010), and summary CAFE standards (U.S. Department of Transportation (NHTSA), 2011) since 1978 is used for the total population and fuel economy values of LDVs.

New vehicles deployed in any given year make up for the number of vehicles scrapped that year plus the projected increase in the total number of vehicles over the previous year, which is assumed to follow the EIA's projections (U.S. Energy Information Administration, 2011). The vehicle scrappage function is expressed as a logistic function of age of the form $d(t) = 1 \Big/ \left\{ A_0 + e^{-(A_1 + A_2 t)} \right\}$ based on Greene & Chen (1981) where t is the age of the vehicle and $d(t)$ is the discard probability (scrappage probability) function. The discard probability function is assumed to only be a function of vehicle age and not the year in which the vehicle was produced. Furthermore, it defines the probability that a vehicle of a certain age will be scrapped during its operation in the subsequent year. Using LDV sales values from 1990 to 2010, total vehicles on road in 2010, and the total emissions from the LDV sector in 2010 (data and sources shown in Appendix E), the parameter coefficients A_0, A_1, and A_2 are determined using the Microsoft® Excel GRG non-linear solver.

The solver changes the values of A_0, A_1, and A_2, and thus of $d(t)$ such that the age distribution of the fleet so obtained minimizes the square of the error between reported and predicted number of total vehicles, and subject to the constraint that the error in reported and predicted values of total sector-wide GHG emissions is less than or equal to 1%. Due to the nonlinear nature of the objective function and constraint in A_0, A_1, and A_2, the optimization was run with 100 starting points of A_0, A_1, and A_2. The set of values of A_0, A_1, and A_2 that gave the lowest objective function value were selected as the global optimizers. These values yield less than 1% inaccuracy in the total vehicle population and total

emissions value. The discard probability function for LDVs based on the 2010 fleet data shown in Appendix E is expressed as follows.

$$d(t) = \frac{1}{0.95 + e^{10.0292 - 0.6512t}}$$

.....Equation 4.1

Note that *d(t)* is the one-year survival probability, that is, conditional on having survived *t* years, *d(t)* gives the probability that the unit will survive until year *t*+1. Figure 4.2 shows the plot of the discard probability function with age. The survival probability *P(t)* is 1–*d(t)*. Other important assumptions and sources are listed in Appendix F.

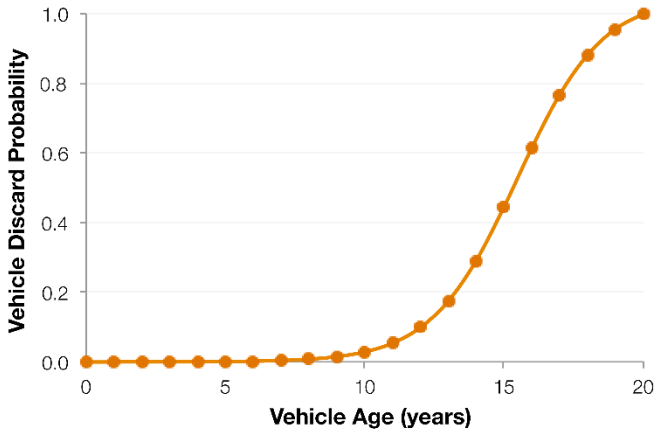

Figure 4.2. Vehicle discard (scrappage) probability as a function of its age. Values indicate the cumulative probability that a vehicle of a given age operating in a given year will be scrapped by the end of that year.

4.2.1.2 Electric Utility Sector

In the utility sector, the nine technology platforms for electricity generation considered in this study are coal (C), natural gas (NG), petroleum (P), biomass (B), nuclear (N), hydro (H), wind (W), solar (S), and geothermal (G). The model does not currently consider distribution or transmission efficiency or energy losses, nor does it include costs for grid infrastructure. Within the sector, discrete

generators are not considered. Instead, megawatt-hours (MWh) generated by each technology type are treated as continuous, and then deployed together and retired in kind. Operating constraints associated with electricity dispatch such as spinning reserves are not included in the scope of the model.

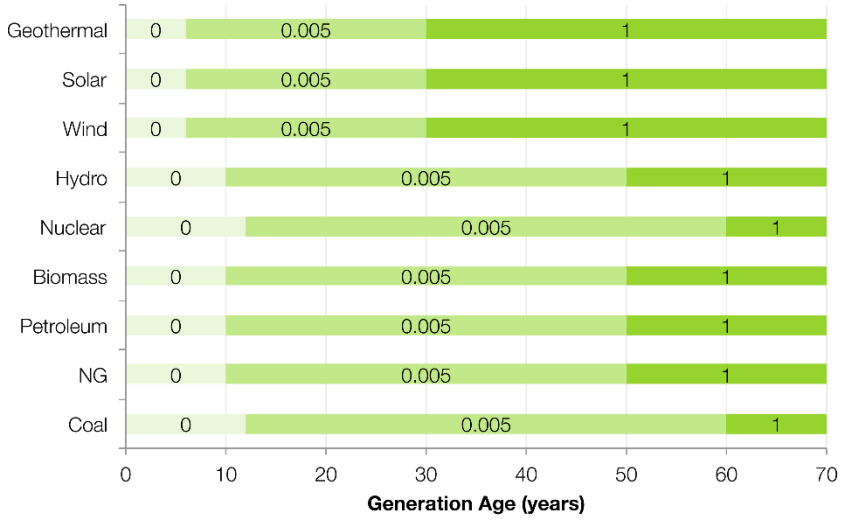

Figure 4.3. Discard probabilities of various generator types used in this study. A discard probability of 1 indicates that the generator has reached the end of its service life.

Installation, operation and maintenance, and fuel costs are obtained from the U.S. EIA's plant cost report (U.S. EIA, 2010). Retirement costs for each generator type are the sum of the decommissioning costs and the additional financing-related remuneration. The latter is calculated assuming that financing of the power plant is completed over a period of 30 years at the market rate with prevalent interests rates and rates of return on equity. As in the case of the LDV sector, retirement costs are higher for newer generation capacities. All unit costs are estimated taking into account the average 2010 capacity factors of each generator technology type. Non-electric vehicle related electricity demand is assumed to follow projections in U.S. Energy Information Administration (2011). Sector-wide total GHG emissions data for 2010 are obtained from U.S. Environmental Protection Agency

(2010). Discard probabilities of various generator technologies are shown in Figure 4.3. Discard probability equals 1 when the capacity reaches its critical age (service life). Other important assumptions and their sources for the utility sector are listed in Appendix F.

Lastly, the model also assumes that all technology types are available for production and sale, and that all technologies that are built are sold (supply equals demand). The global warming impacts of the production processes involved in the manufacture of vehicles and their components (including batteries for EVs), as well as the upstream emissions from fuel supply chains are considerable. However, estimates in the literature for use phase emissions from combustion of fossil fuels directly within the vehicle or at the power plant charging over the vehicle's lifetime range between 65-95% for CVs, 60-80% for HEVs, 50-70% for BEVs, and 65-70% for PHEVs (Hawkins, Singh, Majeau-Bettez, & Strømman, 2013; H.-J. Kim, McMillan, Keoleian, & Skerlos, 2010; Lewis, Kelly, & Keoleian, 2014; H. L. MacLean & Lave, 2003; Samaras & Meisterling, 2008), which indicates that use phase emissions are the predominant contributor to the life cycle the global warming footprint of a vehicle. Further, the emissions for automotive sectors indicated in Figure 1.1, which are also used to identify and set emission targets in this study, are also based on greenhouse gas emissions during the use phase of the vehicle. Emissions from production phase and fuel supply chains are included as part of the industrial sector. The contribution of use phase emissions to the life cycle emissions of power plants is nearly 100%. Thus, this study will focus only on the use phase emissions of vehicles and power plants.

4.2.2 Sets, Inputs, and Decision Variables

4.2.2.1 Sets

N_v	Set of vehicle technologies $\{CV, HEV, BEV, PHEV\}$ or Conventional Vehicle, Hybrid Electric Vehicle, Battery Electric Vehicle, Plug-in Hybrid Electric Vehicle.
N_e	Set of electric generation technologies $\{C, NG, P, B, H, W, \mathrm{S}, \mathrm{G}\}$ or Coal, Natural Gas, Petroleum, Biomass, Nuclear, Hydroelectric, Wind, Solar and Geothermal.
T	Set of ages for technologies. 0 implies a new technology unit.
Y	Set of years in the model are indexed from $0,\ldots,\lvert Y\rvert$. Year 0 is 2010.
$N = N_v \cup N_e$	Set of all technologies.

4.2.2.2 Inputs

$DEPLOYMENT\_COST(i,k)$	Unit cost of purchasing or constructing one new unit of technology $i \in N$ in year $k \in Y$.
$MAINTENANCE\_COST(i,j,k)$	Annual unit maintenance cost of technology $i \in N$ that is of age $j \in T$ in year $k \in Y$.
$FUEL\_COST(i,k)$	Cost per kg of fuel for technology $i \in N$ in year $k \in Y$.
$SCRAPPAGE\_VALUE(i,j,k)$	Market value that owners of technology $i \in N$ stand to receive when scrapping or decommissioning a unit of age $j \in T$ in year $k \in Y$ at the end of its life.
$TAKE\_BACK\_VALUE(i,j,k)$	Additional subsidy amount that owners of technology $i \in N$ stand to receive when scrapping or decommissioning a unit of age $j \in T$ in year $k \in Y$ before the end of its natural life.
$DEM_v(k)$	Annual demand for vehicle miles travelled (VMT) in year $k \in Y$.

$DEM_e(k)$ — Annual demand for MWh in year $k \in Y$. This excludes the demand for electricity generated each year by *BEV* and *PHEV* vehicles which is determined endogenously.

$EN(i, j, k)$ — Annual electricity demand per vehicle of technology $i \in N$ of age $j \in T$ in year $k \in Y$. For technologies *CV* and *HEV* these will be 0 in all years and for all age vehicles.

$GEN_v(i, j, k)$ — Annual usage (VMT) for vehicle technology $i \in N_v$ for units of age $j \in T$ in year $k \in Y$. Miles travelled per vehicle is assumed to be constant for all technologies of all ages, and thus the variation in VMT is only due to changes in number of vehicles with time.

$GEN_e(i, j, k)$ — Annual electricity generation rate of unit of electric technology $i \in N_e$ for units of age $j \in T$ in year $k \in Y$ measured in MWh.

$CARBON\_INTENSITY(i)$ — Carbon intensity of fuel used in technology $i \in N$ (kg CO_2/kg fuel)

$FUEL\_EFFICIENCY_s(i, j, k)$ — Quantity of fuel needed per mile (for $i \in N_v$) or per MWh (for $i \in N_e$) for a unit of age $j \in T$ in year $k \in Y$. Note that *s* refers to the vehicle sector (*v*) or the electric sector (*e*).

$CFnew_v(i, k)$ — Unit purchase and operating cost of a vehicle of technology $i \in N_v$ in year $k \in Y$, defined as:

$$DEPLOYMENT\_COST(i,k) + MAINTENANCE\_COST(i,0,k) + FUEL\_EFFICIENCY_v(i,0,k) \bullet GEN_v(i,0,k) \bullet FUEL\_COST(i,k)$$

$CFold_v(i, j, k)$ — Unit operating cost of an old technology $i \in N_v$ of age $j \in T$ in year $k \in Y$, defined as:

$$MAINTENANCE\_COST(i,j,k) + FUEL\_EFFICIENCY_v(i,j,k) \bullet GEN_v(i,0,k) \bullet FUEL\_COST(i,k)$$

$CFnew_e(i,k)$	Unit construction and operating cost of a new unit of electric generation capacity of technology $i \in N_e$ in year $k \in Y$, defined as: $DEPLOYMENT\_COST(i,k) + MAINTENANCE\_COST(i,0,k) + FUEL\_EFFICIENCY_e(i,0,k) \bullet GEN_e(i,0,k) \bullet FUEL\_COST(i,k)$
$CFold_e(i,j,k)$	Unit operating cost of an old technology $i \in N_e$ of age $j \in T$ in year $k \in Y$, defined as: $MAINTENANCE\_COST(i,j,k) + FUEL\_EFFICIENCY_e(i,j,k) \bullet GEN_e(i,0,k) \bullet FUEL\_COST(i,k)$
$CFret(i,j,k)$	Unit retirement cost of technology $i \in N$ of age $j \in T$ in year $k \in Y$, defined as: $SCRAPPAGE\_VALUE(i,j,k) + TAKE\_BACK\_VALUE(i,j,k)$
r	Discount rate for net present value calculations, assumed as 7%.
$INITFLEET(i,j)$	Initial number of units of technology $i \in N$ of age $j \in T$.
$INITPROD_s$	Initial production capacity in sector *s* (vehicle (*v*) or electric (*e*)).
$P(i,j)$	Cumulative probability that a unit of technology $i \in N$ of age $j \in T$ will survive to the following year.
$Z_{low}(i,k), Z_{hi}(i,k)$	Low and high allowable changes in the percent composition of technology $i \in N$ in year $k \in Y$.
$G_{low}(i,k), G_{hi}(i,k)$	Low and high allowable changes in the percent composition of the new deployment for technology $i \in N$ in year $k \in Y$.
$MARKET\_SHARE(i,k)$	Upper bound on the total market share of technology $i \in N$ in year $k \in Y$.
$EF(i,j,k)$	Emission factor per unit of technology $i \in N$ of age $j \in T$ in year $k \in Y$, defined as

$FUEL\_EFFICIENCY_s(i,j,k)$
$\bullet GEN_s(i,0,k) \bullet CARBON\_INTENSITY(i)$

where *s* refers to either the vehicle (*v*) or energy (*e*) sectors

$EMISSION\_TARGET_s(k)$ Emission target for sector *s* (vehicle (*v*) or energy (*e*)) in year $k \in Y$ in kg CO_2/year.

$PROD\_GROWTH_s(k)$ Production capacity growth rate in sector *s* (vehicle (*v*) or energy (*e*)). This is the rate at which production capacity grows from year 0 to year *k*.

4.2.2.3 Decision Variables

$new(i,k)$ Number of new units of technology $i \in N$ deployed in year $k \in Y$.

$old(i,j,k)$ Number of old or existing units of technology $i \in N$ of age $j \in T$ in existence in year $k \in Y$.

$ret(i,j,k)$ Number of units of technology $i \in N$ of age $j \in T$ retired in year $k \in Y$.

4.2.3 Objective Function

Based on the unit cost inputs and decision variables defined earlier, the objective function of the minimization problem for both sectors can then be written as:

$$\min_{\substack{new \\ old \\ ret}} \sum_{k=1}^{|Y|} \frac{\left\{\sum_{i \in N} new(i,k) \bullet CFnew(i,o,k)\right\} + \left\{\sum_{i \in N}\sum_{j=1}^{|T|}\left[old(i,j,k) \bullet CFold(i,j,k)\right] + \left[ret(i,j,k) \bullet CFret(i,j,k)\right]\right\}}{(1+r)^{k-1}}$$

.....Equation 4.2

This essentially translates to "minimize the net present value of all costs over the analysis time horizon by changing the number of new units sold, number of old units retired, and number of old units present in the fleet." Note that the *FUEL_EFFICIENCY* term in the definition of *CF* includes

any increase in fuel efficiency of a unit of a given technology type over time due to technological improvements, as well as the decrease in fuel efficiency with age of that unit. Also, *CFnew* captures any trends in the deployment costs such as reduction in Lithium ion battery costs, and wind farm commissioning costs.

4.2.4 Constraints

4.2.4.1 Fleet Constraints

The total demand constraint in the auto sector can be expressed as shown in Equation 4.3, and it

$$\forall k \in Y$$

$$\left\{\sum_{i\in N}\sum_{j=1}^{|T|} old_v(i,j,k)\bullet GEN_v(i,j,k)\right\}+\left\{\sum new_v(i,0,k)\bullet GEN_v(i,0,k)\right\}\geq DEM_v(k)$$

.....Equation 4.3

essentially represents the total number of vehicle miles traveled as a function of time. The demand for electricity, expressed in MWh of generation, includes the demand from charging of electric vehicles, and is shown in Equation 4.4. The demand from EV charging is endogenously calculated by running the electric and auto sector models iteratively, with EV charging emissions factors from one iteration (calculated as the generation-weighted average emissions per MWh in the electric sector) used in the subsequent iteration until the root mean square error of emission factors for all years over the analysis time horizon (2011 – 2050) converges to less than 1% with respect to the previous iteration.

$$\forall k \in Y$$

$$\left\{\sum_{i\in N_e}\sum_{j=1}^{|T|} old_e(i,j,k)\bullet GEN_e(i,j,k)\right\}+\left\{\sum_{i\in N_e} new_e(i,0,k)\bullet GEN_e(i,0,k)\right\}$$

$$\geq DEM_e(k)+\left\{\sum_{i\in N_v}\sum_{j=1}^{|T|} old_v(i,j,k)\bullet EN(i,j,k)\right\}+\left\{\sum_{i\in N_e} new_v(i,0,k)\bullet EN(i,0,k)\right\}$$

.....Equation 4.4

In this study, the total population of the LDV sector fleet is assumed to grow at 1% annually, with the miles traveled per year by a vehicle of any technology type and age remaining constant. As such, the annual increase in VMT is assumed to be due to increase in number of vehicles alone. The non-EV related demand in the electric sector is assumed to grow as projected in the AEO 2011 report (U.S. Energy Information Administration, 2011).

The total market share of a given technology can be expressed as the ratio of the sum of old and new units of that technology to the total number of units in the fleet. The model allows the total market share of technologies to be constrained to restrict the manner in which new technologies are introduced into the market or old technologies are phased out of the market. These constraints are implemented by requiring that the *change* in total market shares of a certain technology from the previous year be within the exogenously defined bounds of $-Z_{low}$ and $+Z_{hi}$. The total market share constraints can be written as shown in Equation 4.5. Rollout of new technologies and phasing out of old technologies can also be controlled by restricting the change in new units deployed over the previous year to exogenously defined bounds of $-G_{low}$ and $+G_{hi}$ (Equation 4.6). Together, these two approaches constitute the deployment smoothing constraints.

$$\forall i \in N, k \in Y$$

$$\left\{1 - Z_{low}(i,k)\right\} \bullet \left\{new(i,k-1) + \sum_{j=1}^{|T|} old(i,j,k-1)\right\}$$

$$\leq new(i,k) + \sum_{j=1}^{|T|} old(i,j,k) \leq \left\{1 + Z_{hi}(i,k)\right\} \bullet \left\{new(i,k-1) + \sum_{j=1}^{|T|} old(i,j,k-1)\right\}$$

.....Equation 4.5

$$\forall i \in N, k \in Y$$

$$\left\{1 - G_{low}(i,k)\right\} \bullet new(i,k-1) \leq new(i,k) \leq \left\{1 + G_{hi}(i,k)\right\} \bullet new(i,k-1)$$

.....Equation 4.6

Additionally, the total market share (and not change in total market share) of a given technology in a year can also be constrained as follows.

$$\forall i \in N_v, k \in Y$$
$$new_v(i,k) + \sum_{j=1}^{|T|} old_v(i,j,k) \leq MARKET\_SHARE(i,k) \bullet DEM_v(k)$$
$$\forall i \in N_e, k \in Y$$
$$new_e(i,k) + \sum_{j=1}^{|T|} old_e(i,j,k) \leq MARKET\_SHARE(i,k) \bullet \left\{ \begin{array}{l} DEM_e(k) + \left[\sum_{i \in N_v} \sum_{j=1}^{|T|} old_v(i,j,k) \bullet EN(i,j,k) \right] \\ + \left[\sum_{i \in N_v} new_v(i,k) \bullet EN(i,0,k) \right] \end{array} \right\}$$

.....Equation 4.7

In addition to these fleet constraints, the total new unit production capacity (for all technologies combined) in any given sector can also be restricted to simulate a gradual ramp up in capacity of new vehicles or electricity generation. For instance, this constraint can prevent the sales of 50% more vehicles (25 million) in year 1 of the analysis, which is unlikely to happen since the additional vehicle manufacturing facilities needed to meet this production increase cannot realistically be built in a year. It should be noted that the same effect can be achieved using the new unit deployment smoothing constraint, and restricting the total new unit production capacity is just another way of restricting increase in deployment of new units. As such, the production constraint can be written as:

$$\forall k \in Y$$
$$\sum_{i \in N_v} new_v(i,k) \leq INITPROD_v \bullet PROD\_GROWTH_v(k)$$
$$\sum_{i \in N_e} new_e(i,k) \leq INITPROD_e \bullet PROD\_GROWTH_e(k)$$

.....Equation 4.8

4.2.4.2 Emission Constraints

Sector-wide emissions can be expressed as the sum of emissions from old units that have survived scrappage or forced retirement and the emission from new units. The emission constraints can then be expressed as an annual target for each year of the analysis horizon (Equation 4.9), or as an aggregate constraint over the entire analysis horizon such that the total allowable emissions over a given period equal the sum of the annual emission targets over that same period (Equation 4.10).

$$\forall k \in Y$$

$$\sum_{i \in N_s} new_s(i,k) \bullet EF(i,0,k) + \sum_{i \in N_s} \sum_{j=1}^{|T|} old_v(i,j,k) \bullet EF(i,j,k) \leq EMISSION\_TARGET_s(k)$$

.....Equation 4.9

$$\sum_{k=1}^{|Y|} \left\{ \sum_{i \in N_s} new_s(i,k) \bullet EF(i,0,k) + \sum_{i \in N_s} \sum_{j=1}^{|T|} old_v(i,j,k) \bullet EF(i,j,k) \right\} \leq \sum_{k=1}^{|Y|} EMISSION\_TARGET_s(k)$$

.....Equation 4.10

This model assumes a uniform rate of emission reduction from 2011 through 2050 to achieve a set reduction in GHGs relative to 1990 emission values. The time period of interest to us is until 2050. However, as discussed earlier, the analysis time horizon for both sectors goes well beyond 2050 to account for operating costs beyond 2050. The value of elements in the vector *EMISSION_TARGET* for years beyond 2050 is held at the constant value of the 2050 target. Thus, elements of the *EMISSION_TARGET* vector fall on a straight line with a slope of $\{E(2050) - E(2010)\}/(2050 - 2010)$ until 2050, followed by a straight line with slope 0 beyond 2050. Finally, the non-negativity constraints for the decision variables can be expressed as follows.

$$\forall i \in N, k \in Y$$
$$new(i,k) \geq 0$$

$$\forall i \in N, j \in T, k \in Y$$
$$old(i,j,k) \geq 0$$
$$ret(i,j,k) \geq 0$$

.....Equation 4.11

Additional assumptions and data sources used to construct the model are listed in Appendix F.

4.3 TECHNOLOGICAL COSTS OF DELAYED CLIMATE ACTION

To evaluate the technological costs of delayed climate action, we use the stock-and-flow model and optimization framework described in the previous section. In the context of this study, "climate action" is defined as direct or indirect emission constraining measures to cut annual CO_2 emission levels by 30 to 80% of 1990 emission levels by the year 2050. The range of emission reduction percentages serves to define "windows of opportunities" between the present time and 2050 before which said levels of emission reduction are theoretically feasible. That is, the respective emission reductions can be achieved if technology evolution follows the least-cost-to-society trajectories determined by the optimization model, which in effect acts as a benevolent dictator in the context of this policy analysis. A given technology trajectory includes operation, maintenance, scrappage, and forced retirement of existing units, as well as deployment of new units during the analysis time horizon. Costs and emissions under emission-constrained scenario are compared to a business-as-usual (BAU) scenario for the specific sector under consideration. Technology trajectories under the BAU scenario are also assumed to evolve such that the cost to society is minimized, although the BAU scenario assumes no emission reduction policies and technology cost structures beyond those already in place, such as the Corporate Fuel Economy Standards (CAFE) and federal electric vehicle (EV) tax credits.

Salient features and assumptions behind the BAU and emission constrained scenarios are discussed next.

4.3.1 Business-as-Usual Scenario

Defining the BAU case is of critical importance in any climate policy analysis, because it serves as the benchmark against which costs and emission reductions of the emission-constrained scenarios are compared. In addition to the model assumptions outlined in section 4.2, the main assumptions in the BAU scenario for the U.S. auto sector are: (a) CAFE standards for vehicle fuel economies beyond 2025 (the year until which they are presently defined) continue to follow the linear trajectory set by CAFE standards from 2011-2025, which is defined as $CAFE(year) = 1.3704(year - 2010) + 26.077$ ($R^2 = 0.991$), (b) miles traveled per vehicle per year remain unchanged form year to year, although the total vehicle population follows projections estimated in the AEO 2011 report (U.S. Energy Information Administration, 2011), (c) vehicle scrappage does not exceed naturally expected values determined using Equation , that is, there is no forced retirement of vehicles through take-back programs.

Main assumptions for the electric utility sector include (a) maximum deployment (upper bound) of new coal, biomass, nuclear, hydroelectric, and geothermal generation, and minimum deployment (lower bound) for new natural gas generation follows the projects outlined in the AEO 2011 report (U.S. Energy Information Administration, 2011), and (b) generation capacity (MWh) scrappage does not exceed naturally expected values shown in Figure 4.3, that is, there is no forced retirement of power plants. It should be noted that forced retirement of generation capacity involves compensating the utility service provider for lost revenue over the balance of the power plant life and buying its debt

to shareholders and banks if the forced retirement occurs before the end of its financing period. Typical forced retirement compensation values for a coal plant 20 and 40 years into its service life are $7631/MWh and $588/MWh respectively, which is an order of magnitude higher than values reported by utilities that have recently retired or are planning to retire old coal fired capacity. Further, the AEO 2011 report estimates that roughly 40 GW of old fossil fuel capacity will be retired by 2035. This is roughly half of the 74 GW of total fossil fuel capacity older than 50 years (typical service life for fossil fuel generators) operational in 2010 according to eGRID 2010 data (U.S. Environmental Protection Agency, 2014a). Since the optimization model naturally scraps any capacity older than its service life, the scrappage assumed here is still higher than the AEO 2011 reference case assumption of 40 GW, and closer to the 60 GW estimate provided in the recent early release version of AEO 2014 (U.S. Energy Information Administration, 2014).

4.3.2 Climate Action Scenario

The climate action scenario assumes that regulatory measures such as sector-wide emission targets, emission permits and trading schemes, or carbon tax will be put in place starting from the year in the climate action is initiated, and continuing through the year 2050 and beyond so as to reduce and maintain annual emission levels in 2050 and beyond to 30-60% of the 1990 values. This emission "constraint" is implemented in two ways in this study depending on the analysis. The first approach treats 2005 as the baseline climate action year since it was the year in which the Kyoto Protocol (United Nations, 1997) went into effect, and assumes a linear annual reduction in emissions through 2050 such that the annual sector-specific emission in 2050, E_{2050}, is 1-p times (p = 30-60%) the 1990 emission value, E_{1990}. The sum of the annual "ideal" emissions E_{ideal} (that is if climate action had

initiated in 2005) from 2005 till the end of the analysis time horizon (2005 + $|Y|$), minus the sum of the annual emission deficit accrued between 2005 and the climate action year y_{CA} (due deviation of actual emissions E_{actual} from the ideal emissions E_{ideal}) is then treated as the emission budget B for the years between the climate action year y_{CA} and 2050. This can be expressed mathematically as follows.

$$B = \sum_{y=2005}^{2010+|Y|} E_{ideal}(y) - \sum_{y=2011}^{y_{CA}} \left\{ E_{actual}(y) - E_{ideal}(y) \right\}$$

where,

$$\forall y \in [2005, 2050]$$
$$E_{ideal}(y) = (y - 2005) \bullet \left\{ \frac{(1-p) E_{1990} - E_{2005}}{2050 - 2005} \right\} + E_{2005}$$
and
$$\forall y \in [2051, 2010 + |Y|]$$
$$E_{ideal}(y) = (2050 - 2005) \bullet \left\{ \frac{(1-p) E_{1990} - E_{2005}}{2050 - 2005} \right\} + E_{2005}$$

.....Equation 4.12

Based on Equation 4.10 and Equation 4.12, the emission budget constraint can be rewritten as:

$$\sum_{k=1}^{|Y|} \left\{ \sum_{i \in N_s} new_s(i,k) \bullet EF(i,0,k) + \sum_{i \in N_s} \sum_{j=1}^{|T|} old_v(i,j,k) \bullet EF(i,j,k) \right\} \leq B$$

.....Equation 4.13

The second approach of implementing an emission constraint is by including the emissions in the objective function as a cost. This approach requires emissions to be ascribed a certain cost penalty, which is implemented in this analysis using estimates of social cost of carbon (SCC). Expressing emissions as costs eliminates the need to impose an emission budget constraint, and therefore, this

approach is used when setting a specified p% reduction in annual emissions by 2050 leads to infeasibility in the optimization process. Further, the second approach can also be used to estimate the SCC required for achieving a certain emission reduction. Assuming that the SCC linearly increases with time as estimated in the literature (United States Government, 2013), the objective function under the second approach can be written based on Equation 4.2 and Equation 4.10 as follows.

$$\min_{\substack{new \\ old \\ ret}} \sum_{k=1}^{|Y|} \left\{ \frac{\left\{ \sum_{i \in N} new(i,k) \bullet \left(CFnew(i,0,k) + SCC(k) \bullet EF(i,0,k) \right) \right\} + \left\{ \sum_{i \in N} \sum_{j=1}^{|T|} \left[old(i,j,k) \bullet \left(CFold(i,j,k) + SCC(k) \bullet EF(i,j,k) \right) \right] + \left[ret(i,j,k) \bullet CFret(i,j,k) \right] \right\}}{(1+r)^{k-1}} \right\}$$

.....Equation 4.14

The total emissions in the climate action scenario will be less than the BAU scenario, although the technology trajectory required to achieve this emission reduction will require additional costs relative to the BAU scenario for more expensive technology deployment and retirement. Thus, if E_{BAU} and E_{CA}, and C_{BAU} and C_{CA} are the total emissions and expenditures (including deployment, operation, maintenance, and forced retirement) respectively in the BAU and climate action scenarios over the analysis time horizon, the average carbon abatement cost $C_{abatement}$ in \$ per unit of CO_2 avoided in the climate action scenario is expressed as follows.

$$C_{abatement}\left(\frac{\$}{\text{ton CO}_2 \text{ avoided}} \right) = \frac{C_{CA} - C_{BAU} \ (\$)}{E_{BAU} - E_{CA} \ (\text{ton CO}_2)}$$

.....Equation 4.15

Different values of emission reduction percentages p will lead to different absolute values of C_{BAU} and C_{CA}. Further, for a given value of p, different of climate action year y_{CA} will also give different absolute values of C_{CA} (C_{BAU} remains unchanged since it does not depend on emission targets). To overcome this problem and enable comparison of results across different values of p and y_{CA}, we define the ratio $R = C_{CA}/C_{BAU}$ as a standard metric.

Costs and emissions under the BAU and climate action scenarios will vary significantly based on the underlying assumptions for critical parameters such as fuel economy, battery technology costs, vehicle value depreciation rate, emission factors for grid charging of EVs, miles traveled per vehicle per year, and fuel prices in the auto sector, and overnight capital costs, retirement costs (interest rate, return on equity, risk), fuel prices, and rate of increase in demand in the electric utility sector. To account for the effects of these parameters on the technological costs of delayed climate action, we also perform an uncertainty analysis. The levels and values of parameters and assumptions used in the uncertainty analysis and their sources are listed in Appendix H.

4.4 RESULTS AND DISCUSSION

Following the optimization framework described earlier and imposing emissions reductions in the climate action case in the form of a collective emissions budget from 2011 through 2050, we estimate the technological costs of meeting said reductions in both the automotive and electric utility sectors in the U.S. We evaluate the technology trajectories and abatement costs, and track their respective evolution for 80%, 60%, 50%, 40%, and 30% reduction of CO_2 emissions from each sector by 2050 relative to its respective 1990 emission level, with the 60% reduction case used as the nominal case for the uncertainty analysis. For a given percentage emission reduction p, we define climate inaction

within each sector as technology evolution that follows the BAU trajectory defined in section 4.3.1. Thus, if we climate action is initiated in 2020, for instance, the optimization model will assume technology evolution from 2011 through 2019 to follow its BAU trajectory, and then find the technology trajectory needed from 2020 to 2050 to achieve a total of p% reduction in emission levels by 2050 relative to the sector's 1990 level.

4.4.1 Light Duty Vehicle Sector

Figure 4.4 shows the ratio of technological costs of climate action relative to the BAU scenario (R) for various levels of emissions reduction in the auto sector by 2050. The analysis reveals that the window of opportunity to achieve 80% reduction in emissions has already passed, meaning that even under the assumptions of a benevolent dictatorship and favorable cost and fuel economy progression, reducing auto sector emissions to 80% of its 1990 values is highly unlikely. Regardless of the percentage reduction in emissions by 2050, the R curve is observed to follow a "hockey-stick" shape, wherein climate action costs relative to BAU remain almost constant up to an inflection point, beyond which they steeply rise until the point in time when achieving the respective percentage emission reduction is no longer feasible (indicated by × in Figure 4.4).

The sharp rise in climate action costs is due to the forced retirement of 60-180 million vehicles over a ten-year period, and their replacement with more expensive electric vehicles. The slow turnover of vehicle fleets owing to the typical design life of 20 years for a vehicle thus leads to a certain amount emissions to be "locked-in" unless the turnover is expedited through high forced retirements or take-back programs. Whether through high social cost of inaction in the form of ecosystem damages, adaptation, and resulting economic output loses, or through technological costs of retirement of old

vehicles and replacement with more expensive cleaner vehicles, delaying climate action pushes the costs of carbon abatement on to future generations despite anticipated improvements in technology costs and fuel efficiencies.

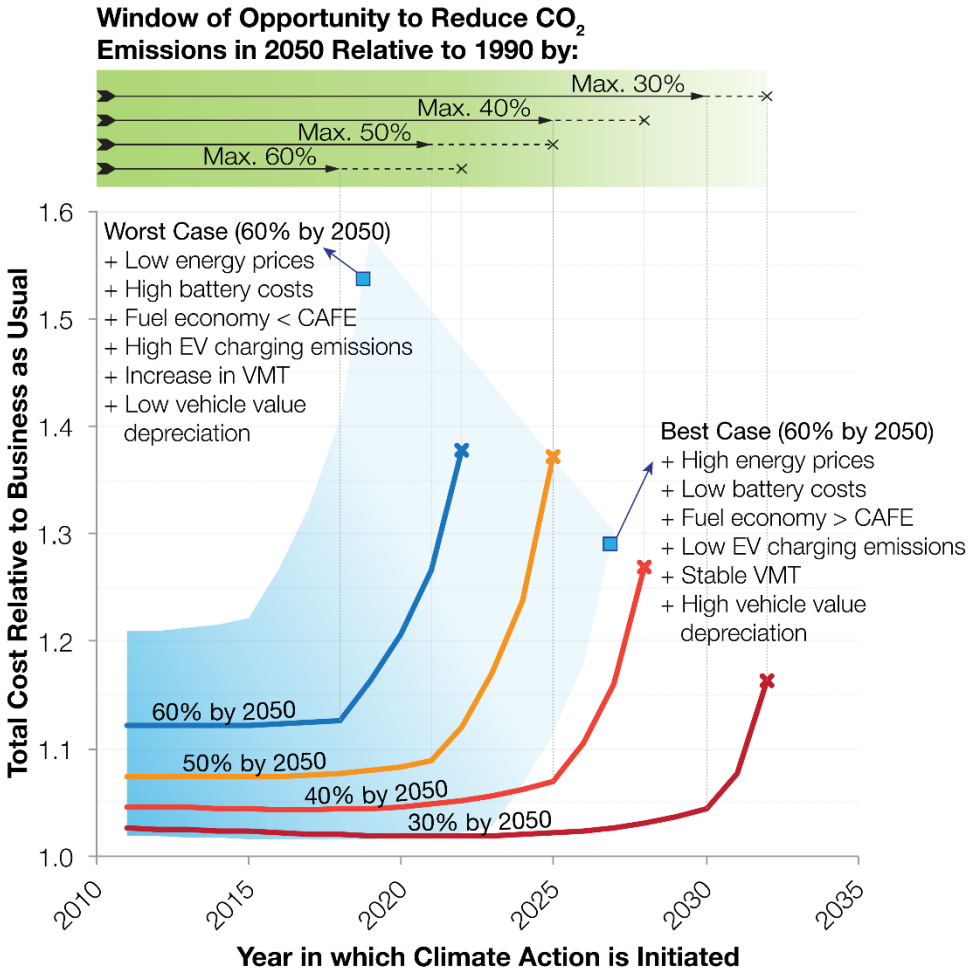

Figure 4.4. Technological costs of climate inaction, and windows of opportunity to achieve 30-60% reductions in emission levels by 2050 relative to 1990 levels in the auto sector.

The window of opportunity to reduce automotive emissions by 60% by 2050 considering the best and the worst case projections in technology costs, fuel prices, and fuel efficiency is roughly between 2015 and 2025. It must be noted that this analysis assumes that every vehicle that needs to be deployed

is produced by the producer and purchased by consumers. Thus, the analysis ignores production and consumer preference constraints, which stand to only further constrain the achievable emissions, and the figures for windows of opportunity presented here are optimistic estimates compared to reality. The analysis also reveals that under the likely (nominal) case of projected improvements in fuel economy, technology costs (such as batteries), and fuel prices, climate action must be initiated at the very latest before 2030 to achieve an emission reduction target as low as 30%.

Another interesting outcome of the analysis is that technological costs under climate action remain effectively flat compared to costs under the BAU scenario. This means that expected reductions in costs and improvements in fuel economies and EV charging are not sufficient, even in the best case, to justify waiting for an optimal action time in the future on the basis of minimizing total cost to society. The role of EV charging emissions or in other words the grid mix in the electric utilities sector is also of great importance. The nominal case assumes that the electric sector itself achieves a minimum of 30% reduction in its emissions by 2050 assuming a similar least-cost approach. However, if the electricity mix remains largely reliant on fossil fuels, such that the generation-weighted average emission factor for EV charging fails to fall below 0.4 tons of CO_2/MWh by 2030 (about 0.56 tons of CO_2/MWh in 2011), the estimates of theoretically achievable emission reductions and window of opportunity to achieve a given level of emission reduction will further decrease in value.

Retirement of old vehicles and replacement with costlier but cleaner vehicles may seem like an expensive option for carbon abatement. However, it remains significantly more inexpensive than waiting for existing vehicle fleets to be decommissioned naturally through scrappage at the end of their

service life, and then being replaced by even more expensive vehicles such as BEVs to compensate for the emissions of the now scrapped vehicle over the period of its operation towards the end of its life. Figure 4.5 shows this comparison.

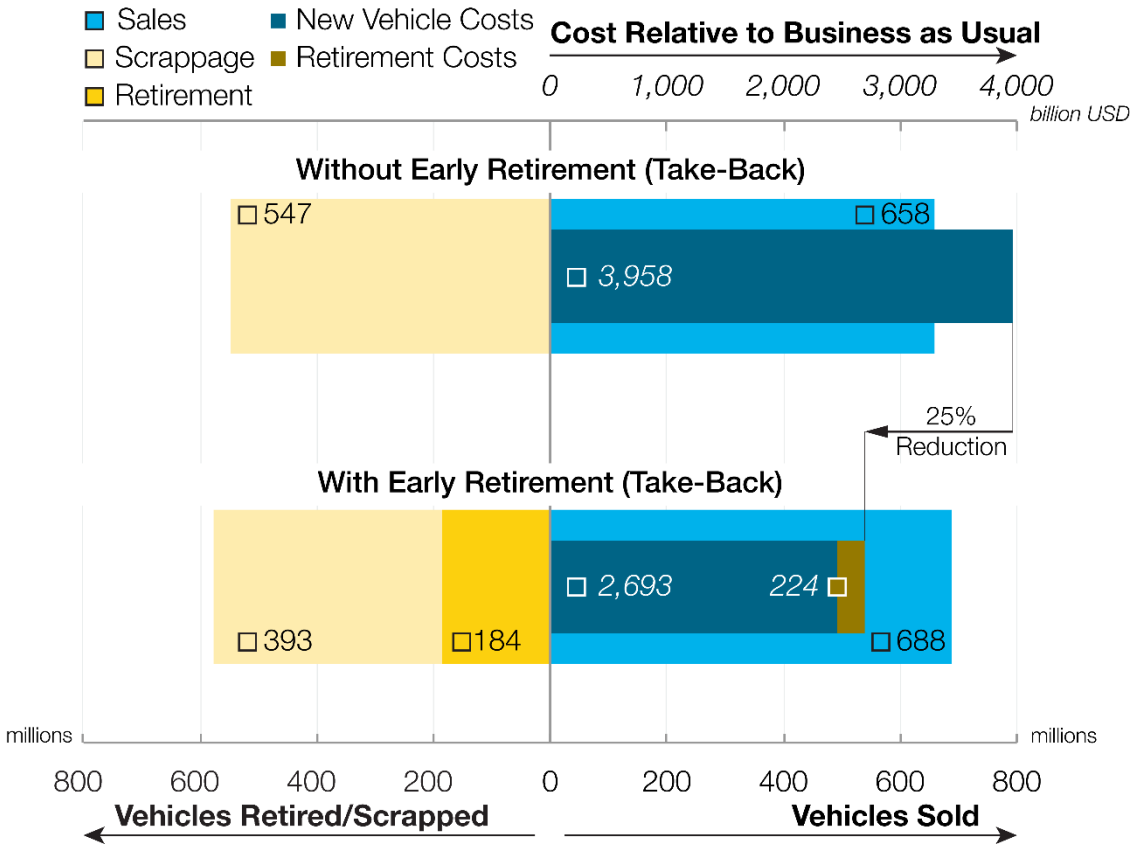

Figure 4.5. Comparison of climate action costs with and without forced retirement of vehicles through take-back programs. Climate action year assumed here as 2021.

It can be observed that by forced retirement (take-back) over a period of thirty years (2021-2050) of about 184 million vehicles, aged between 15 and 20, 95% of which would have been scrapped in one to four years in any case, incurs an additional cost of 224 billion USD, but still is cheaper overall by 25% than not retiring such old vehicles. This difference in costs emanates from the fact that retired old vehicles in the near term can still be replaced by HEVs or PHEVs to meet the emission reduction target, but delays from allowing old vehicles to reach the end of their service life naturally would

necessitate replacement with significantly more expensive BEVs to meet the same emission reduction target but in a shorter period of time.

With this background on the emission reduction amounts and their respective action timelines, the question then remains as to how to enforce the emission constraint or budget. One way is by imposing a sector-wide carbon penalty, which can then be translated into fuel taxes, fuel economy standards, or other policy instruments. The analysis of such policy instruments will require rigorous macro-economic assessments that are beyond the scope of this dissertation. However, the amount of carbon penalty needed to achieve a given amount of emission reduction can be estimated using this model by ascribing a certain cost to carbon emissions, and including those costs in the cost-minimization framework. As a starting point for this analysis, we use the social cost of carbon (SCC) estimates provided by the U.S. government for regulatory impact analysis (United States Government, 2013). We first use both the low (average) and high (95% percentile) values of SCC, adjusted to the discount rate used in this study, as carbon penalties to estimate the emission reduction that can be achieved with the respective SCC values. We find that even with the high SCC value, maximum achievable emission reduction assuming immediate climate action is well below 60%. Maintaining the identical slope of the high SCC curve, we then offset the high SCC curve until emission reductions under immediate climate action reaches 60%. Figure 4.6 shows the results from this analysis. The analysis reveals that to achieve a 60% reduction in emissions by 2050, the SCC or carbon penalty should be approximately 30 USD/ton CO_2 higher than the high (95 percentile) estimate provided in the literature (United States Government, 2013). Further, the low range of SCC estimates can reduce sectoral emissions by less than 20% by 2050.

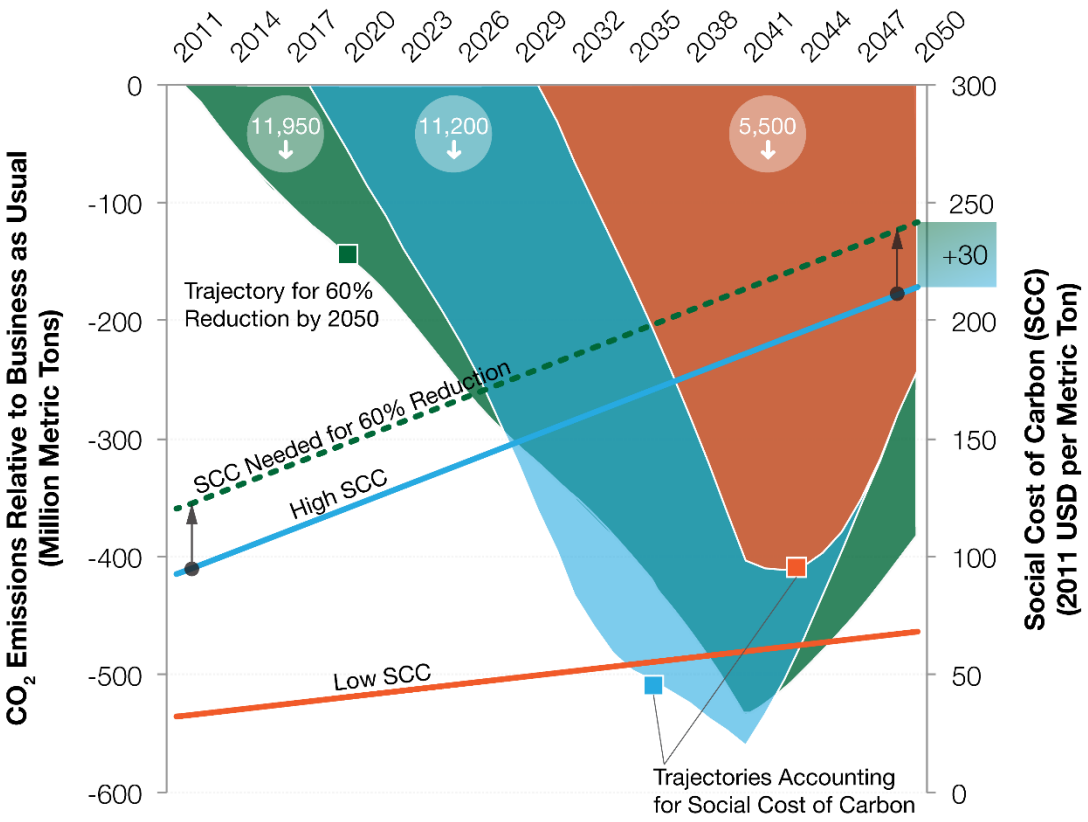

Figure 4.6. Estimation of the carbon penalty of social cost of carbon (SCC) needed to achieve 60% reduction in emissions by 2050 under immediate climate action in the auto sector.

Under immediate climate action, our analysis reveals that the average technological cost of carbon abatement in the automotive sector is about 33 USD/ton of CO_2 avoided. The costs and emissions used to derive this number are benchmarked against costs and emissions in the BAU scenario, and include cost of deployment of new units, operation and maintenance of new and old units, and retirement of old units. Figure 4.7 shows the technology trajectories under BAU and immediate climate action 60% reduction by 2050 scenarios in the auto sector. In the BAU scenario, we see predominantly CV-based new vehicle fleets until about 2040, beyond which PHEVs are the technology of choice from a purely cost point of view. In the climate action case however, this switch from CVs to PHEVs would need to occur twenty years earlier starting in 2020, with PHEVs switching

to BEVs around 2045. Scrappage of vehicles is indicated as shaded and on the negative part of the ordinate axis.

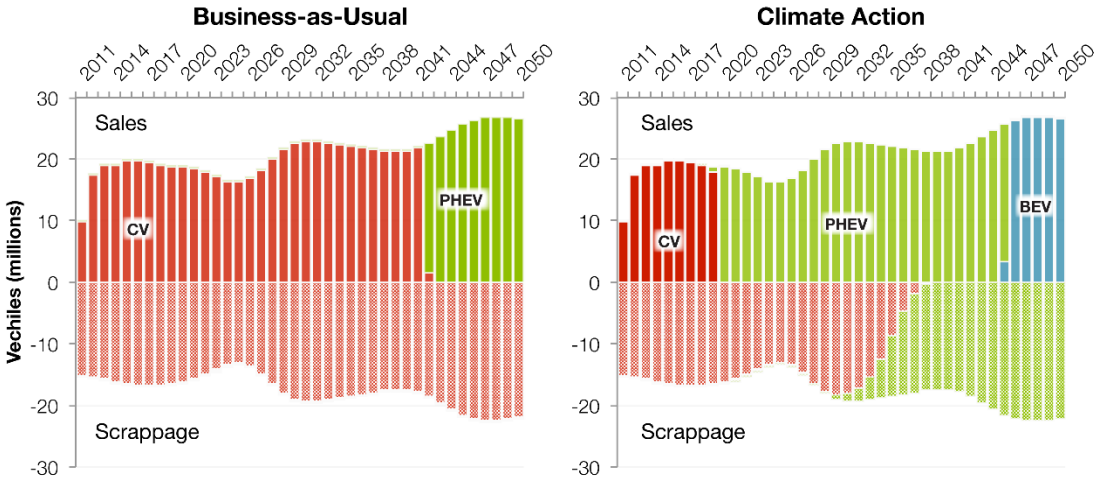

Figure 4.7. Auto sector technology trajectories under BAU scenario (left) and climate action scenario (right) assuming immediate action for 60% emission reduction by 2050.

The abrupt changes in technology in new vehicle sales occur due to the absence of market share or deployment smoothing constraints in this analysis. As described earlier, the purpose of this analysis is to predict ideal technology trajectories that minimize the total abatement cost to society, and are a representation of what *should* ideally happen as a result of climate action. It should be noted that new vehicles deployed in any given year make up for the number of vehicles scrapped that year plus the increase in total vehicle population. The oscillation (with an approximately 14-year period) in the number of new units deployed roughly follows the new vehicle sales from 1990 to 2010 (initial fleet condition for the model). This is due to the fact that vehicle mortality in any given year is assumed to follow the same logistic probability curve explained in section 4.2.1.1 on which the 2010 fleet composition is based. This cyclic behavior of the number of vehicles scrapped is also observed in a recent analysis of the effect of vehicle scrappage rates on vehicle sales by Citi Investment Research and

Analysis (Vellequette, 2013), and the periodicity of roughly 14 years observed in this study closely matches the 15-year periodicity predicted in the Citi study.

4.4.2 Electric Utility Sector

Similar sets of analyses, as performed for the auto sector, were performed for the electric utility sector. Iterative runs of the auto sector and electric sector models until convergence of EV loads on the electric grid reveal that EV charging load will become significant starting around 2025 at a value of 0.5% of the total electric sector demand, and linearly rise to about 12% of the total electric sector demand in 2050 under the assumptions employed in the model. In the electric utility sector, we observe that an 80% reduction in emissions by 2050 is in fact possible (see Figure 4.8). To enable a consistent comparison across sectors, however, we still treat the 60% emission reduction by 2050 case as the nominal case for the uncertainty analysis. Unlike the auto sector, we do not observe a "hockey-stick" shape for the climate action technological cost curves, that is, there is not flat region for abatement costs relative to BAU over any period of time. Instead, the technological costs of climate action closely follow a fourth order increase with every year of delay (Figure 4.9), regardless of the percentage reduction in emissions desired. It is interesting to note, however, that the magnitude of the ratio of technological costs under climate action and BAU scenarios, R, is considerably higher in the electric sector ($R \approx 1.4$ under nominal case for immediate action for 60% reduction by 2050) compared to the auto sector ($R \approx 1.125$ under nominal case for immediate action for 60% reduction by 2050). This is primarily due to the fact that forced retirement of generation capacity in the utility sector is necessary right away (immediate climate action) to achieve any amount of reduction between 30-80% by 2050.

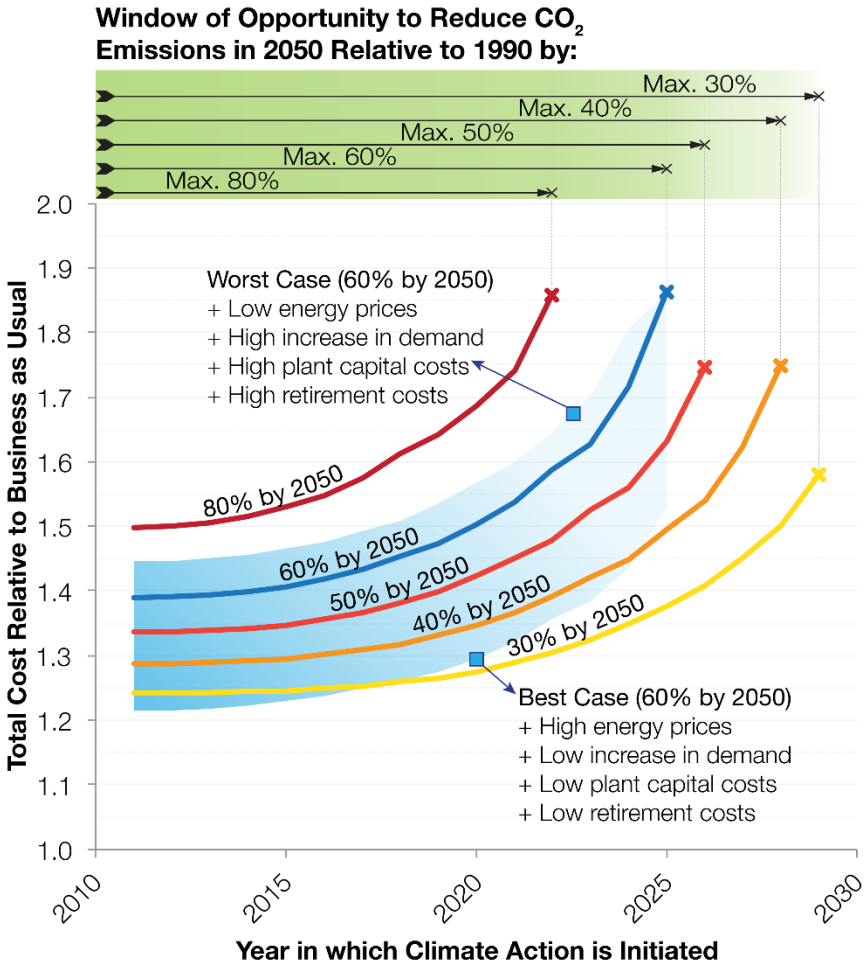

Figure 4.8. Technological costs of climate inaction, and windows of opportunity to achieve 30-80% reductions in emission levels by 2050 relative to 1990 levels in the electric utility sector.

The window of opportunity to achieve 30-60% of reduction in emissions by 2050, however, is similar to the auto sector. In both the auto and electric utility sectors, we thus observe that the technological costs of climate action rise significantly with delays, and the window of opportunity for climate action to reduce emissions by at least 30% rapidly narrows and ultimately closes by about 2030. It should again be noted that the analysis assumes no market or production constraints, and that introducing such constraints only stands to further shorten this window.

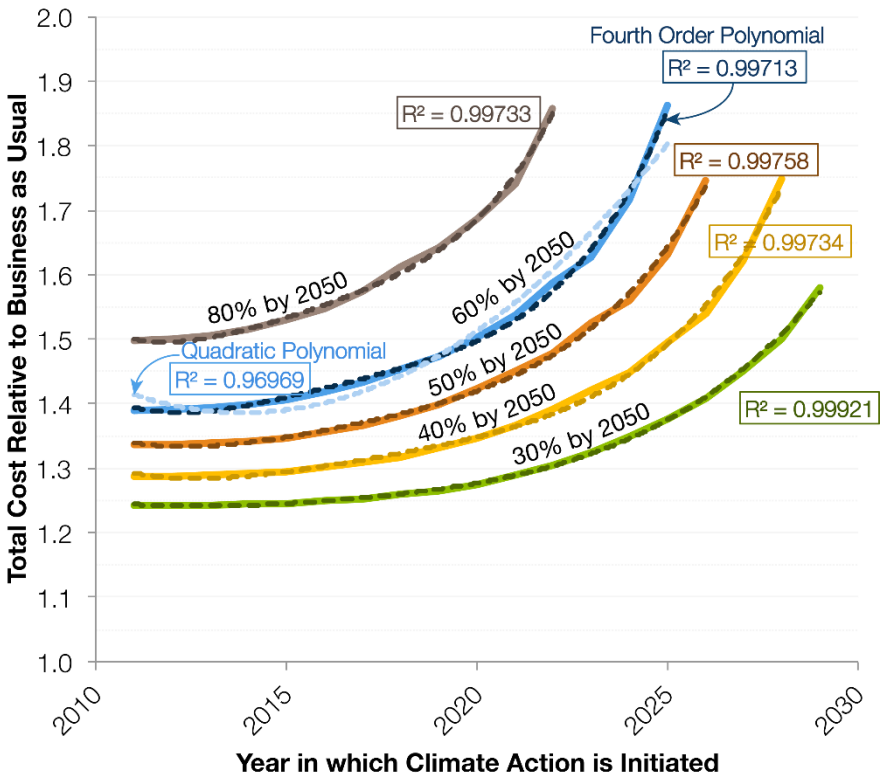

Figure 4.9. Technological costs of climate action follow a fourth order increase with every year of climate action delay.

Forced retirement of old fossil fuel-based capacity is critical to climate action in the electric sector (see Figure 4.10). Under immediate climate action for 60% reduction in emissions by 2050 in the electric sector, coal (C), natural gas (NG), petroleum (P), and nuclear (N) generating capacity older than its service life would need to be retired immediately and replaced with new NG capacity. Similar to the switch from CVs to PHEVs in the auto sector, the electricity sector would also need to switch to wind for new capacity addition around 2025. This scenario assumes that new nuclear capacity additions are unlikely to exceed the small growth of 0.2% (annually) projected in the AEO 2011 report (U.S. Energy Information Administration, 2011). However, from the point of view of capital and operating costs, nuclear capacity addition has a lower cost than wind, although nuclear capacity addition has 2-3 times the lead times for wind or solar power when considering new capacity addition.

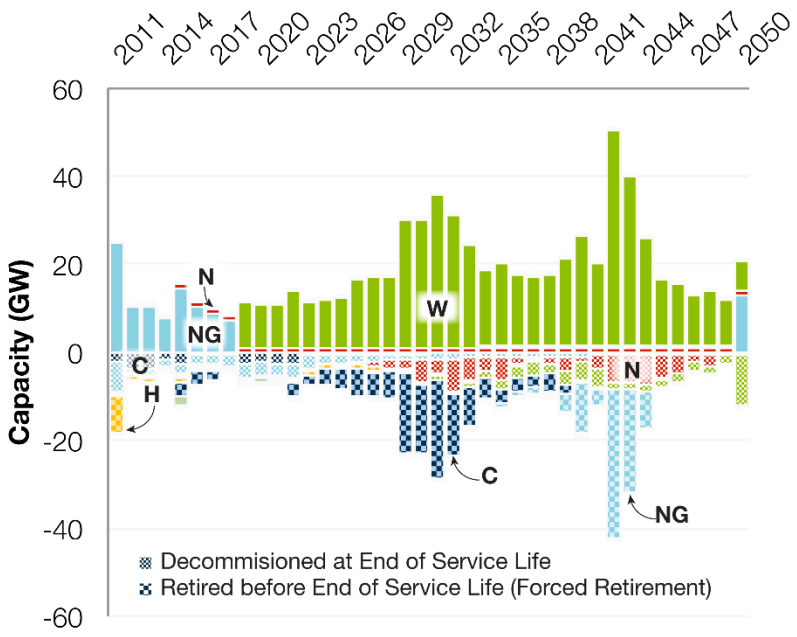

Figure 4.10. Technology trajectory for immediate climate action in the electric sector for 60% emission reduction by 2050.

The analysis also assumes the levelized cost of electricity from utility scale solar projects (S) based on the EIA's latest (2013) estimates for plant costs and capacity factors (U.S. Energy Information Administration, 2013d). Based on these figures, the levelized cost of electricity (LCOE) for on-shore wind capacity (W) is about 1.2 USD/kWh and for photovoltaic (PV) solar is about 4.2 USD/kWh. However, advances in the utility scale PV technology, costs, and coupled storage systems to increase the utilization (capacity factor) can potentially make PV solar generation cost competitive with on-shore wind, particularly if the U.S. Department of Energy's SunShot Initiative target of 1 USD/W is achieved in the near term (Gowrishankar, Hutton, Fluhrer, & Dasgupta, 2006; Mileva, Nelson, Johnston, & Kammen, 2013). This scenario has not been modeled in the uncertainty analysis presented in this study, but will be included in the next iteration of the model and its inputs.

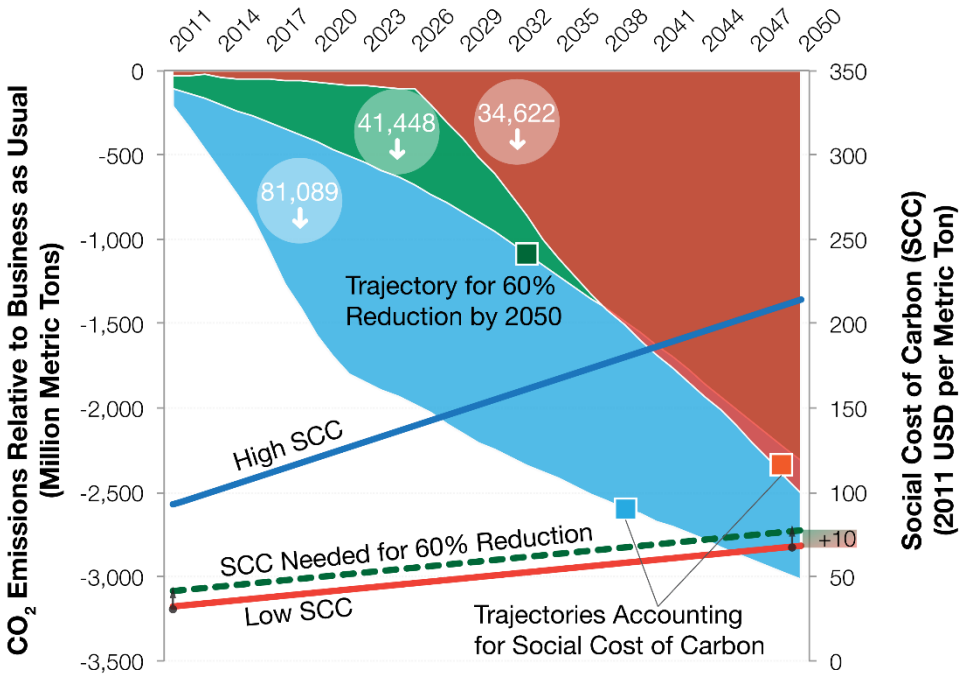

Figure 4.11. Estimation of the carbon penalty of social cost of carbon (SCC) needed to achieve 60% reduction in emissions by 2050 under immediate climate action in the auto sector.

Unlike the auto sector, we find that in the electric sector, the lower (average) estimate of SCC can achieve significant emission reduction, and by setting the carbon penalty to roughly USD 10/metric ton higher than the low SCC estimate (as opposed to the high SCC estimate in the auto sector), emission reductions of 60% by 2050 can be achieved as shown in Figure 4.11. The reason behind this drastic change is that it is significantly inexpensive to reduce carbon emissions from the electric sector compared to the auto sector. The average abatement cost assuming immediate climate action for 60% reduction by 2050 in the electric sector is roughly USD 22/ton CO_2 avoided, more than 30% lower than the corresponding value for the auto sector. This is because over the service life of a typical fossil fuel-based unit in the electric sector (MWh of generating capacity), the ratio of total amount spent on operating costs (mainly fuel costs) to the amount spent on capital costs is typically about 4:1 compared to about 3:2 in the automotive sector based on our analysis. As a result, the marginal return

on capital investment in terms of savings in operating costs is considerably higher in the electric sector than in the auto sector, which translates to the observed higher return on investment in terms of emission reduction.

4.5 RECOMMENDATIONS AND CONCLUSIONS

4.5.1 Climate Action Window

The least cost trajectories and technological costs of climate action over various scenarios examined for both the automotive and electric sectors in this study provide certain key insights into the question of carbon management through prevention in these sectors. First, we find little evidence that introducing delays in imposing formal emission constraints through suitable policy instruments with the anticipation that improvements in costs and efficiencies of established and nascent technologies will compensate for the delays. In the auto sector, technological costs of abatement for a given percentage reduction in emissions by 2050 remain practically constant until forced retirement becomes essential to meet said emission targets. Beyond this point, the costs increase steeply with every year of delay, and the ability to meet even a 30% reduction target by 2050 vanishes at the latest by 2030. In the electric sector, the technological costs of abatement increase roughly as a fourth order polynomial with every year of delay, with the window of opportunity for reducing a minimum of 30% of emissions by 2050 similarly closing by 2030 at the latest under all conditions examined. We highlight that these costs are purely the technological costs associated with deploying, operating and retiring technology units, and do not include social costs of ecosystem damages and climate change adaptation, which have already been shown to increase considerably with delayed climate action.

Secondly, the inertia in fleet turnover introduced due to product lifetimes necessitates forced retirement of units (vehicles or MWh of generation capacity) before their service life beyond a certain point in time due to climate inaction. Despite significantly higher costs compared to the immediate climate action case wherein retirement is either not necessary (auto sector) or is lower (electric utility sector), retirement and substitution with cleaner technologies in delayed climate action cases (between 2020 and 2030) is still a cheaper option than not retiring. This is because the capital costs of new technologies such as battery electric vehicles or on-shore wind plants needed to compensate for emissions from older fossil fuel-based units allowed to operate until the end of their service life is significantly high. Finally, we confirm that the cost to reduce emissions from the electric sector are more than 30% lower than abatement costs in the automotive sector. This opens the possibility of concerted carbon mitigation efforts between the two sectors, particularly given the rising trend towards electric vehicles.

4.5.2 Implications for Technology Investments

If climate action (60% emission reduction relative to 1990) were to be initiated in the near future, the abatement costs and emission reduction relative to the BAU scenario would need to follow the progression shown in Figure 4.12 to minimize the total cost to society. In both the electric and automotive sectors, the initial years of climate action from now through 2030 will have to involve large capital investments on the part of electric power plant owners and vehicle owners respectively in switching to less carbon-intensive technologies.

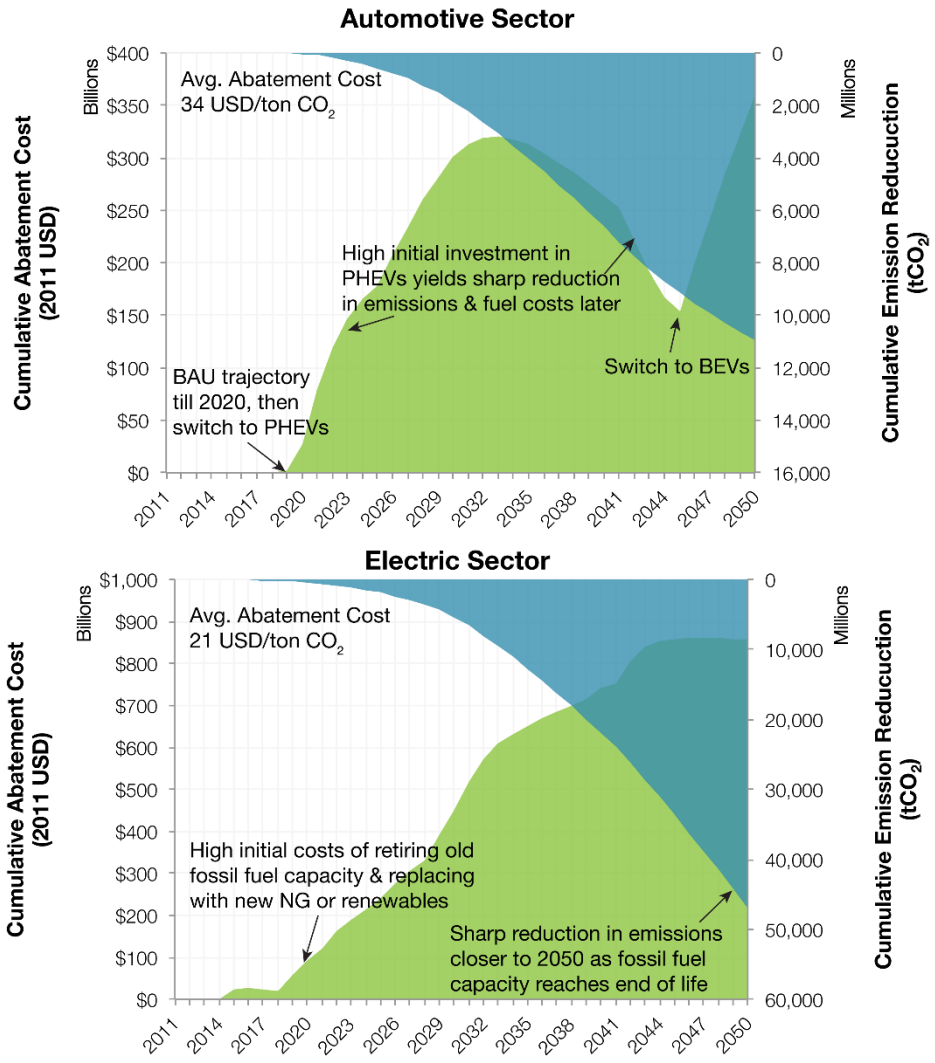

Figure 4.12. Cumulative abatement costs and emission reduction relative to BAU in the automotive and electric sectors assuming climate action starting 2015.

In the case of the automotive sector, the model data and results indicate that a switch from conventional gasoline- or diesel-powered vehicles to plugin hybrids i.e. PHEVs is necessary. Here, we emphasize that our analysis examines *existing* technologies and their cost progressions, and thus it chooses PHEVs as the optimal technology of choice from 2020 – 2045, and BEVs thereafter (Figure 4.7, right). In the electric sector, the results indicate a switch to new and efficient NG (combined cycle) plants until about 2020, followed by a switch to new wind power (Figure 4.10). However, from

the point of view of informing producers, consumers, and policy makers on decisions over incentives or R&D spending, these results simply indicate the costs and emission intensities of technologies capable of achieving a specific amount of total emission reduction at least cost to society. Using these costs and emission intensities as upper bounds, policy decisions can then be made to incentivize existing technologies, or set targets for novel and innovative technologies. Figure 4.13 shows there cost and emission intensity progression in both the automotive and electric sectors for achieving 60% emission reduction by 2050.

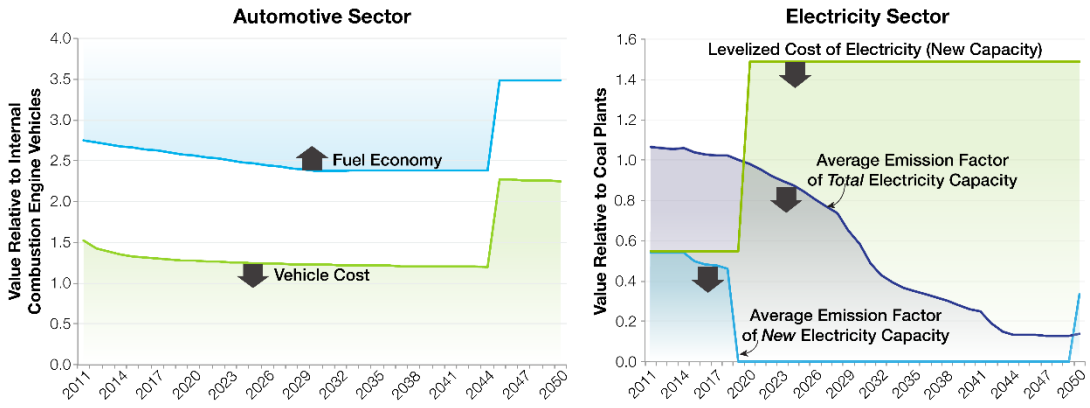

Figure 4.13. Cost, fuel economy, and emission factor targets for existing and next generation technologies in the automotive and electric sectors to achieve 60% emission reduction by 2050.

Note that emission intensity for the automotive sector is expressed as miles per gallon (mpg), and thus the vehicle fuel economy values shown in Figure 4.13 (left) are a lower bound. The model and its conclusions surrounding climate action windows are thus robust not only within the bounds of the cost and efficiency improvements in existing technologies, but also to potential disruptive technological innovations. In fact, the levels of cost (per vehicle or per MWh) and emission intensities obtained through such an analysis using this model can be used as design targets for technologies that are in research phase or have been developed but are yet to be commercialized.

4.5.3 Using the Model and Framework for Robust Policy Design and Evaluation

The optimization model and policy analysis framework presented in this chapter and described in Figure 4.14 can be scaled up or down to facilitate decision-making over technology investments and policy design, and environmental planning at different scales. For instance, the model could be expanded to include energy and/or transportation fleets in developing countries such as China and India that are significant GHG emitters to determine investment portfolios and incentives that minimize carbon abatement costs across countries through appropriate mechanisms such as emission permits. The model could also be applied for the purposes of planning or estimating levels of technology subsidies, premiums for take-back programs for old vehicles, and emissions prices (for trading schemes) for regional emission mitigation programs such as the State of California's Global Warming Solutions Act (Pavley & Nunez, 2006).

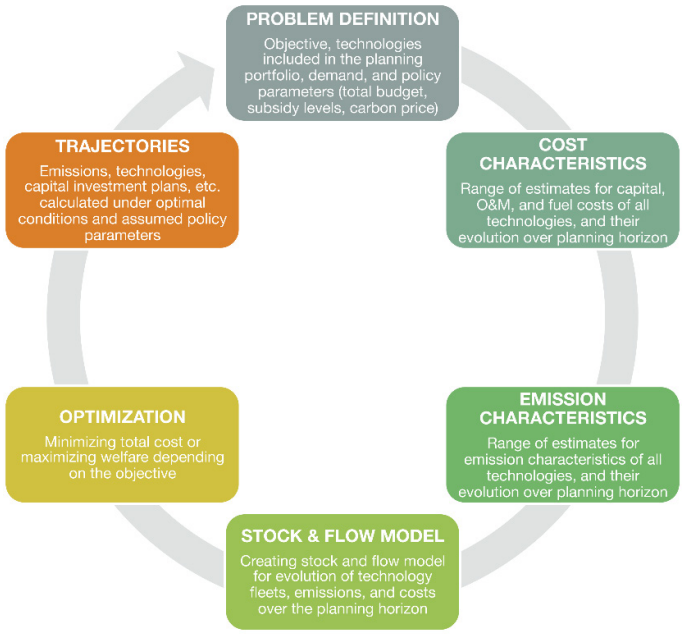

Figure 4.14. Process for building and applying the model to inform or evaluate policy decisions on carbon abatement at regional and global scales.

The framework behind the model is developed so as to maintain linearity in the optimization formulation. To evaluate various scenarios of technology portfolios, or test the outcomes under different levels of subsidies and other policy instruments, the model will need to be run sequentially or iteratively depending on the desired analysis. The ability to runt he model iteratively can also allow the inclusion of micro- or macro-economic sub-modules, which may otherwise introduce non-linearity in a model. For instance, if the price elasticity of electricity demand is known, one can endogenously estimate the sectoral demand for electricity by running the model iteratively until convergence, instead of using demand as an exogenous parameter. Another example could be the introduction of a vehicle demand model based on vehicle attributes such as class, price, subsidy, and cost of ownership to endogenously estimate upper bounds on the market penetration of a given technology. The market shares can then be imposed as constraints in the optimization model, and the price of carbon to achieve a certain level of emission reduction can be evaluated by iteratively adjusting the market shares and carbon price until convergence.

A comprehensive assessment of the uncertainties in parameters that define technology costs, technology improvements, fuel costs, and technology evolution (e.g. survival probability of vehicles) is needed to test whether the conclusions of the analyses hold true under the best and worst case scenarios, and if so, the ranges of values for parameters under which the conclusions hold true. It should be noted that a high degree of uncertainty can sometimes be inevitable when dealing with technologies that are not yet mature, or are even yet to be developed for that matter. As such, the uncertainty associated with very specific outcomes of a desired analysis (in the context of this framework), such as a subsidy value for a given technology in a given year, is likely to be high and we

caution against the blind interpretation of such values. Instead, by keeping the objectives of the analysis more qualitative and at a high level of decision-making, such as ascertaining whether the window of opportunity for climate action expands or shrinks with expected (or disruptive) improvements in technology (see sections 4.3 and 4.5.1), the outcomes of the model are more robust to such uncertainties.

CHAPTER 5

ENGINEERING SIGNIFICANCE AND FUTURE WORK

Quantifying Life Cycle Risks in CCS due to Trade-Offs in CO_2 Quality and Process Costs

Numerous studies in the literature have examined the life cycle environmental impacts of CCS from coal and natural gas power plants (Khoo & Tan, 2006; Koornneef et al., 2008; E. S. Rubin, Chen, & Rao, 2007; Schreiber, Zapp, & Kuckshinrichs, 2009; Singh et al., 2011). The estimates of CO_2 emissions for every metric ton of CO_2 captured range from 200-350 kg including on-site or from upstream processes depending on the fuel source, and separation method used. The energy penalties assumed in these studies however only take into account the basic steps of separation and compression involved in CO_2 capture. They do not account for the steps that may be required to purify the CO_2 to a level that is safe (from an environmental and occupational standpoint) for transportation, as well as sequestration or use as an industrial feedstock. Thus, they do not account for the influence of the quality of CO_2 on the net energy balance and carbon footprint (Zapp et al., 2012), which may lead to underestimation of CCS impacts. As identified in the IMPACTS project in the European Union (Lilliestråle et al., 2014), "there is a need to build new knowledge on the fundamental properties of CO_2 mixtures with impurities and their impact on the CCS chain integrity and economics."

Our recent work (Supekar & Skerlos, 2014) on the effects of quality requirements for merchant market CO_2 on the energy consumption and emissions from the CO_2 recovery process begins to

address this knowledge gap by providing ranges of environmental impacts for various purity standards defined by EIGA (European Industrial Gases Association, 2008). However, as discussed earlier, the impurity levels in CO_2 recovered form co-product sources or natural wells for merchant market applications or EOR are considerably lower than levels found in flue gases of electric power generation plants. As a result, CCS plants at power generation facilities will likely require additional pre-treatment steps such as flue gas desulfurization (FGD), selective catalytic reduction (SCR), and electrostatic precipitation (ESP) to condition the flue gas for further purification. It should be noted that this pre-treatment is needed to prevent formation of heat-stable salts and uneconomically high consumption of the chemical absorbent during the absorption enrichment step. A detailed process- and thermodynamics-based model of the CO_2 recovery process is thus central to the accurate estimation of the net benefits of CCS.

The success of large-scale CCS is closely tied to the availability of a reliable transportation network. Most of the CO_2 in the merchant market is transported via road networks in heavy-duty trucks. However, the massive quantities of CO_2 that will potentially be captured from power plants in CCS operations will have to be transported via a network of onshore or offshore pipelines to sequestration sites. Currently, the U.S. has about 6000 km of pipeline network built to transport roughly 50 MMT of CO_2 recovered from natural wells and a few co-product sources for use in EOR operations. These pipes range in diameter from 305 mm - 752 mm, and have a capacity ranging from 4.4 – 20 MMT/year. Figure 5.1 shows the capital and operation costs of pipelines as a function of the pipe diameter. These costs have been developed based on an extensive review of the literature on pipeline costs in the EOR, oil, and natural gas industry, and do not include the cost of boosting stations that

may be necessary to make up for pressure losses in pipelines extending over several hundred kilometers. Transportation of CO_2 for CCS thus also needs to be designed carefully such that existing and new pipeline networks are equipped to handle varying qualities of CO_2, while striking an optimal balance between capital costs, operating costs, and system reliability.

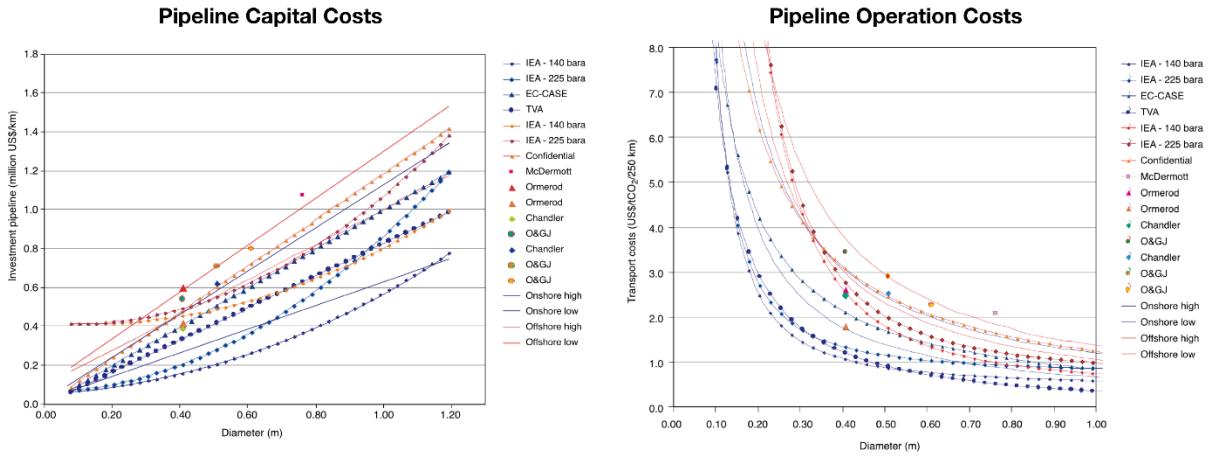

Figure 5.1. Estimated capital and operation costs of CO_2 transportation pipelines carrying recovered CO_2 at 10 MPa pressure (Intergovernmental Panel on Climate Change, 2005).

Additionally, from a consequential life cycle assessment standpoint, it is essential to consider that although the sequestration of CO_2 generated from fossil fuel combustion in EOR will keep this CO_2 out of the atmosphere for a long period of time, the fossil fuels extracted from the earth's crust will create additional CO_2, which may or may not be sequestered in future. In this context, it has been argued (Hertwich, 2014; Plevin, Delucchi, & Creutzig, 2014) that carbon abatement technologies are effective insofar as they prevent the further extraction of carbonaceous materials that may lead to equal or more GHG emissions in the future through chemical or biological pathways. From a life cycle standpoint, it is important to take this end-of-life application of sequestered CO_2 into account to evaluate the true benefits of CCS.

To address the engineering and questions surrounding CO_2 quality, recovery process characterization, and transportation network design, future research in this area will seek to quantify the environmental and economic risks associated with carbon capture and sequestration (CCS) projects by building upon the work on CO_2 recovery and life cycle emissions presented in this thesis (see Figure 5.2).

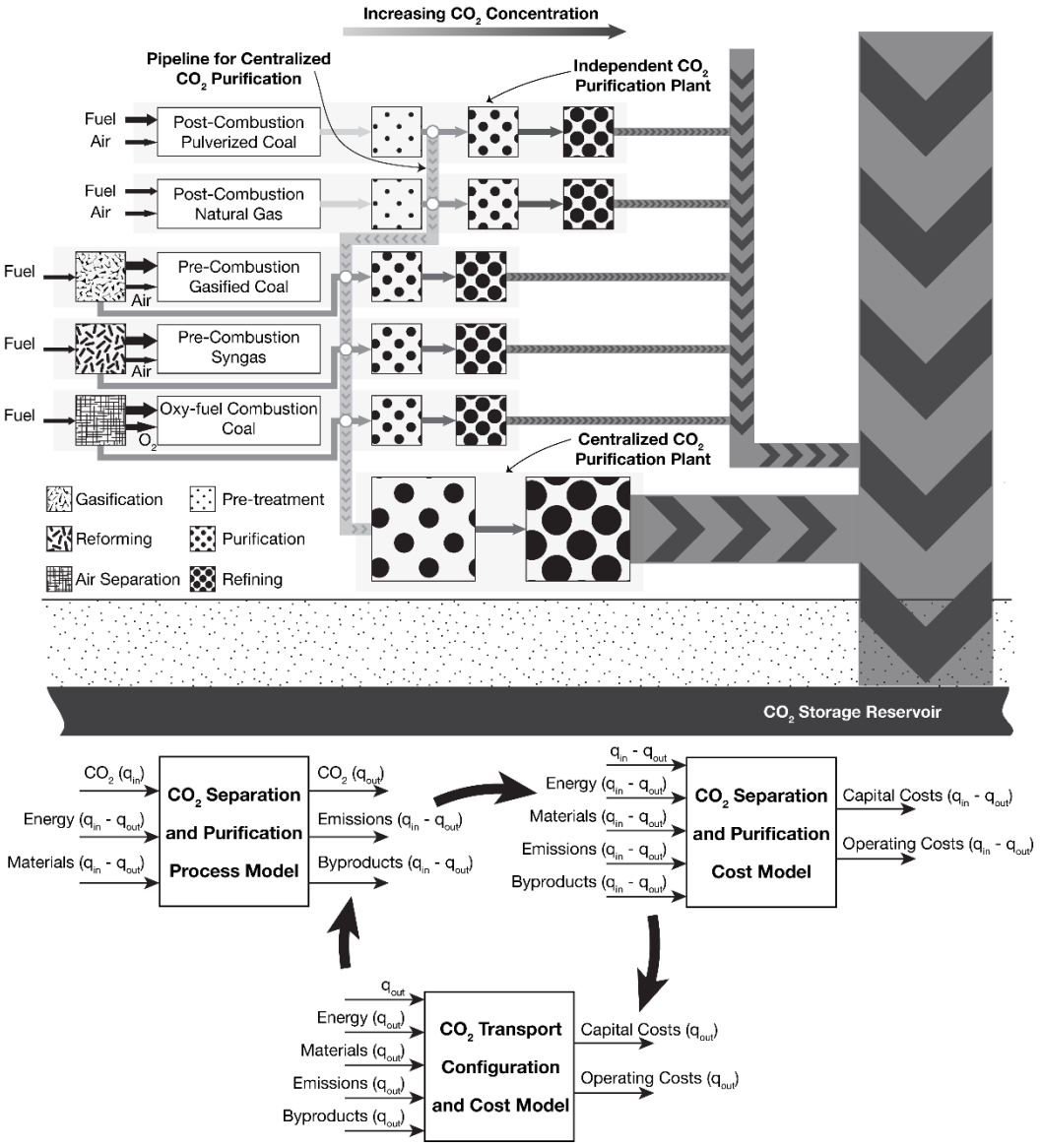

Figure 5.2. Framework for a detailed characterization and optimization of large-scale CCS projects and CO_2 transportation networks.

The major outcomes of this research will be (1) characterization of the individual and collective impact of CO_2 impurities on each step in the CCS process, (2) translation of these impacts to potential environmental emissions and economic costs for various current and potential technologies producing CO_2 as a byproduct of electric power generation, (3) development of an integrated model of the CCS process and assessment of its life cycle environmental impacts, costs, and risks in a design-optimization framework to determine the optimal values of critical process variables and pipeline network design configurations, (4) application of the integrated assessment model to identify the most suitable candidates for CCS retrofits in the U.S. utility generator fleet, and (5) consequential life cycle analysis of CO_2 recovered and purified in using large scale CCS systems for use in enhanced oil recovery operations.

Charting Cost-Optimal Carbon Abatement Policy Measures for the Energy and Automotive Sector

The work presented in this thesis on cost-optimal carbon abatement technology pathways assumes an ideal world where consumers buy what producers produce. However, in reality, consumers exercise their choice when purchasing a product, and the producers also face delays in rollout of their products due to production capacity ramp time, and regulatory processes. To account for these factors in the cost-optimal policy design framework, the optimization model from this thesis will be coupled with a system dynamics-based simulation model that will analyze market-related factors such as consumer choice to endogenously determine technology market share evolution. This combined optimization-simulation iterative model will elucidate (1) the technology trajectories that are most likely to help achieve 2050 CO_2 emission targets while accounting for the delays introduced by technology turnover,

production ramping, and policy-enforcement, and (2) the optimal policy portfolio and optimal levels of individual instruments needed to achieve the desired technology trajectories. The ability of the model to run at variously time-scales, and learn from the economic and emission outcomes of previous years' policy decisions can thus facilitate dynamic policy-making, which can be of significant value to technical bodies advising law-makers on climate policy. The dynamic policy making approach can be applied sector-wide or on a smaller scale limited to a specific power control area or state.

APPENDICES

Appendix A Recovered CO_2 purity grades, processing steps, and operating conditions used to estimate production emissions from various sources.

	Standard Purity	**High Purity**	**Sources**	**Notes**
Outlet purity range	≥ 99.5%	99.9 - 99.999%	(All Gas, 2001; Matheson Gas, 2010),	-
Purification train components	MEA absorber/stripper (only for post-combustion capture), gas/liquid separators, scrubber, carbon filter, desiccant drier	MEA absorber/stripper (only for post-combustion capture), gas/liquid separators, scrubber, carbon filter, desiccant drier, distillation tower	(Finley, 2006; Häring, 2008; Overcash et al., 2007; Rushing, 2013; The Wittemann Company, 2012)	Additional catalytic oxidation step for hydrogen and natural well sources
CO_2 output pressure and temperature (for sequestration)	99.5 bar, 35 °C	99.5 bar, 35 °C	(IPCC, 2005)	Compression step not necessary in natural well source; source pressure is 47 bar
CO_2 output pressure and temperature (for merchant market)	18 bar, -22 °C	18 bar, -22 °C	(Finley, 2006; Häring, 2008; Overcash et al., 2007; Rushing, 2013)	Compression step not necessary in natural well source; source pressure is 47 bar
Source of electricity at recovery plant	U.S. Average Mix or NGCC-CCS/PC-CCS for post-combustion capture	U.S. Average Mix or NGCC-CCS/PC-CCS for post-combustion capture	(*Ecoinvent Database v2.2*, 2010)	-
Source of heat at recovery plant	Natural Gas for high purity and NGCC-CCS plants, and coal for PC-CCS	Natural Gas for high purity and NGCC-CCS plants, and coal for PC-CCS	(U.S. Environmental Protection Agency, 1998a, 1998b)	-

	Standard Purity	High Purity	Sources	Notes
Scrubber	Wet spray tower	Wet spray tower	(U.S. EPA, 2003b)	Removes particulates, acid gases, water soluble impurities
Compressor	Screw type multistage	Screw type multistage	(Rushing, 2013)	-
Carbon filter	Coconut shell granular activated carbon (GAC)	Coconut shell granular activated carbon (GAC)	(Finley, 2006; Häring, 2008; Hung, 2012)	Removes sulfides, volatile organics, hydrocarbons
Carbon bed regeneration	Steam at 200 - 400 °C for 8 - 12 hours, 93 °C air drying for 3 - 4 hours, and ambient air cooling for 3 - 4 hours; steam consumption 1.5 - 3.5 kg/kg impurity	Steam at 400 - 600 °C for 8 - 12 hours, 93 °C air drying for 3 - 4 hours, and ambient air cooling for 3 - 4 hours; steam consumption of 3.5 - 6.0 kg/kg impurity	(Häring, 2008; Kohl & Nielson, 1997)	-
Dryer desiccant	Alumina	Molecular Sieves	(*Ecoinvent Database v2.2*, 2010; Finley, 2006; Kohl & Nielson, 1997)	Removes moisture
Dryer bed regeneration	Dry CO_2 at 205 - 315 °C for 3 - 5 hours, and ambient air cooling for 2 - 3 hours; dry CO_2 consumption 8% of dryer inlet flow	Dry CO_2 at 315 - 400 °C for 8 hours, and ambient air cooling for 3 hours; dry CO_2 consumption 8% of drier inlet flow	(Häring, 2008; Kohl & Nielson, 1997)	75% of the energy from the heat source is lost to heating the desiccant bed, vessel, and vent gases(Kohl & Nielson, 1997)
Catalytic oxidation	Oxygen at 20 bar, 420 °C over platinum group or metal oxide catalyst	Oxygen at 20 bar, 420 °C over metal oxide catalyst	(*Ecoinvent Database v2.2*, 2010; Häring, 2008; Kohl & Nielson, 1997; Overcash et al., 2007; Topsøe, 2010)	Removes VOCs, hydrocarbons, and sulfides
Distillation	Not required	Pure CO_2 used in the stripper with a reflux ratio of 0.1 - 0.3	(Häring, 2008)	Removes trace air gases
Liquefaction	Centralized ammonia chillant system	Centralized ammonia chillant system	(Häring, 2008; Overcash et al., 2007; Rushing, 2013)	Chilled ammonia also used in some heat exchangers

Appendix B Range of values used to estimate process inputs and environmental impacts from production of various grades of CO_2 from different sources.

	Nominal	High	Low	Units	Sources	Notes
CO_2 Capture Efficiency	85%	90%	65%	-	(IPCC, 2005)	-
Specific enthalpy of regeneration steam	2733	2795	2733	kJ/kg steam	(Erga, Juliussen, & Lidal, 1995; Overcash et al., 2007)	-
Regeneration steam consumption	1.7	1.8	1.7	kg steam/kg CO_2	(Erga et al., 1995; Kothandaraman, 2010)	-
Activated carbon regeneration steam flow rate	3.5	6	1.5	kg/kg impurity	(Kohl & Nielson, 1997)	-
Activated carbon regeneration steam temperature	400	600	200	°C	(Kohl & Nielson, 1997)	-
Activated carbon regeneration steam enthalpy	3277	3705	2873	kJ/kg steam	-	-
Activated carbon purification time	12	12	8	hours	(Kohl & Nielson, 1997)	-
Drying regeneration gas temperature	315	400	205	°C	(Kohl & Nielson, 1997)	High and nominal values for molsieve, low value for alumina desiccant
Drying time	8	12	8	hours	(Kohl & Nielson, 1997)	-
Distillation stripper reflux ratio	0.25	0.3	0.1	-	(Häring, 2008)	Corresponding to yields of 80%, 50%, and 90%
PC/NGCC impurities	1%	3%	0.5%	-	(IPCC, 2005)	Impurity levels post-MEA wash
Ammonia/Ethanol source impurities	3%	3%	1%	-	(Feinberg & Karpuk, 1990)	-

	Nominal	High	Low	Units	Sources	Notes
Hydrogen source impurities	3%	3%	1%	-	(Feinberg & Karpuk, 1990)	-
Natural well impurities	3%	5%	2%	-	(Feinberg & Karpuk, 1990)	-

Appendix C Environmental impacts of 1 MWh of electricity production for sale in PC, PC-CCS, NG, and NGCC-CCS power plants.

Pulverized Coal (PC)

			On-Site	Upstream	Total
PC	GWP	*kg CO2 eq.*	1.02E+03	4.39E+01	1.07E+03
	OZDP	*kg CFC-11 eq.*	3.52E-05	1.35E-06	3.65E-05
	SMOG	*kg O3 eq.*	3.79E+01	2.99E+00	4.09E+01
	ACIDP	*mol H+ eq.*	1.09E+02	7.35E+00	1.16E+02
	EUTP	*kg N eq.*	6.76E-02	4.92E-03	7.26E-02
	RESP	*kg PM10 eq.*	3.11E-01	1.06E-01	4.17E-01
	ECOTX	*CTUe*	1.59E+01	1.79E+00	1.77E+01
	ENER	*MJ*	9.67E+03	7.66E+01	9.75E+03
	WATER	*kg*	6.91E+02	1.59E+03	2.28E+03
PC-CCS	GWP	*kg CO2 eq.*	3.91E+02	1.66E+02	5.57E+02
	OZDP	*kg CFC-11 eq.*	1.36E-05	7.78E-06	2.13E-05
	SMOG	*kg O3 eq.*	7.66E+01	1.63E+01	9.29E+01
	ACIDP	*mol H+ eq.*	1.35E+02	3.96E+01	1.75E+02
	EUTP	*kg N eq.*	1.30E-01	2.87E-01	4.17E-01
	RESP	*kg PM10 eq.*	1.36E-01	2.29E-01	3.65E-01
	ECOTX	*CTUe*	1.25E+01	4.88E+01	6.13E+01
	ENER	*MJ*	1.84E+04	3.46E+03	2.18E+04
	WATER	*kg*	1.31E+03	7.66E+03	8.97E+03

Natural Gas Combined Cycle (NGCC)

			On-Site	Upstream	Total
NGCC	GWP	*kg CO2 eq.*	3.44E+02	3.73E+01	3.81E+02
	OZDP	*kg CFC-11 eq.*	0.00E+00	2.40E-06	2.40E-06
	SMOG	*kg O3 eq.*	7.13E+00	2.13E+00	9.26E+00
	ACIDP	*mol H+ eq.*	1.15E+01	3.61E+00	1.52E+01
	EUTP	*kg N eq.*	1.27E-02	3.77E-03	1.64E-02
	RESP	*kg PM10 eq.*	4.41E-02	7.34E-03	5.14E-02
	ECOTX	*CTUe*	1.92E+00	3.70E-01	2.29E+00
	ENER	*MJ*	6.78E+03	1.19E+02	6.90E+03
	WATER	*kg*	2.00E+02	7.37E+02	9.37E+02
NGCC-CCS	GWP	*kg CO2 eq.*	8.91E+01	5.84E+01	1.48E+02
	OZDP	*kg CFC-11 eq.*	0.00E+00	3.96E-06	3.96E-06
	SMOG	*kg O3 eq.*	1.19E+01	3.13E+00	1.51E+01
	ACIDP	*mol H+ eq.*	1.60E+01	7.06E+00	2.30E+01
	EUTP	*kg N eq.*	1.78E-02	6.47E-02	8.26E-02
	RESP	*kg PM10 eq.*	1.22E-02	1.91E-02	3.13E-02
	ECOTX	*CTUe*	1.78E+00	1.06E+01	1.24E+01
	ENER	*MJ*	8.73E+03	3.80E+02	9.11E+03
	WATER	*kg*	2.57E+02	2.08E+03	2.33E+03

Appendix D Material and energy input, and environmental impacts of production of 1 metric ton of industrial and high purity grades of recovered CO_2.

Material and Energy Inputs

		Ammonia/Ethanol			**Hydrogen**			**Natural Wells**		
		Nom	Low	High	Nom	Low	High	Nom	Low	High
Industrial Purity										
Electricity	*kWh*	159.9	159.7	159.9	209.8	209.6	209.8	-16.3	-16.4	-16.1
NG	*kg*	6.8	0.0	14.1	4.5	0.0	11.8	18.4	12.6	32.7
Compressed Air	*kg*	13.9	13.9	13.9	13.9	13.9	13.9	11.5	11.5	11.5
Oxygen	*kg*	0.0	0.0	0.0	5.5	5.5	5.5	14.6	14.6	14.6
GAC	*g*	13.3	13.3	13.3	13.3	13.3	13.3	13.3	13.3	13.3
Alumina	*g*	19.9	19.9	19.9	19.9	19.9	19.9	39.8	39.8	39.8
Potable Water	*kg*	747	549	912	747	549	912	95	28	272
High Purity										
Electricity	*kWh*	186.1	170.3	191.3	248.5	225.2	256.2	-8.9	-13.1	-7.3
NG	*kg*	8.5	0.0	18.4	5.6	0.0	15.3	23.1	13.9	42.5
Compressed Air	*kg*	17.4	15.3	18.1	17.4	15.3	18.1	14.3	12.6	14.9
Oxygen	*kg*	0.0	0.0	0.0	6.9	6.1	7.2	18.3	16.1	19.0
GAC	*g*	13.3	13.3	13.3	13.3	13.3	13.3	13.3	13.3	13.3
Alumina	*g*	19.9	19.9	19.9	19.9	19.9	19.9	39.8	39.8	39.8
Potable Water	*kg*	1,740	1,411	1,991	1,740	1,411	1,991	119	30	354

Environmental Impacts

		Ammonia/Ethanol			**Hydrogen**			**Natural Wells**		
		Nom	Low	High	Nom	Low	High	Nom	Low	High
Industrial Purity										
GWP	*kg CO2 eq.*	146.6	121.6	173.3	175.9	159.4	202.6	1,175	1,154	1,225
SMOG	*kg O3 eq.*	6.0	5.5	6.5	7.5	7.2	8.0	0.9	0.5	2.0
ACIDP	*mol H+ eq.*	54.3	44.9	64.3	64.4	58.3	74.4	24.3	16.4	43.8
EUTP	*g N eq.*	471.7	469.2	473.6	611.6	609.8	613.6	-23.3	-25.1	-19.0
RESP	*g PM10 eq.*	159.6	128.8	192.6	189.0	168.7	221.9	73.9	47.7	138.1
ECOTX	*CTUe*	130.2	102.3	159.9	151.6	133.3	181.3	68.1	44.4	126.1
ENER	*MJ*	2,385	1,964	2,834	2,846	2,570	3,294	995	638	1,871
WATER	*kg*	1,836	1,439	2,166	1,954	1,557	2,284	226	89	581
High Purity										
GWP	*kg CO2 eq.*	173.4	130.2	213.4	210.0	171.8	251.4	1,197	1,162	1,267
SMOG	*kg O3 eq.*	7.0	5.9	7.9	8.9	7.7	9.9	1.6	0.8	3.0
ACIDP	*mol H+ eq.*	63.8	48.0	78.7	76.5	62.6	91.8	32.9	19.1	59.9
EUTP	*g N eq.*	549.9	500.7	567.9	725.0	655.4	750.1	2.5	-14.0	12.9
RESP	*g PM10 eq.*	189.1	137.8	237.7	225.8	181.8	275.9	101.5	56.4	190.5
ECOTX	*CTUe*	154.0	109.2	197.5	180.9	143.3	225.4	92.2	51.9	172.5
ENER	*MJ*	2,819	2,099	3,488	3,396	2,766	4,088	1,383	762	2,598
WATER	*kg*	3,879	3,185	4,395	4,027	3,315	4,548	305	108	783

Appendix E Vehicle Sales, Emissions, and Total Vehicle Population Data to Estimate Vehicle Scrappage Rate Curve.

Year	Total LDV Sales*	CVs	HEVs**	BEVs	PHEVs
1990	13,859,700	13,859,700	-	-	-
1991	12,309,400	12,309,400	-	-	-
1992	12,857,300	12,857,300	-	-	-
1993	13,882,700	13,882,700	-	-	-
1994	15,044,900	15,044,900	-	-	-
1995	14,717,600	14,717,600	-	-	-
1996	15,089,500	15,089,500	-	-	-
1997	15,114,100	15,114,100	-	-	-
1998	15,533,600	15,533,600	-	-	-
1999	16,879,400	16,879,383	17	-	-
2000	17,343,700	17,334,350	9,350	-	-
2001	17,118,300	17,098,018	20,282	-	-
2002	16,821,900	16,785,865	36,035	-	-
2003	16,639,100	16,591,500	47,600	-	-
2004	16,866,800	16,782,601	84,199	-	-
2005	16,948,200	16,738,489	209,711	-	-
2006	16,504,100	16,251,464	252,636	-	-
2007	16,089,100	15,736,826	352,274	-	-
2008	13,195,000	12,882,614	312,386	-	-
2009	10,401,400	10,111,129	290,271	-	-
2010	11,554,600	11,280,390	274,210	-	-

Total LDV Population in 2010* **	230,444,440 vehicles
Total CO_2 Emissions from LDVs in 2010** **	1,134.4 Mt CO_2

*Vehicle sales data source: Wards Auto (2014)

**HEV sales data source: U.S. Department of Energy (AFDC) (2014)

***Data source: U.S. Department of Transportation (FHWA) (2010)

****Data source: U.S. Environmental Protection Agency (2013)

Appendix F Total and Age-wise Breakdown of Electric Generation Capacity and Total Emissions Data for 2010.

Age*	Build Year	Coal	NG	Petroleum	Biomass	Nuclear	Hydro	Wind	Solar	Geothermal
0	2012	3953	10127	580	388	0	345	12953	1616	192
1	2011	4159	10880	349	273	0	161	6936	705	7
2	2010	5836	7626	1048	257	0	22	4681	240	24
3	2009	1999	10718	100	432	0	26	9922	101	213
4	2008	1584	8853	94	259	0	18	8499	33	64
5	2007	1514	7712	322	321	0	20	5279	107	67
6	2006	597	10113	206	262	0	21	2650	1	53
7	2005	478	16818	165	44	0	30	2159	3	30
8	2004	617	25354	285	130	0	79	393	0	0
9	2003	90	52804	319	174	0	83	1609	0	0
10	2002	11	65757	994	54	0	16	773	2	7
11	2001	520	43336	571	247	0	140	1404	5	0
12	2000	129	30068	685	73	0	4	56	0	61
13	1999	328	9285	228	125	0	189	701	0	0
14	1998	4	2112	171	162	0	3	176	0	61
15	1997	90	4475	405	148	0	63	20	0	0
16	1996	1913	4262	294	262	1270	61	28	0	51
17	1995	2635	6852	182	146	0	123	30	0	0
18	1994	1073	9255	107	375	0	277	102	0	0
19	1993	193	4903	132	384	1215	159	4	0	48
20	1992	1603	5001	276	168	0	204	7	0	98
21	1991	3406	3348	840	1004	0	167	77	0	0
22	1990	2229	5089	273	623	3596	464	157	92	88
23	1989	3284	3647	538	817	2514	575	99	92	355
24	1988	1851	2801	144	626	6424	542	27	70	301
25	1987	4253	2629	92	819	7968	275	110	34	36
26	1986	6435	1380	226	365	9893	635	87	69	68
27	1985	7338	1616	104	536	8795	1203	111	30	455
28	1984	11166	1059	97	315	8153	631	149	15	213
29	1983	6692	418	160	133	3505	719	378	0	306

Age*	Build Year	Coal	NG	Petroleum	Biomass	Nuclear	Hydro	Wind	Solar	Geothermal
30	1982	12443	1028	243	273	1221	656	20	0	128
31	1981	10506	805	2208	362	4499	279	18	0	0
32	1980	16001	423	1202	290	1922	1227	0	0	251
33	1979	10647	2406	1118	104	865	2126	0	0	110
34	1978	12172	2654	2543	120	2113	2322	0	0	0
35	1977	12549	5188	1312	141	6976	519	0	0	0
36	1976	8863	4016	2688	240	3897	1615	0	0	0
37	1975	11275	9310	3862	0	6670	2031	17	0	110
38	1974	11879	9184	6551	46	9677	554	0	0	0
39	1973	16602	7183	2154	5	4412	1254	0	0	110
40	1972	10925	8114	4457	58	6432	221	0	0	110
41	1971	12466	9254	2064	98	2463	1187	0	0	110
42	1970	11823	6823	1398	54	2266	1135	0	0	0
43	1969	13131	4908	1230	137	1192	1907	0	0	0
44	1968	9810	4371	2167	194	0	1951	0	0	0
45	1967	8214	6635	1052	170	0	2432	0	0	0
46	1966	4110	3222	750	143	0	1415	0	0	0
47	1965	5935	3523	739	245	0	1605	0	0	0
48	1964	4538	2817	821	124	0	2178	0	0	0
49	1963	4134	3817	347	64	0	2522	0	0	0
50	1962	3529	2636	527	84	0	2416	0	0	0
51	1961	4520	2592	662	33	0	3482	0	0	0
52	1960	4098	2302	220	87	0	1644	0	0	0
53	1959	6628	3014	409	109	0	1741	0	0	0
54	1958	6298	3478	576	120	0	2749	0	0	0
55	1957	3667	1197	274	72	0	1478	0	0	0
56	1956	1486	1861	112	54	0	1233	0	0	0
57	1955	5877	1236	420	112	0	1736	0	0	0
58	1954	5564	1889	384	109	0	1287	0	0	0
59	1953	4341	705	48	45	0	1955	0	0	0
60	1952	2464	579	85	91	0	1693	0	0	0
61	1951	1514	1086	300	92	0	1372	0	0	0

Age*	Build Year	Coal	NG	Petroleum	Biomass	Nuclear	Hydro	Wind	Solar	Geothermal
62	1950	1121	528	120	39	0	1200	0	0	0
63	1949	691	345	151	111	0	1242	0	0	0
64	1948	142	452	32	55	0	803	0	0	0
65	1947	32	54	107	0	0	169	0	0	0
66	1946	56	12	18	0	0	59	0	0	0
67	1945	6	6	7	0	0	366	0	0	0
68	1944	106	2	1	0	0	1006	0	0	0
69	1943	90	60	0	0	0	1078	0	0	0
70	1942	12	73	8	3	0	1101	0	0	0
Capacity Factors		0.5139	0.2880	0.4683	0.8136	0.4030	0.2696	0.1536	0.4770	0.5139
Total Generation*		4,027,337	GWh							
Total Emissions**		2,156.8	Mt CO_2							

*Capacity and generation data source: (U.S. Energy Information Administration, 2013a, 2013b; U.S. Environmental Protection Agency, 2014b)

**Emissions data source: (U.S. Environmental Protection Agency, 2013)

Appendix G Additional Input Data and Assumptions for Least-Cost Climate Action Analysis.

Automotive (LDV) Sector

Input Parameter / Data Set	Notes	Source
2010 vehicle fleet composition by age	Fleet composition derived using auto sales data since 1990 and discard probabilities for vehicles which are determined using an S-curve function	(U.S. Department of Energy (AFDC), 2014; Wards Auto, 2014)
Vehicle discard probability	Cumulative discard probabilities for vehicles estimated using an S-curve function that minimizes error in total number of vehicles in 2010 while maintaining an error of <1% in the fleet-wide emissions from LDVs in 2010	(U.S. Department of Transportation (FHWA), 2010)
Vehicle critical age	Assumed as 20 years for all technology types	
Gasoline vehicle fuel economy	CVs and PHEVs (gas driving) from 1990 to 2010 follow CAFE values; HEVs assumed to have 13% better mpg than CV; fuel economy assumed to improve by based on estimates in the literature	(McKinsey & Company, 2009; Meszler, German, Mock, & Bandivadekar, 2012; TNO et al., 2011)
Electric vehicle fuel economy	MWh/miles assumed to reduce at 0.5% annually after 2010	(U.S. Department of Energy & U.S. Environmental Protection Agency, 2014)
Combined vehicle fuel economy	Formula for mpge obtained from EPA rule (Eg/Em.Ee)	(U.S. Department of Energy, 2000)
CAFE fuel economy standards	Years 1990-2025 follow CAFE standards that have been published so far; standards for 2026 and later calculated by linear extrapolation of 2008-2025 numbers	(U.S. Department of Transportation (NHTSA), 2011; U.S. Environmental Protection Agency & U.S. Department of Transportation (NHTSA), 2010, 2012)
New vehicle deployment costs	Assumption based on sales-weighted average for vehicle type excluding subsidies for each vehicle type in 2011	(U.S. Energy Information Administration, 2011)
Vehicle maintenance cost	Assumption; maintenance costs assumed to increase by 5% with every year of aging	Assumption
Vehicle retirement costs	Retirement cost equals value of vehicle calculated using average annual depreciation rate based on literature	(Allgemeiner Deutscher Automobil-Club e.v., 2014)
Gasoline prices	Gas prices assumed to follow EIA projections	(U.S. Energy Information Administration, 2011)
Retail consumer electricity prices	Residential electricity price assumed to follow EIA projections	(U.S. Energy Information Administration, 2011)

Input Parameter / Data Set	Notes	Source
Vehicle miles traveled on gasoline	Average VMT/LDV for US in 2010	(U.S. Department of Transportation (FHWA), 2012)
Vehicle miles traveled on battery power	Miles on battery powered propulsion assumed to be 60% of average VMT/LDV for PHEVs	Assumption
CO2 emissions from burning gasoline	Constant	(U.S. Environmental Protection Agency & U.S. Department of Transportation (NHTSA), 2010)
CO2 emissions from wall charging of EVs	EF calculated by running utility optimization model and assuming maximum additional load from LDV charging calculated under maximum EV penetration case	
Battery cost reduction	Rate are which batteries becomes cheaper assumed to follow non-exponential power curve based on literature data	(Hensley, Knupfer, & Pinner, 2009; Valentine-urbschat & Bernhart, 2009)
Technology cost reduction	Rate at which the technology becomes cheaper over the years (different from battery cost reduction which is in addition to this reduction); assumed to be 0% for CVs and HEVs, and 1% for BEVs and PHEVs	Assumption

Electric Utility Sector

Input Parameter/Data Set	Notes	Source
2010 generation fleet composition by age	Installed capacity, generation, and generator age data obtained from eGRID; Generation capacity older than 70 years, which comprised of only 3% of total capacity, is excluded from the fleet, but total generation and emission values are kept identical to actual reported values	(U.S. Energy Information Administration, 2013a, 2013b; U.S. Environmental Protection Agency, 2014b)
Capacity discard probability	Assumed to be 0.005 until natural retirement	Assumption
Capacity critical age	Assumed 60 years for coal, nuclear, hydro, and wind, 50 years for natural gas, and 30 years for the rest	
Deployment & O&M costs, heat rates, emission factors	Value assumed to be the average of different kinds of generation units using the same fuel; $/kW converted to $/MWh considering 2010 capacity factors	(U.S. Energy Information Administration, 2013e)
Capacity retirement cost	Decommissioning costs obtained for retirement of an entire plant using a certain type of fuel, and then divided by the nominal capacity of a plant using the particular fuel; forced retirement costs include decommissioning cost plus the payment for lost revenue, and any remaining debt; capital recovery factor includes ROI/interest rate (10-12%), risk (1-3%), and tax (5%), loan term for capital cost is assumed to be 30 years	Powerplant financing: (Bozzuto, 2006; Peppiatt, 2012) Decommissioning costs: Coal, NG, Petroleum - (Malley & Zarider, 2012); Hydro - (Brazos River Authority, 2007); Nuclear - (U.S. Nuclear Regulatory Commission, 2012); Wind - (Hewson, 2008); Solar - (Belectric, 2011)
Fuel Costs	Fuel costs based on average heating values of different kinds of generation units using the same fuel, and fuel prices in 2010; Fuel prices of coal assumed to increase at 0.5% annually, petroleum at 3% annually, and rest at 1% annually based on historic trends in prices of these fuels	(U.S. Energy Information Administration, 2011)

Appendix H Levels of parameter values used for uncertainty analyses of delayed climate action cost study.

Automotive (LDV) Sector

Parameter Group	Parameter	Control Variable	Value in Best Case	Value in Nominal Case	Value in Worst Case
1	FE_Gas	% increase in FE (mpg)	High	Nom	Low
	FE_Elec	% increase in FE (mile/kWh)	High	Nom	Low
	FE_Comb	% increase in FE (mpg)	High	Nom	Low
2	Cost_Body	$/vehicle body	Low	Nom	High
	Cost_Batt	$/kWh	Low	Nom	High
	Cost_Maint	$/vehicle	Low	Nom	High
3	Cost_Ret	% decrease in $/vehicle with time	High	Nom	Low
4	Miles	Miles travelled per vehicle per year	Low	Nom	High
5	Gas_Price	% increase in $/gal	High	Nom	Low
	Elec_Price	% increase in $/kWh	High	Nom	Low
6	Charging EF	% decrease in tCO2/kWh with time	High	Nom	Low

Electric Utility Sector

Parameter Group	Parameter	Control Variable	Value in Best Case	Value in Nominal Case	Value in Worst Case
1	Overnight Capital Cost	Annual Reduction in Overnight Capital Costs	High	Nom	Low
2	Retirement Cost	Interest, return on equity, risk	Low	Nom	High
3	Fuel Prices	% increase in fuel prices	High	Nom	Low
4	Generation	% increase in annual generation	Low	Nom	High
	EV Market Penetration	Additional % point increase in annual generation after 2025 due to EV charging	Low	Nom	High

Appendix I Parameter values and their respective sources for uncertainty analyses of delayed climate action cost study.

Automotive (LDV) Sector

	Low	Nom	High
Gasoline MPG			
FE improve 2011-2030	1.25%	1.50%	1.75%
FE improve 2030-2050	0.50%	0.50%	0.50%
Electric MPG			
FE improve 2011-2030	0.75%	1.00%	1.25%
FE improve 2030-2050	0.50%	0.50%	0.50%
Annual % decrease in vehicle value			
CV	10.0%	16.8%	20.0%
HEV	10.0%	15.2%	20.0%
BEV	10.0%	16.5%	20.0%
PHEV	10.0%	15.2%	20.0%
Miles travelled per vehicle per year	12,000	12,500	13,200
Annual % increase in gasoline price	1.12%	1.50%	2.00%
Annual % increase in electricity price	0.01%	0.50%	1.00%
Battery cost ($/kWh) as a function of years (x), x $\in$Y	$751.04\ x^{-0.421}$	$800.49\ x^{-0.302}$	$837.10\ x^{-0.213}$
Average annual reduction in EV charging emission factor	0.61%	0.61%	0.74%

Electric Utility Sector

	Low	Nom	High
Annual % change in overnight capital cost	0.0%	0.0%	2.0%
Retirement Cost	1.25%	1.50%	1.75%
Interest Rate on Debt	10%	12%	8%
Interest Rate on Equity	12%	14%	10%
Risk for Established Tech	3%	3%	3%
Risk for New Tech	6%	8%	6%
Annual % change in fuel prices	0.50%	0.50%	0.50%
Coal	-1.70%	0.30%	2.30%
Natural Gas	1.60%	2.30%	2.80%
Fuel Oil (Petroleum)	-2.90%	4.30%	4.40%
Annual % increase in non-EV demand	0.8%	0.5%	1.0%
Annual % increase in EV charging demand	0.5%	0.1%	0.75%

REFERENCES

Advanced Cryogenics. (2013). U.S. Carbon Dioxide Plant Database. Tavernier, FL. Retrieved from http://www.carbondioxideconsultants.com/

All Gas. (2001). Carbon Dioxide (CO_2) CGA-320. Retrieved from http://www.allgas.com/datapages/co2.pdf

Allgemeiner Deutscher Automobil-Club e.v. (2014). *ADAC Autokosten 2014* (Vol. 12, p. 42). Munich, Germany. Retrieved from http://www.adac.de/_mmm/pdf/autokostenuebersicht_47085.pdf

Aramcharoen, a., & Mativenga, P. T. (2009). Size effect and tool geometry in micromilling of tool steel. *Precision Engineering*, *33*(4), 402–407. doi:10.1016/j.precisioneng.2008.11.002

Aresta, M. (2003). Carbon Dioxide Utilization: Greening Both the Energy and Chemical Industry: An Overview. In C. Liu, R. G. Mallinson, & M. Aresta (Eds.), *Utilization of Greenhouse Gases*. Washington, DC: American Chemical Society. doi:10.1021/bk-2003-0852

Aresta, M., & Dibenedetto, A. (2007). Utilisation of CO_2 as a chemical feedstock: opportunities and challenges. *Dalton Transactions (Cambridge, England : 2003)*, (28), 2975–92. doi:10.1039/b700658f

Argonne National Laboratory. (2012). GREET Model 2012. Argonne, IL. Retrieved from https://greet.es.anl.gov/greet_2_series

Arif, M., Rahman, M., & San, W. Y. (2011). Ultraprecision ductile mode machining of glass by micromilling process. *Journal of Manufacturing Processes*, *13*(1), 50–59. doi:10.1016/j.jmapro.2010.10.004

Arsecularatne, J. A., Zhang, L. C., & Montross, C. (2006). Wear and tool life of tungsten carbide, PCBN and PCD cutting tools. *International Journal of Machine Tools and Manufacture*, *46*(5), 482–491. doi:10.1016/j.ijmachtools.2005.07.015

Baker, A. H., & Garvey, M. D. (2013, May). Carbon Dioxide - A Market Flooded by Demand. *CryoGas International*, 28–34. Retrieved from http://cryogas.com/may-2013-vol-51-no-05/

Bandivadekar, A., Bodek, K., Cheah, L., Evans, C., Groode, T., Heywood, J., … Weiss, M. (2008). *On the Road in 2035*.

Bare, J. (2011). TRACI 2.0: the tool for the reduction and assessment of chemical and other environmental impacts 2.0. *Clean Technologies and Environmental Policy*, *13*(5), 687–696. doi:10.1007/s10098-010-0338-9

BBI International. (2014). U.S. Ethanol Plants. Retrieved from http://www.ethanolproducer.com/plants/listplants/US/Existing/All

Beckman, E. J. (2004). Supercritical and near-critical CO2 in green chemical synthesis and processing. *The Journal of Supercritical Fluids*, *28*(2-3), 121–191. doi:10.1016/S0896-8446(03)00029-9

Belectric. (2011). *Decommissioning Plan - Fleshman/Kost Road 3 MW Solar Farm* (p. 14). Sacramento, CA. Retrieved from www.planningdocuments.saccounty.net/DocOpen.aspx?PDCID=13854

Bissacco, G., Hansen, H. N., & De Chiffre, L. (2005). Micromilling of hardened tool steel for mould making applications. *Journal of Materials Processing Technology*, *167*(2-3), 201–207. doi:10.1016/j.jmatprotec.2005.05.029

Blowers, P., & Titus, M. (2004). Use of life-cycle inventory as a screening tool for environmental performance: Supercritical carbon dioxide in the semiconductor industry. *Environmental Progress*, *23*(4), 284–290. doi:10.1002/ep.10047

Boyd, S. (2011). *Life-Cycle Assessment of Semiconductors*. Springer.

Bozzuto, C. (2006). Power Plant Economics. Retrieved from https://wpweb2.tepper.cmu.edu/ceic/SeminarPDFs/Carl_Bozzuto_Seminar.pdf

Brandão, M., Levasseur, A., Kirschbaum, M. U. F., Weidema, B. P., Cowie, A. L., Jørgensen, S. V., … Chomkhamsri, K. (2012). Key issues and options in accounting for carbon sequestration and temporary storage in life cycle assessment and carbon footprinting. *The International Journal of Life Cycle Assessment*, *18*(1), 230–240. doi:10.1007/s11367-012-0451-6

Brazos River Authority. (2007). Board Votes Unanimously to Decommission Hydro Plant at Possum Kingdom Lake. Retrieved January 23, 2013, from http://www.brazos.org/generalPdf/47ZEE_Decommissioning.pdf

Butler, M. P., Reed, P. M., Fisher-Vanden, K., Keller, K., & Wagener, T. (2014). Inaction and climate stabilization uncertainties lead to severe economic risks. *Climatic Change*, *127*(3-4), 463–474. doi:10.1007/s10584-014-1283-0

Byers, J. P. (Ed.). (2006). *Metalworking Fluids* (Second Edi., p. 480). Boca Raton, FL: CRC Press. Retrieved from http://www.crcpress.com/product/isbn/9781574446890

Cervero, R., & Duncan, M. (2006). 'Which Reduces Vehicle Travel More: Jobs-Housing Balance or Retail-Housing Mixing? *Journal of the American Planning Association*, *72*(4), 475–490. doi:10.1080/01944360608976767

Cheng, C., Phipps, D., & Alkhaddar, R. M. (2005). Treatment of spent metalworking fluids. *Water Research*, *39*(17), 4051–63. doi:10.1016/j.watres.2005.07.012

Cherubini, F., & Strømman, A. H. (2011). Life cycle assessment of bioenergy systems: state of the art and future challenges. *Bioresource Technology*, *102*(2), 437–51. doi:10.1016/j.biortech.2010.08.010

Clarens, A. F., Hayes, K. F., & Skerlos, S. J. (2006). Feasibility of Metalworking Fluids Delivered in Supercritical Carbon Dioxide. *Journal of Manufacturing Processes*, *8*(1), 47–53. doi:10.1016/S1526-6125(06)70101-3

Clarens, A. F., MacLean, D. J., Hayes, K. F., Park, Y.-E., & Skerlos, S. J. (2009). Solubility of a Metalworking Lubricant in High-Pressure CO2 and Effects in Three Machining Processes. In *Transactions of NAMRI/SME* (Vol. 37, pp. 645–652).

Clarens, A. F., Park, Y., Temme, J., Hayes, K., Zhao, F., & Skerlos, S. (2009). Evaluation of Cooling Potential and Tool Life in Turning Using Metalworking Fluids Delivered in Supercritical Carbon Dioxide. In *ASME 2009 International Manufacturing Science and Engineering Conference, Volume 1* (pp. 67–75). ASME. doi:10.1115/MSEC2009-84140

Clarens, A. F., Resurreccion, E. P., White, M. A., & Colosi, L. M. (2010). Environmental life cycle comparison of algae to other bioenergy feedstocks. *Environmental Science & Technology*, *44*(5), 1813–9. doi:10.1021/es902838n

Clarens, A. F., Zimmerman, J. B., Keoleian, G. A., Hayes, K. F., & Skerlos, S. J. (2008). Comparison of Life Cycle Emissions and Energy Consumption for Environmentally Adapted Metalworking Fluid Systems. *Environmental Science & Technology*, *42*(22), 8534–8540. doi:10.1021/es800791z

Corporate Value Chain (Scope 3) Accounting and Reporting Standard. (2012) (p. 152). Washington, DC. Retrieved from http://www.ghgprotocol.org/files/ghgp/public/Corporate-Value-Chain-Accounting-Reporing-Standard_041613.pdf

De Visser, E., Hendriks, C., Barrio, M., Mølnvik, M. J., de Koeijer, G., Liljemark, S., & Le Gallo, Y. (2008). Dynamis CO2 quality recommendations. *International Journal of Greenhouse Gas Control*, *2*(4), 478–484. doi:10.1016/j.ijggc.2008.04.006

DeSimone, J. M. (2002). Practical approaches to green solvents. *Science (New York, N.Y.)*, *297*(5582), 799–803. doi:10.1126/science.1069622

Desimone, J. M., & Tumas, W. (Eds.). (2003). *Green Chemistry Using Liquid and Supercritical Carbon Dioxide* (First Edit.). Cary, NC, USA: Oxford University Press. Retrieved from http://site.ebrary.com/lib/umich/docDetail.action?docID=10085244

Dornfeld, D., Min, S., & Takeuchi, Y. (2006). Recent Advances in Mechanical Micromachining. *CIRP Annals - Manufacturing Technology*, *55*(2), 745–768. doi:10.1016/j.cirp.2006.10.006

Du, Y., Cai, F., Kong, D.-L., & He, L.-N. (2005). Organic solvent-free process for the synthesis of propylene carbonate from supercritical carbon dioxide and propylene oxide catalyzed by insoluble ion exchange resins. *Green Chemistry*, *7*(7), 518. doi:10.1039/b500074b

Ecoinvent Database v2.2. (2010). Switzerland.

Egashira, K., & Mizutani, K. (2002). Micro-drilling of monocrystalline silicon using a cutting tool. *Precision Engineering*, *26*(3), 263–268. doi:10.1016/S0141-6359(01)00113-1

Ehmann, K. F., Bourell, D., Culpepper, M. L., Hodgson, T. J., Kurfess, T. R., Madou, M., … Devor, R. E. (2005). *International Assessment of Research and Development in Micromanufacturing*. Baltimore, MD. Retrieved from http://www.dtic.mil/cgi-bin/GetTRDoc?Location=U2&doc=GetTRDoc.pdf&AD=ADA466761

Eide, J. (2013). *Rethinking CCS – Strategies for Technology Development in Times of Uncertainty by*. Massachusetts Institute of Technology. Retrieved from http://sequestration.mit.edu/pdf/2013_JanEide_Thesis.pdf

Ekvall, T., & Finnveden, G. (2001). Allocation in ISO 14041—a critical review. *Journal of Cleaner Production*, *9*(3), 197–208. doi:10.1016/S0959-6526(00)00052-4

El Baradie, M. A. (1996). Cutting fluids: Part I. Characterisation. *Journal of Materials Processing Technology*, *56*(1-4), 786–797. doi:10.1016/0924-0136(95)01892-1

Erga, O., Juliussen, O., & Lidal, H. (1995). Carbon dioxide recovery by means of aqueous amines. *Energy Conversion and Management*, *36*(6-9), 387–392. doi:10.1016/0196-8904(95)00027-B

European Industrial Gases Association. (2008). *Carbon dioxide source qualification quality standards and verification* (p. 13). Brussels, Belgium. Retrieved from http://www.ascoco2.com/fileadmin/user_upload/ascoco2.com/Bilder_und_Dokumente/CO2-_und_Trockeneislieferungen/EIGA_Spezifikationen_CO2.pdf

Farm Futures. (2014). Ammonia Prices Surge Higher. Retrieved from http://farmfutures.com/mdfm/Faress1/author/252/2014/4/WFertR040714.pdf

Federal Greenhouse Gas Accounting and Reporting Guidance. (2010) (p. 47). Washington, DC. Retrieved from http://www.whitehouse.gov/sites/default/files/microsites/ceq/ghg_guidance_document_0.pdf

Feinberg, D., & Karpuk, M. (1990). *CO_2 Sources for Microalgae-Based Liquid Fuel Production*. Golden, CO. Retrieved from http://www.nrel.gov/docs/legosti/old/3820.pdf

Filiz, S., Conley, C. M., Wasserman, M. B., & Ozdoganlar, O. B. (2007). An experimental investigation of micro-machinability of copper 101 using tungsten carbide micro-endmills. *International Journal of Machine Tools and Manufacture*, *47*(7-8), 1088–1100. doi:10.1016/j.ijmachtools.2006.09.024

Filiz, S., Xie, L., Weiss, L. E., & Ozdoganlar, O. B. (2008). Micromilling of microbarbs for medical implants. *International Journal of Machine Tools and Manufacture*, *48*(3-4), 459–472. doi:10.1016/j.ijmachtools.2007.08.020

Finley, R. (2006). *Illinois State Geological Survey Evaluation of CO_2 Capture Options from Ethanol Plants*. Champaign, IL. Retrieved from http://www.sequestration.org/resources/publish/phase2_capture_topical_rpt.pdf

Fratila, D. (2010). Macro-level environmental comparison of near-dry machining and flood machining. *Journal of Cleaner Production*, *18*(10-11), 1031–1039. doi:10.1016/j.jclepro.2010.01.017

Garvey, M. D. (2010, May). The US Merchant Carbon Dioxide Market Report. *CryoGas International*, 32–34. Retrieved from http://cryogas.com/may-2010-vol-48-no-05/

Garvey, M. D. (2014, May). The US Merchant CO_2 Report. *CryoGas International*, *52*(5), 26–29. Retrieved from http://cryogas.com/may-2014-vol-52-no-05/

Garvey, M. D., & Turley, C. E. (2011, May). The 2010 U.S. Carbon Dioxide Market Report: A Changing Landscape. *CryoGas International*, 24–28. Retrieved from http://cryogas.com/may-2011-vol-49-no-05/

Garvey, M. D., & Turley, C. E. (2012, May). Change is Good - The 2011 Carbon Dioxide Report. *CryoGas International*, 26–30. Retrieved from http://cryogas.com/may-2012-vol-50-no-05/

Gowrishankar, V., Hutton, D., Fluhrer, C., & Dasgupta, N. (2006). Making Photovoltaic Power Competitive with Grid Power. *2006 IEEE 4th World Conference on Photovoltaic Energy Conference*, 2532–2535. doi:10.1109/WCPEC.2006.279761

Green Chemistry Award 2014 Winner. (2014). Retrieved from http://www.rsc.org/ScienceAndTechnology/Awards/GreenChemistry/2014-Winner.asp

Greene, D. L., & Chen, C. K. E. (1981). Scrappage and survival rates of passenger cars and light trucks in the U.S., 1966–1977. *Transportation Research Part A: General*, *15*(5), 383–389. doi:10.1016/0191-2607(81)90144-8

Greene, D. L., Leiby, P. N., & Bowman, D. (2007). *Integrated Analysis of Market Transformation Scenarios with HyTrans*.

Grimes-Casey, H. G., Keoleian, G. a, & Willcox, B. (2009). Carbon emission targets for driving sustainable mobility with US light-duty vehicles. *Environmental Science & Technology*, *43*(3), 585–90. Retrieved from http://www.ncbi.nlm.nih.gov/pubmed/19244987

Guinée, J. B., Heijungs, R., Huppes, G., Zamagni, A., Masoni, P., Buonamici, R., … Rydberg, T. (2011). Life cycle assessment: past, present, and future. *Environmental Science & Technology*, *45*(1), 90–6. doi:10.1021/es101316v

Häring, H.-W. (Ed.). (2008). *Industrial Gases Processing* (1st ed.). Munich: Wiley-VCH.

Hattori, T. (2011). Ultrapure Water-Related Problems and Waterless Cleaning Challenges. In *ECS Transactions* (Vol. 34, pp. 371–376). doi:10.1149/1.3567606

Hawkins, T. R., Singh, B., Majeau-Bettez, G., & Strømman, A. H. (2013). Comparative Environmental Life Cycle Assessment of Conventional and Electric Vehicles. *Journal of Industrial Ecology*, *17*(1), 53–64. doi:10.1111/j.1530-9290.2012.00532.x

Hensley, R., Knupfer, S., & Pinner, D. (2009). *Electrifying cars: How three industries will evolve* (p. 10). Detroit, MI. Retrieved from http://www.lne.be/themas/beleid/mina4/leeswijze/projecten/elektromobiliteit/mc-kinsey.pdf

Hertwich, E. (2014). Understanding the Climate Mitigation Benefits of Product Systems: Comment on "Using Attributional Life Cycle Assessment to Estimate Climate-Change Mitigation…." *Journal of Industrial Ecology*. doi:10.1111/jiec.12150

Hewson, T. (2008). Wind Decmmissioning Costs - Lessons Learned. Retrieved January 23, 2013, from https://www.wind-watch.org/documents/wind-decommissioning-costs-lessons-learned/

Hung, J. J. (2012). *The production of activated carbon from coconut shells using pyrolysis and fluidized bed reactors*. University of Arizona.

Hyatt, J. A. (1984). Liquid and supercritical carbon dioxide as organic solvents. *The Journal of Organic Chemistry*, *49*(26), 5097–5101. doi:10.1021/jo00200a016

Intergovernmental Panel on Climate Change. (2005). *Carbon Dioxide Capture and Storage*. (B. Metz, O. Davidson, H. de Coninck, M. Loos, & L. Meyer, Eds.) (p. 442). Cambridge, UK and New York, USA: Cambridge University Press. Retrieved from www.cambridge.org/9780521863360

Intergovernmental Panel on Climate Change. (2007). *Climate Change 2007: Synthesis Report. Contribution of Working Groups I, II and III to the Fourth Assessment Report of the Intergovernmental Panel on Climate Change*. (R. K. Pachauri, A. Reisinger, & Core Writing Team, Eds.) (Vol. 32). Geneva, Switzerland.

IPCC. (2001). *Climate Change 2001 : Synthesis Report*. (R. T. Watson & Core Writing Team, Eds.). Cambridge, U.K.: Cambridge University Press.

IPCC. (2005). *Special Report on Carbon Dioxide Capture and Storage*. (B. Metz, O. Davidson, H. de Coninck, M. Loos, & L. Meyer, Eds.). New York: Cambridge University Press.

Jiménez-González, C., Kim, S., & Overcash, M. R. (2000). Methodology for developing gate-to-gate Life cycle inventory information. *The International Journal of Life Cycle Assessment*, *5*(3), 153–159. doi:10.1007/BF02978615

Jun, M. B. G., Joshi, S. S., DeVor, R. E., & Kapoor, S. G. (2008). An Experimental Evaluation of an Atomization-Based Cutting Fluid Application System for Micromachining. *Journal of Manufacturing Science and Engineering*, *130*(3), 031118. doi:10.1115/1.2738961

Kakinuma, Y., Yasuda, N., & Aoyama, T. (2008). Micromachining of Soft Polymer Material applying Cryogenic Cooling. *Journal of Advanced Mechanical Design, Systems, and Manufacturing*, *2*(4), 560–569. doi:10.1299/jamdsm.2.560

Karnib, M., Kabbani, A., Holail, H., & Olama, Z. (2014). Heavy Metals Removal Using Activated Carbon, Silica and Silica Activated Carbon Composite. *Energy Procedia*, *50*, 113–120. doi:10.1016/j.egypro.2014.06.014

Kenneth G. Hancock Memorial Award. (1999) (p. 11). Washington, DC. Retrieved from http://www.acs.org/content/dam/acsorg/funding/awards/gci/hancock/Hancock-Award-Winner-Archive.pdf

Khoo, H. H., & Tan, R. B. H. (2006). Life Cycle Investigation of CO2 Recovery and Sequestration. *Environmental Science & Technology*, *40*(12), 4016–4024. doi:10.1021/es051882a

Kim, C.-J., Mayor, J. R., & Ni, J. (2004). A Static Model of Chip Formation in Microscale Milling. *Journal of Manufacturing Science and Engineering*, *126*(4), 710. doi:10.1115/1.1813475

Kim, H.-J., McMillan, C. A., Keoleian, G. a., & Skerlos, S. J. (2010). Greenhouse Gas Emissions Payback for Lightweighted Vehicles Using Aluminum and High-Strength Steel. *Journal of Industrial Ecology*, *14*(6), 929–946. doi:10.1111/j.1530-9290.2010.00283.x

Kim, S., & Overcash, M. (2000). Allocation procedure in multi-output process: an illustration of ISO 14041. *The International Journal of Life Cycle Assessment*, *5*(4), 221–228. doi:10.1007/BF02979363

Klocke, F., & Eisenblätter, G. (1997). Dry Cutting. *CIRP Annals - Manufacturing Technology*, *46*(2), 519–526. doi:10.1016/S0007-8506(07)60877-4

Kohl, A. L., & Nielson, R. (1997). *Gas Purification* (5th ed.). Houston: Gulf Publishing Company.

Koornneef, J., van Keulen, T., Faaij, A., & Turkenburg, W. (2008). Life cycle assessment of a pulverized coal power plant with post-combustion capture, transport and storage of CO2. *International Journal of Greenhouse Gas Control*, *2*(4), 448–467. doi:10.1016/j.ijggc.2008.06.008

Kothandaraman, A. (2010). *Carbon Dioxide Capture by Chemical Absorption: A Solvent Comparison Study*. Massachussetts Institute of Technology. Retrieved from http://dspace.mit.edu/handle/1721.1/59877

KPMG. (2013). *KPMG Global Semiconductor Survey*. Retrieved from https://www.kpmg.com/US/en/IssuesAndInsights/ArticlesPublications/Documents/kpmg-global-semiconductor-survey-optimistic-2013.pdf

Krishnan, N., Boyd, S., Somani, A., Raoux, S., Clark, D., & Dornfeld, D. (2008). A hybrid life cycle inventory of nano-scale semiconductor manufacturing. *Environmental Science & Technology*, *42*(8), 3069–75. doi:10.1021/es071174k

Krishnan, N., Williams, E. D., & Boyd, S. B. (2008). Case studies in energy use to realize ultra-high purities in semiconductor manufacturing. In *2008 IEEE International Symposium on Electronics and the Environment* (pp. 1–6). IEEE. doi:10.1109/ISEE.2008.4562913

Kromer, M. A., Bandivadekar, A., & Evans, C. (2010). Long-term greenhouse gas emission and petroleum reduction goals: Evolutionary pathways for the light-duty vehicle sector. *Energy*, *35*(1), 387–397. doi:10.1016/j.energy.2009.10.006

Lee, K., & Dornfeld, D. A. (2002). An Experimental Study on Burr Formation in Micro Milling Aluminum and Copper. In *Proceedings of the North American Manufacturing Research Institution of the Society of Manufacturing Engineers* (p. 8). West Lafayette, IN: Society of Manufacturing Engineers.

Lewis, A. M., Kelly, J. C., & Keoleian, G. a. (2014). Vehicle lightweighting vs. electrification: Life cycle energy and GHG emissions results for diverse powertrain vehicles. *Applied Energy*, *126*, 13–20. doi:10.1016/j.apenergy.2014.03.023

Li, K.-M., & Chou, S.-Y. (2010). Experimental evaluation of minimum quantity lubrication in near micro-milling. *Journal of Materials Processing Technology*, *210*(15), 2163–2170. doi:10.1016/j.jmatprotec.2010.07.031

Lilliestråle, A., Mølnvik, M. J., Tangen, G., Jakobsen, J. P., Munkejord, S. T., Morin, A., & Størset, S. Ø. (2014). The IMPACTS Project: The Impact of the Quality of CO_2 on Transport and Storage Behaviour. *Energy Procedia*, *51*(1876), 402–410. doi:10.1016/j.egypro.2014.07.047

Lin, A. Y., Panchangam, S. C., & Lo, C. (2009). The impact of semiconductor, electronics and optoelectronic industries on downstream perfluorinated chemical contamination in Taiwanese rivers. *Environmental Pollution (Barking, Essex : 1987)*, *157*(4), 1365–72. doi:10.1016/j.envpol.2008.11.033

Liow, J. L. (2009). Mechanical micromachining: a sustainable micro-device manufacturing approach? *Journal of Cleaner Production*, *17*(7), 662–667. doi:10.1016/j.jclepro.2008.11.012

Liu, X., DeVor, R. E., & Kapoor, S. G. (2006). An Analytical Model for the Prediction of Minimum Chip Thickness in Micromachining. *Journal of Manufacturing Science and Engineering*, *128*(2), 474. doi:10.1115/1.2162905

Liu, X., DeVor, R. E., Kapoor, S. G., & Ehmann, K. F. (2004). The Mechanics of Machining at the Microscale: Assessment of the Current State of the Science. *Journal of Manufacturing Science and Engineering*, *126*(4), 666. doi:10.1115/1.1813469

Liu, Y., Asthana, R., & Rohatgi, P. (1991). A map for wear mechanisms in aluminium alloys. *Journal of Materials Science*, *26*(1), 99–102. doi:10.1007/BF00576038

Looking Back on 15 Years of Greenhouse Gas Accounting. (2014). Retrieved from http://www.wri.org/blog/2014/01/looking-back-15-years-greenhouse-gas-accounting

Lucca, D. a., Seo, Y. W., & Komanduri, R. (1993). Effect of Tool Edge Geometry on Energy Dissipation in Ultraprecision Machining. *CIRP Annals - Manufacturing Technology*, *42*(1), 83–86. doi:10.1016/S0007-8506(07)62397-X

MacLean, D. J., Hayes, K. F., Barnard, T., Hull, T., Park, Y. E., & Skerlos, S. J. (2009). Impact of Supercritical Carbon Dioxide Metalworking Fluids on Tool Life in Turning of Sintered Steel and Milling of Compacted Graphite Iron. In *ASME 2009 International Manufacturing Science and Engineering Conference, Volume 1* (pp. 43–48). ASME. doi:10.1115/MSEC2009-84026

MacLean, H. L., & Lave, L. B. (2003). Life cycle assessment of automobile/fuel options. *Environmental Science & Technology*, *37*(23), 5445–52. Retrieved from http://www.ncbi.nlm.nih.gov/pubmed/14700331

Malley, E., & Zarider, D. (2012). *Decommissioning Obsolete Power Plants: WHY DO IT NOW?* (p. 5). Lowell, MA. Retrieved from http://www.trcsolutions.com/Documents/White Papers/Decommissioning_Obsolete_Power_Plants_TRC_Ed_Malley_David_Zarider.pdf

Manufactures Summary by State: 2009. (2012). Retrieved from https://www.census.gov/compendia/statab/2012/tables/12s1012.xls

Matheson Gas. (2010). Carbon Dioxide. Retrieved from http://www.mathesongas.com/pdfs/products/Carbon-Dioxide-Pure-Gas.pdf

McCollum, D., & Yang, C. (2009). Achieving deep reductions in US transport greenhouse gas emissions: Scenario analysis and policy implications. *Energy Policy*, *37*(12), 5580–5596. doi:10.1016/j.enpol.2009.08.038

McCormick, M. (2012). *A Greenhouse Gas Accounting Framework for Carbon Capture and Storage Projects*. Arlington, VA. Retrieved from http://www.c2es.org/docUploads/CCS-framework.pdf

McCoy, S. T., Pollak, M., & Jaramillo, P. (2011). Geologic sequestration through EOR: Policy and regulatory considerations for greenhouse gas accounting. *Energy Procedia*, *4*, 5794–5801. doi:10.1016/j.egypro.2011.02.576

McKinsey & Company. (2009). *Roads toward a low-carbon future: Reducing CO2 emissions from passenger vehicles in the global road transportation system* (p. 36). New York, NY. Retrieved from http://www.google.com/url?sa=t&rct=j&q=&esrc=s&source=web&cd=1&cad=rja&uact=8&ved=0CCAQFjAA&url=http://www.mckinsey.com/~/media/mckinsey/dotcom/client_service/Sustainability/PDFs/roads_toward_low_carbon_future_new.ashx&ei=b3m8VNLzIou

Melzer, L. S. (2012). *Carbon Dioxide Enhanced Oil Recovery (CO2 EOR): Factors Involved in Adding Carbon Capture, Utilization and Storage (CCUS) to Enhanced Oil Recovery* (p. 18). Midland, TX. Retrieved from http://neori.org/Melzer_CO2EOR_CCUS_Feb2012.pdf

Mendicino, L., Mccormack, K., Gibson, S., & Covington, J. (1998). Energy conservation through water usage reduction in the semiconductor industry, 131–140.

Meszler, A. D., German, J., Mock, P., & Bandivadekar, A. (2012). *Summary of the EU cost curve development methodology* (No. 2012-5) (p. 41). Washington, DC. Retrieved from http://www.theicct.org/sites/default/files/publications/ICCT_CostCurveSummary_wkp20121102.pdf

Meyer, J. P. (2007). *Summary of Carbon Dioxide Enhanced Oil Recovery (CO2 EOR) Injection Well Technology*. Plano, TX. Retrieved from http://www.api.org/~/media/Files/EHS/climate-change/Summary-carbon-dioxide-enhanced-oil-recovery-well-tech.pdf

Mileva, A., Nelson, J. H., Johnston, J., & Kammen, D. M. (2013). SunShot solar power reduces costs and uncertainty in future low-carbon electricity systems. *Environmental Science & Technology*, *47*(16), 9053–60. doi:10.1021/es401898f

MIT CC&ST Program. (2014). Carbon Capture and Sequestration Project Database. Retrieved from http://sequestration.mit.edu/tools/projects/index.html

Morrow, W. R., Gallagher, K. S., Collantes, G., & Lee, H. (2010). Analysis of policies to reduce oil consumption and greenhouse-gas emissions from the US transportation sector. *Energy Policy*, *38*(3), 1305–1320. doi:10.1016/j.enpol.2009.11.006

NAICS Association. (2014). Sector 31-33 -- Manufacturing. Retrieved from http://www.naics.com/naics-code-description/?code=31

National Institute of Standards and Technology. (2011). Thermo-physical Properties of Fluid Systems. Retrieved from http://webbook.nist.gov

National Renewable Energy Laboratory. (2012). U.S. Life Cycle Inventory Database. Retrieved from https://www.lcacommons.gov/nrel/search

Ndiaye, P. M., Franceschi, E., Oliveira, D., Dariva, C., Tavares, F. W., & Oliveira, J. V. (2006). Phase behavior of soybean oil, castor oil and their fatty acid ethyl esters in carbon dioxide at high pressures. *The Journal of Supercritical Fluids*, *37*(1), 29–37. doi:10.1016/j.supflu.2005.08.002

Ng, C. K., Melkote, S. N., Rahman, M., & Senthil Kumar, A. (2006). Experimental study of micro- and nano-scale cutting of aluminum 7075-T6. *International Journal of Machine Tools and Manufacture*, *46*(9), 929–936. doi:10.1016/j.ijmachtools.2005.08.004

Nguyen, T., Zarudi, I., & Zhang, L. C. (2007). Grinding-hardening with liquid nitrogen: Mechanisms and technology. *International Journal of Machine Tools and Manufacture*, *47*(1), 97–106. doi:10.1016/j.ijmachtools.2006.02.010

Overcash, M., Li, Y., Griffing, E., & Rice, G. (2007). A life cycle inventory of carbon dioxide as a solvent and additive for industry and in products. *Journal of Chemical Technology & Biotechnology*, *82*(11), 1023–1038. doi:10.1002/jctb.1747

Pacala, S., & Socolow, R. (2004). Stabilization wedges: solving the climate problem for the next 50 years with current technologies. *Science (New York, N.Y.)*, *305*(5686), 968–72. doi:10.1126/science.1100103

Pacific Northwest National Lab. (2014). U.S. and Canada Merchant Hydrogen Production Capacities. Retrieved from http://hydrogen.pnl.gov/filedownloads/hydrogen/datasheets/merchant_hydrogen_producers.xls

Pavley, F., & Nunez, F. (2006). *California Assembly Bill No. 32 - Global Warming Solutions Act of 2006* (p. 13). Sacramento, CA. Retrieved from http://www.arb.ca.gov/cc/docs/ab32text.pdf

Peppiatt, S. (2012). Introduction to Power Station Project Financing. *Berkeley Journal of International Law*, *13*(1-2), 46–64. Retrieved from http://scholarship.law.berkeley.edu/cgi/viewcontent.cgi?article=1137&context=bjil

Plevin, R. J., Delucchi, M. a., & Creutzig, F. (2014). Using Attributional Life Cycle Assessment to Estimate Climate-Change Mitigation Benefits Misleads Policy Makers. *Journal of Industrial Ecology*, *18*(1), 73–83. doi:10.1111/jiec.12074

Product Life Cycle Accounting and Reporting Standard. (2011) (p. 148). Washington, DC. Retrieved from http://www.ghgprotocol.org/files/ghgp/public/Product-Life-Cycle-Accounting-Reporting-Standard_041613.pdf

Pušavec, F., Govekar, E., Kopač, J., & Jawahir, I. S. (2011). The influence of cryogenic cooling on process stability in turning operations. *CIRP Annals - Manufacturing Technology*, *60*(1), 101–104. doi:10.1016/j.cirp.2011.03.096

Pusavec, F., Hamdi, H., Kopac, J., & Jawahir, I. S. (2011). Surface integrity in cryogenic machining of nickel based alloy—Inconel 718. *Journal of Materials Processing Technology*, *211*(4), 773–783. doi:10.1016/j.jmatprotec.2010.12.013

Raventos, M., Duarte, S., & Alarcon, R. (2002). Application and possibilities of supercritical CO_2 extraction in food processing industry: an overview. *Food Science and Technology International*, *8*(5), 269–284. doi:10.1106/108201302029451

Rentziou, A., Gkritza, K., & Souleyrette, R. R. (2012). VMT, energy consumption, and GHG emissions forecasting for passenger transportation. *Transportation Research Part A: Policy and Practice*, *46*(3), 487–500. doi:10.1016/j.tra.2011.11.009

Rogelj, J., McCollum, D. L., Reisinger, A., Meinshausen, M., & Riahi, K. (2013). Probabilistic cost estimates for climate change mitigation. *Nature*, *493*(7430), 79–83. doi:10.1038/nature11787

Rubin, E. S., Chen, C., & Rao, A. B. (2007). Cost and performance of fossil fuel power plants with CO_2 capture and storage. *Energy Policy*, *35*(9), 4444–4454. doi:10.1016/j.enpol.2007.03.009

Rubin, J. B., Davenhall, L. B., Barton, J., Taylor, C. M. V., & Tiefert, K. (1998). A comparison of chilled DI water/ozone and CO/sub 2/-based supercritical fluids as replacements for photoresist-stripping solvents. In *Twenty Third IEEE/CPMT International Electronics Manufacturing Technology Symposium (Cat. No.98CH36205)* (pp. 308–314). IEEE. doi:10.1109/IEMT.1998.731087

Rushing, S. A. (2011). Carbon Dioxide Apps Are Key In Ethanol Project Developments. Retrieved from http://www.ethanolproducer.com/articles/7674/carbon-dioxide-apps-are-key-in-ethanol-project-developments

Rushing, S. A. (2013). Personal communication with Sam Rushing, Advanced Cryogenics Ltd., Tavernier, Florida, USA, 23 August 2013.

Samaras, C., & Meisterling, K. (2008). Life Cycle Assessment of Greenhouse Gas Emissions from Plug-in Hybrid Vehicles: Implications for Policy. *Environmental Science & Technology*, *42*(9), 3170–3176. doi:10.1021/es702178s

Schreiber, A., Zapp, P., & Kuckshinrichs, W. (2009). Environmental assessment of German electricity generation from coal-fired power plants with amine-based carbon capture. *The International Journal of Life Cycle Assessment*, *14*(6), 547–559. doi:10.1007/s11367-009-0102-8

Shiau, C.-S. N., Kaushal, N., Hendrickson, C. T., Peterson, S. B., Whitacre, J. F., & Michalek, J. J. (2010). Optimal Plug-In Hybrid Electric Vehicle Design and Allocation for Minimum Life Cycle Cost, Petroleum Consumption, and Greenhouse Gas Emissions. *Journal of Mechanical Design*, *132*(9), 091013. doi:10.1115/1.4002194

SimaPro v.7.3.3. (2012). Amersfoort, The Netherlands: PRé Consultants.

Singh, B., Strømman, A. H., & Hertwich, E. G. (2011). Comparative life cycle environmental assessment of CCS technologies. *International Journal of Greenhouse Gas Control*, *5*(4), 911–921. doi:10.1016/j.ijggc.2011.03.012

Stephenson, D. A., & Agapiou, J. S. (2005). *Metal Cutting Theory and Practice* (Second., p. 864). Boca Raton, FL: CRC Press.

Stern, N. (2008). The Economics of Climate Change. *American Economic Review*, *98*(2), 1–37. doi:10.1257/aer.98.2.1

Su, Y., He, N., Li, L., & Li, X. L. (2006). An experimental investigation of effects of cooling/lubrication conditions on tool wear in high-speed end milling of Ti-6Al-4V. *Wear*, *261*(7-8), 760–766. doi:10.1016/j.wear.2006.01.013

Subramaniam, B., Rajewski, R. A., & Snavely, K. (1997). Pharmaceutical processing with supercritical carbon dioxide. *Journal of Pharmaceutical Sciences*, *86*(8), 885–90. doi:10.1021/js9700661

Sun, S., Brandt, M., & Dargusch, M. S. (2010). Machining Ti–6Al–4V alloy with cryogenic compressed air cooling. *International Journal of Machine Tools and Manufacture*, *50*(11), 933–942. doi:10.1016/j.ijmachtools.2010.08.003

Supekar, S. D., & Skerlos, S. J. (2014). Market-driven emissions from recovery of carbon dioxide gas. *Environmental Science & Technology*, *48*(24), 14615–23. doi:10.1021/es503485z

Svensson, R., Odenberger, M., Johnsson, F., & Strömberg, L. (2004). Transportation systems for CO_2–application to carbon capture and storage. *Energy Conversion and Management*, *45*(15-16), 2343–2353. doi:10.1016/j.enconman.2003.11.022

The Greenhouse Gas Protocol - A Corporate Accounting and Reporting Standard. (2004) (p. 116). Washington, DC. Retrieved from http://www.wri.org/sites/default/files/pdf/ghg_protocol_2004.pdf

The Wittemann Company. (2012). Wittemann Company Profile. Retrieved from http://www.pureco2nfidence.com/launch/images/downloads/wittemann_capabilities.pdf

TNO, AEA, CE Delft, Ökopol, TML, Ricardo, & IHS Global Insight. (2011). *Support for the revision of Regulation (EC) No 443 / 2009 on CO2 emissions from cars* (p. 364). Delft, The Netherlands. Retrieved from http://ec.europa.eu/clima/policies/transport/vehicles/cars/docs/study_car_2011_en.pdf

Tom, J. W., & Debenedetti, P. G. (1991). Particle formation with supercritical fluids—a review. *Journal of Aerosol Science*, *22*(5), 555–584. doi:10.1016/0021-8502(91)90013-8

Topsøe, H. (2010). Purification of crude CO2 gases. Retrieved from http://www.topsoe.com/business_areas/air_pollution_control/~/media/PDF files/CATOX/Purification_of_crude_CO2_gases.ashx

Tsai, W.-T., Chen, H.-P., & Hsien, W.-Y. (2002). A review of uses, environmental hazards and recovery/recycle technologies of perfluorocarbons (PFCs) emissions from the semiconductor manufacturing processes. *Journal of Loss Prevention in the Process Industries*, *15*(2), 65–75. doi:10.1016/S0950-4230(01)00067-5

Turton, H., & Barreto, L. (2006). Long-term security of energy supply and climate change. *Energy Policy*, *34*(15), 2232–2250. doi:10.1016/j.enpol.2005.03.016

U.S. Census Bureau. (2005). *Industrial Gases : Fourth Quarter 2004*. *Current Industrial Reports* (p. 4). Retrieved from http://www.census.gov/industry/1/mq325c044.pdf

U.S. Department of Energy. (2000). *Electric and Hybrid Vehicle Research, Development, and Demonstration Program; Petroleum-Equivalent Fuel Economy Calculation* (Vol. 65, p. 7). Washington, DC. Retrieved from http://www.gpo.gov/fdsys/pkg/FR-2000-06-12/pdf/00-14446.pdf

U.S. Department of Energy (AFDC). (2014). U.S. PEV Sales by Model. Retrieved from http://www.afdc.energy.gov/data/10567

U.S. Department of Energy, & U.S. Environmental Protection Agency. (2014). fueleconomy.gov. Retrieved January 23, 2013, from http://www.fueleconomy.gov

U.S. Department of Transportation (FHWA). (2010). MV1 - State Motor Vehicle Registrations. Retrieved from http://www.fhwa.dot.gov/policyinformation/statistics/2010/mv1.cfm

U.S. Department of Transportation (FHWA). (2012). *Annual vehicle distance traveled in miles and related data* (p. 1). Washington, DC. Retrieved from http://www.fhwa.dot.gov/policyinformation/statistics/2010/pdf/vm1.pdf

U.S. Department of Transportation (NHTSA). (2011). *Summary of Fuel Economy Performance* (p. 17). Washington D.C.

U.S. DoE/EIA. (2011). *Emissions of Greenhouse Gases in the United States*. Washington D.C. Retrieved from http://www.eia.gov/environment/emissions/ghg_report/pdf/0573%282009%29.pdf

U.S. EIA. (2010). *Updated Estimates of Power Plant Capital and Operating Costs*. Retrieved from http://www.eia.gov/oiaf/beck_plantcosts/pdf/updatedplantcosts.pdf

U.S. Energy Information Administration. (2011). *Annual Energy Outlook 2011* (Vol. 0383, p. 245). Washington, DC. Retrieved from www.eia.gov/forecasts/aeo/

U.S. Energy Information Administration. (2013a). Net Generation by Energy Source: Electric Utilities, 2001 - 2012. Retrieved January 19, 2015, from http://www.eia.gov/electricity/annual/xls/epa_03_02_a.xlsx

U.S. Energy Information Administration. (2013b). Net Generation from Renewable Sources: Electric Utilities, 2002 - 2012. Retrieved January 19, 2015, from http://www.eia.gov/electricity/annual/xls/epa_03_02_b.xlsx

U.S. Energy Information Administration. (2013c). U.S. Refinery Hydrogen Production Capacity. Retrieved from http://www.eia.gov/dnav/pet/hist_xls/8_NA_8PH_NUS_6a.xls

U.S. Energy Information Administration. (2013d). *Updated Capital Cost Estimates for Utility Scale Electricity Generating Plants* (p. 201). Washington, DC. Retrieved from http://www.eia.gov/forecasts/capitalcost/pdf/updated_capcost.pdf

U.S. Energy Information Administration. (2013e). Updated estimates of power plant capital and operating costs. Retrieved January 23, 2014, from http://www.eia.gov/forecasts/capitalcost/xls/table1.xls

U.S. Energy Information Administration. (2014). *AEO 2014 Early Release Overview* (Vol. 2014, p. 18). Washington, DC. Retrieved from http://www.eia.gov/forecasts/aeo/er/pdf/0383er(2014).pdf

U.S. Environmental Protection Agency. (1998a). *Bituminous And Sub-bituminous Coal Combustion (AP42 Fifth Ed. Vol. I, Chapter 1: External Combustion Sources)* (p. 52). Washington, DC. Retrieved from http://www.epa.gov/ttnchie1/ap42/ch01/final/c01s01.pdf

U.S. Environmental Protection Agency. (1998b). *Natural Gas Combustion (AP42 Fifth Ed. Vol. I, Chapter 1: External Combustion Sources)* (p. 10). Retrieved from http://www.epa.gov/ttnchie1/ap42/ch01/final/c01s04.pdf

U.S. Environmental Protection Agency. (2010). Greenhouse Gas Reporting Program: 2010 Data Sets. Retrieved from http://www.epa.gov/ghgreporting/documents/xls/ghgp_data_2010_09012013_FINAL.xlsx

U.S. Environmental Protection Agency. (2013). *Inventory of U.S. Greenhouse Gas Emissions and Sinks: 1990-2011* (p. 503). Washington, DC. Retrieved from http://www.epa.gov/climatechange/Downloads/ghgemissions/US-GHG-Inventory-2013-Main-Text.pdf

U.S. Environmental Protection Agency. (2014a). eGRID Ninth Edition. Retrieved from http://www.epa.gov/cleanenergy/energy-resources/egrid/

U.S. Environmental Protection Agency. (2014b). Year 2010 eGRID 9th edition Version 1.0. Retrieved January 23, 2013, from http://www.epa.gov/cleanenergy/documents/egridzips/eGRID_9th_edition_V1-0_year_2010_Data.xls

U.S. Environmental Protection Agency, & U.S. Department of Transportation (NHTSA). (2010). *Light-Duty Vehicle Greenhouse Gas Emission Standards and Corporate Average Fuel Economy Standards; Final Rule* (p. 406). Washington, DC. Retrieved from http://www.nhtsa.gov/staticfiles/rulemaking/pdf/cafe/CAFE-GHG_MY_2012-2016_Final_Rule_FR.pdf

U.S. Environmental Protection Agency, & U.S. Department of Transportation (NHTSA). (2012). *2017 and Later Model Year Light-Duty Vehicle Greenhouse Gas Emissions and Corporate Average Fuel Economy Standards* (Vol. 77, p. 578). Washington, DC. Retrieved from http://www.nhtsa.gov/staticfiles/rulemaking/pdf/cafe/2017-25_CAFE_Final_Rule.pdf

U.S. EPA. (2003a). *Air Pollution Control Technology Fact Sheet - Packed-Bed & Packed-Tower Wet Scrubber (EPA-452/F-03-015)* (p. 6). Retrieved from http://www.epa.gov/ttn/catc/dir1/fpack.pdf

U.S. EPA. (2003b). *Air Pollution Control Technology Fact Sheet - Spray-Chamber & Spray-Tower Wet Scrubber (EPA-452/F-03-016)* (p. 6). Retrieved from http://www.epa.gov/ttn/catc/dir1/fsprytwr.pdf

U.S. EPA. (2014). Presidential Green Chemistry Challenge Award Recipients. Retrieved from http://www2.epa.gov/green-chemistry/presidential-green-chemistry-challenge-award-recipients-technology#carbonDioxide

U.S. Geological Survey. (2012a). Nitrogen (Fixed) - Ammonia Statistics. Retrieved from http://minerals.usgs.gov/minerals/pubs/historical-statistics/ds140-nitro.xlsx

U.S. Geological Survey. (2012b). Nitrogen Statistics and Information. Retrieved from http://minerals.usgs.gov/minerals/pubs/commodity/nitrogen/myb1-2011-nitro.xls

U.S. Nuclear Regulatory Commission. (2012). Decommissioning. Retrieved January 23, 2013, from http://www.nrc.gov/reading-rm/basic-ref/students/decommissioning.html

United Nations. (1997). *Kyoto Protocol to the United Nations Framework Convention on Climate Change* (p. 21). Kyoto, Japan. Retrieved from http://unfccc.int/resource/docs/convkp/kpeng.pdf

United States Government. (2013). *The Social Cost of Carbon* (p. 22). Washington, DC. Retrieved from http://www.whitehouse.gov/sites/default/files/omb/assets/inforeg/technical-update-social-cost-of-carbon-for-regulator-impact-analysis.pdf

Valentine-urbschat, M., & Bernhart, W. (2009). *Powertrain 2020 – The Future Drives Electric* (p. 100). Munich, Germany. Retrieved from http://www.sustainable-innovations.org/EE/Roland_Berger_Powertrain_2020_20110215.pdf

Van Vuuren, D. P., Hoogwijk, M., Barker, T., Riahi, K., Boeters, S., Chateau, J., … Kram, T. (2009). Comparison of top-down and bottom-up estimates of sectoral and regional greenhouse gas emission reduction potentials. *Energy Policy*, *37*(12), 5125–5139. doi:10.1016/j.enpol.2009.07.024

Vellequette, L. P. (2013). Economist sees scrappage juicing U.S. sales in next two years. Retrieved from http://www.autonews.com/article/20130806/RETAIL01/130809904#axzz2nkshVW4H

Veltman, K., Singh, B., & Hertwich, E. G. (2010). Human and environmental impact assessment of postcombustion CO2 capture focusing on emissions from amine-based scrubbing solvents to air. *Environmental Science & Technology*, *44*(4), 1496–502. doi:10.1021/es902116r

Vogler, M. P., Kapoor, S. G., & DeVor, R. E. (2004). On the Modeling and Analysis of Machining Performance in Micro-Endmilling, Part II: Cutting Force Prediction. *Journal of Manufacturing Science and Engineering*, *126*(4), 695. doi:10.1115/1.1813471

Vogtländer, J. G., Brezet, H. C., & Hendriks, C. F. (2001). Allocation in recycling systems. *The International Journal of Life Cycle Assessment*, *6*(6), 344–355. doi:10.1007/BF02978865

Volkswagen AG. (2013). Volkswagen to use CO2 as future refrigerant for air conditioning systems. Retrieved from http://www.volkswagenag.com/content/vwcorp/info_center/en/news/2013/03/cooling.html

Von der Assen, N., Jung, J., & Bardow, A. (2013). Life-cycle assessment of carbon dioxide capture and utilization: avoiding the pitfalls. *Energy & Environmental Science*, *6*(9), 2721. doi:10.1039/c3ee41151f

Wang, S., & Clarens, A. F. (2013). Analytical model of metalworking fluid penetration into the flank contact zone in orthogonal cutting. *Journal of Manufacturing Processes*, *15*(1), 41–50. doi:10.1016/j.jmapro.2012.09.015

Wang, Z. Y., & Rajurkar, K. P. (2000). Cryogenic machining of hard-to-cut materials. *Wear*, *239*(2), 168–175. doi:10.1016/S0043-1648(99)00361-0

Wards Auto. (2014). U.S. Car and Truck Sales, 1931-2013. Retrieved from http://wardsauto.com/keydata/historical/UsaSa01summary

Weidema, B. (2000). Avoiding Co-Product Allocation in Life-Cycle Assessment. *Journal of Industrial Ecology*, *4*(3), 11–33. doi:10.1162/108819800300106366

Weidema, B. (2003). *Market information in life cycle assessment*. Retrieved from http://www.norlca.org/resources/780.pdf

Weidema, B., Frees, N., & Nielsen, A.-M. (1999). Marginal production technologies for life cycle inventories. *The International Journal of Life Cycle Assessment*, *4*(1), 48–56. doi:10.1007/BF02979395

Weinert, K., Inasaki, I., Sutherland, J. W., & Wakabayashi, T. (2004). Dry Machining and Minimum Quantity Lubrication. *CIRP Annals - Manufacturing Technology*, *53*(2), 511–537. doi:10.1016/S0007-8506(07)60027-4

Weinert, K., & Petzoldt, V. (2008). Machining NiTi micro-parts by micro-milling. *Materials Science and Engineering: A*, *481-482*(May 2006), 672–675. doi:10.1016/j.msea.2006.10.220

Whitefoot, K. S., & Skerlos, S. J. (2012). Design incentives to increase vehicle size created from the U.S. footprint-based fuel economy standards. *Energy Policy*, *41*, 402–411. doi:10.1016/j.enpol.2011.10.062

Williams, J. H., DeBenedictis, A., Ghanadan, R., Mahone, A., Moore, J., Morrow, W. R., … Torn, M. S. (2012). The technology path to deep greenhouse gas emissions cuts by 2050: the pivotal role of electricity. *Science (New York, N.Y.)*, *335*(6064), 53–9. doi:10.1126/science.1208365

Wilson, M. E., Kota, N., Kim, Y., Wang, Y., Stolz, D. B., LeDuc, P. R., & Ozdoganlar, O. B. (2011). Fabrication of circular microfluidic channels by combining mechanical micromilling and soft lithography. *Lab on a Chip*, *11*(8), 1550–5. doi:10.1039/c0lc00561d

Yahoo. (2013). Global Semiconductor Market Outlook to 2017. Retrieved from http://finance.yahoo.com/news/global-semiconductor-market-outlook-2017-162800646.html

Yu, C.-H., Huang, C.-H., & Tan, C.-S. (2012). A review of CO2 capture by absorption and adsorption. *Aerosol and Air Quality Research*, 745–769. doi:10.4209/aaqr.2012.05.0132

Zapp, P., Schreiber, A., Marx, J., Haines, M., Hake, J.-F., & Gale, J. (2012). Overall environmental impacts of CCS technologies—A life cycle approach. *International Journal of Greenhouse Gas Control*, *8*, 12–21. doi:10.1016/j.ijggc.2012.01.014

Zimmerman, J. B., Takahashi, S., Hayes, K. F., & Skerlos, S. J. (2003). Experimental and statistical design considerations for economical evaluation of metalworkingfluids metalworking luidsusing the the tapping torque test. *Lubrication Engineering*, *59*(3), 17–24.